Lignin bioconversion and upgrading to value-added products by marine protist, *Thraustochytrium striatum*

by

Xiang Li

B.S., Tongji University, 2015
M.S., Clemson University, 2017

AN ABSTRACT OF A DISSERTATION

submitted in partial fulfillment of the requirements for the degree

DOCTOR OF PHILOSOPHY

Department of Grain Science and Industry
College of Agriculture

KANSAS STATE UNIVERSITY
Manhattan, Kansas

2019

Abstract

Lignin, an important component of lignocellulose, has been regarded as a promising feedstock for biofuel and bioproducts. For lignin utilization and upgrading, diverse strategies have been applied including thermochemical and biological ways. In this study, lignin-derived materials were used as carbon source and converted into bioproducts through microbial fermentation by a novel species, *Thraustochytrium striatum*. It was found that this strain was able to utilize various types of lignin compounds and produce fatty acids and carotenoids simultaneously. In the screening of several lignin model compounds as carbon sources, *T. striatum* can grow on most compounds at different concentrations, while achieving the best growth in 3,4-dihydroxybenzoic acid (3,4-DHBA) and 4-hydroxybenzoic acid (4-HBA). In both batch and fed-batch cultivation modes, *T. striatum* can accumulate a significant amount of long-chain fatty acids and carotenoids. *T. striatum* was also proven to degrade polymeric lignin.

However, the depolymerization ability of *T. striatum* was relatively weak and therefore the fermentation process was optimized to improve lignin degradation and utilization. Among different nitrogen sources tested, the inorganic NH_4Cl was the best and application of organic nitrogen sources would inhibit the utilization of lignin. Mineral elements were able to improve lignin utilization by functioning as co-factors of ligninolytic enzymes and inducing their production at transcriptional level. Different external lignin depolymerization systems including commercial laccase, fungal secretome and Fenton reagent were observed to develop synergistic effects with *T. striatum*. In the presence of laccase both cell growth and lignin utilization were improved, while different kinds of laccase employed different mechanisms. The fungus-derived laccase was indicated to primarily work on breakdown of inter-unit linkages in lignin molecules, and plant-derived laccase possibly attacked aromatic ring structure. With the function of laccase,

more low-molecular-weight fragments would be generated, and laccase-catalyzing reaction would shift the equilibrium toward depolymerization and prevent repolymerization of smaller fragments. On the contrary, lignin peroxidase-dominant fungal secretome and Fenton reagent facilitate lignin degradation while not cell growth.

Black liquor prepared from corn stover alkaline pretreatment was also studied as a lignin-rich waste stream of bioprocessing and biorefinery. *T. striatum* was found to grow with black liquor and reached the cell mass concentration of 5.2 g/L under optimal conditions (pH=7, NH_4Cl=2 g/L) and reduce total lignin concentration of black liquor from 8.18 to 3.09 g/L within 7-day incubation. Aromatic monomers including *p*-coumaric acid, ferulic acid, vanillin, and syringaldehyde were observed to be consumed and converted while polymeric lignin fragments were also depolymerized and degraded. A strong adaptation of *T. striatum* to a wide pH range (3~9) was also observed during black liquor fermentation. The investigation on metabolism of *T. striatum* has identified diverse peroxidase and laccase-type enzymes for lignin depolymerization and multiple pathways for aromatic compounds degradation.

Lignin bioconversion and upgrading to value-added products by marine protist, *Thraustochytrium striatum*

by

Xiang Li

B.S., Tongji University, 2015
M.S., Clemson University, 2017

A DISSERTATION

submitted in partial fulfillment of the requirements for the degree

DOCTOR OF PHILOSOPHY

Department of Grain Science and Industry
College of Agriculture

KANSAS STATE UNIVERSITY
Manhattan, Kansas

2019

Approved by:

Major Professor
Dr. Yi Zheng

Copyright

Abstract

Lignin, an important component of lignocellulose, has been regarded as a promising feedstock for biofuel and bioproducts. For lignin utilization and upgrading, diverse strategies have been applied including thermochemical and biological ways. In this study, lignin-derived materials were used as carbon source and converted into bioproducts through microbial fermentation by a novel species, *Thraustochytrium striatum*. It was found that this strain was able to utilize various types of lignin compounds and produce fatty acids and carotenoids simultaneously. In the screening of several lignin model compounds as carbon sources, *T. striatum* can grow on most compounds at different concentrations, while achieving the best growth in 3,4-dihydroxybenzoic acid (3,4-DHBA) and 4-hydroxybenzoic acid (4-HBA). In both batch and fed-batch cultivation modes, *T. striatum* can accumulate a significant amount of long-chain fatty acids and carotenoids. *T. striatum* was also proven to degrade polymeric lignin.

However, the depolymerization ability of *T. striatum* was relatively weak and therefore the fermentation process was optimized to improve lignin degradation and utilization. Among different nitrogen sources tested, the inorganic NH_4Cl was the best and application of organic nitrogen sources would inhibit the utilization of lignin. Mineral elements were able to improve lignin utilization by functioning as co-factors of ligninolytic enzymes and inducing their production at transcriptional level. Different external lignin depolymerization systems including commercial laccase, fungal secretome and Fenton reagent were observed to develop synergistic effects with *T. striatum*. In the presence of laccase both cell growth and lignin utilization were improved, while different kinds of laccase employed different mechanisms. The fungus-derived laccase was indicated to primarily work on breakdown of inter-unit linkages in lignin molecules, and plant-derived laccase possibly attacked aromatic ring structure. With the function of laccase,

more low-molecular-weight fragments would be generated, and laccase-catalyzing reaction would shift the equilibrium toward depolymerization and prevent repolymerization of smaller fragments. On the contrary, lignin peroxidase-dominant fungal secretome and Fenton reagent facilitate lignin degradation while not cell growth.

Black liquor prepared from corn stover alkaline pretreatment was also studied as a lignin-rich waste stream of bioprocessing and biorefinery. *T. striatum* was found to grow with black liquor and reached the cell mass concentration of 5.2 g/L under optimal conditions (pH=7, NH_4Cl=2 g/L) and reduce total lignin concentration of black liquor from 8.18 to 3.09 g/L within 7-day incubation. Aromatic monomers including *p*-coumaric acid, ferulic acid, vanillin, and syringaldehyde were observed to be consumed and converted while polymeric lignin fragments were also depolymerized and degraded. A strong adaptation of *T. striatum* to a wide pH range (3~9) was also observed during black liquor fermentation. The investigation on metabolism of *T. striatum* has identified diverse peroxidase and laccase-type enzymes for lignin depolymerization and multiple pathways for aromatic compounds degradation.

Table of Contents

List of Figures

List of Tables

List of Abbreviations

3,4-DHBA: 3,4-dihydroxybenzoic acid;

3-FB: 3-fluorobenzoate;

3MGA: 3-O-methylgallic acid;

4-HBA: 4-hydroxybenzoic acid;

ACE: acetovanillone;

AL CS: alkaline extracted lignin from alkaline pretreated corn stover;

ALPHA: aqueous lignin purification with hot acid process;

ASW: artificial seawater;

CAT: catechol;

CFU: colony forming unit;

CHP: combined heat and power;

CMA: *p*-Coumaric acid;

COD: chemical oxygen demand;

CRE: *p*-cresol;

DCW: dry cell weight;

DHA: docosahexaenoic acid;

DMR-EH: deacetylation-mild alkaline treatment-followed by mechanical refining and enzymatic hydrolysis;

DMSO: dimethyl sulfoxide;

DyP: dye-decoloring peroxidase;

EHR: enzymatic hydrolysis residue;

EOL LP: ethanol extracted lignin from Loblolly pine;

EPA: eicosapentaenoic acid;

EPS: extracellular polymeric substance;

FAME: fatty acid methyl ester;

FAS: fatty acid synthase;

FEA: ferulic acid;

FID: flame ionization detector;

GO: gene ontology;

GPC: gel permeation chromatography;

GUA: guaiacol;

GYP: glucose-yeast extract-peptone;

HBS: high-biomass strain;

HSQC: heteronuclear single quantum coherence;

KEGG: Kyoto encyclopedia of genes and genome;

KOG: eukaryotic orthologous groups;

KPL: kraft pine lignin;

LiP: lignin peroxidase;

LPMO: lytic polysaccharide monooxygenase;

MnP: manganese peroxidase;

M_n: number-average molecular weight;

M_w: weight-average molecular weight;

NTG: N-methyl-N'-nitro-N-nitrosoguanidine;

OD: optical density;

OPEFB: oil palm empty fruit bunch;

PBAT: polybutyrate adipate terephthalate;

PBS: phosphate buffered saline;

PCA: protocatchuic acid;

PDC: 2-pyrone-4,6-dicarboxylic acid;

PET: polyethylene terephthalate;

PHA: polyhydroxyalkanoate;

PULCFA: polyunsaturated long-chain fatty acid;

RES: resorcinol;

SEM: scanning electron microscopy;

SLRP: sequential liquid lignin recovery and purification process;

SYA: syringic acid;

SYR: syringaldehyde;

TCA: trans-cinnamic acid;

TFA: total fatty acids;

TGA: triacylglycerol;

THF: tetrahydrofuran;

VAA: vanillic acid;

VAN: vanillin;

VP: versatile peroxidase.

Acknowledgements

I would like to thank Dr. Zheng for his patient guidance and support through the entire course of my study, which helped me to acquire much knowledge and enjoyment through scientific research. I would also like to thank my committee members, Dr. Sun, Dr. Li, and Dr. Wang as well as the outside chair Dr. Tomich, for their valuable advice on experimental design and dissertation revisions. I would like to thank my colleagues, friends and family for their continuing support, encouragement and inspiration.

Chapter 1 - Literature review on lignin bioconversion

1. Introduction

The energy independence and fossil fuel's adverse environmental impacts have strongly promoted the development of renewable clean energy. Bioenergy has been believed to be one option for the sustainable development of society, environment and economy. Lignocellulose, one of the most abundant materials in biosphere, has been regarded as a promising feedstock for the production of bioenergy and bioproducts , as it does not compete with food production's need of water, fertilizer or land (1). Among the three major components of lignocellulose, cellulose and hemicellulose are mainly composed of monosaccharides such as glucose, xylose, arabinose, and mannose, and they can be hydrolyzed and converted into bioethanol through biological conversion. On the contrary, lignin is a highly-branched and heterogeneous polyphenolic polymer. The monomers that constitute lignin molecules are extremely diverse while forming various types of C-C and C-O linkages (e.g., β-O-4, β-β and β-5 linkages) (**Figure 1.1**) (1, 2). The compositional and structural complexities of lignin render it resistant to chemical and biological degradation, therebymaking the utilization of lignin a grand challenge. In the pulping/paper and biorefinery industries, lignin usually has to be removed through chemical (3), hydrothermal (4, 5) or biological ways (6) before proceeding to paper making or biofuel production, which would yield a large amount of lignin in the solid and/or liquid waste streams. For instance, the annual production of about 100 million metric tons of chemical wood pulps worldwide can generate approximately 45 and 2 million metric tons/year of kraft lignin and lignosulfonates, respectively (7). The primary disposal method for the lignin-rich waste is direct combustion to acquire energy and recover alkali (8, 9), and a cost-efficient approach for lignin valorization has yet to be developed.

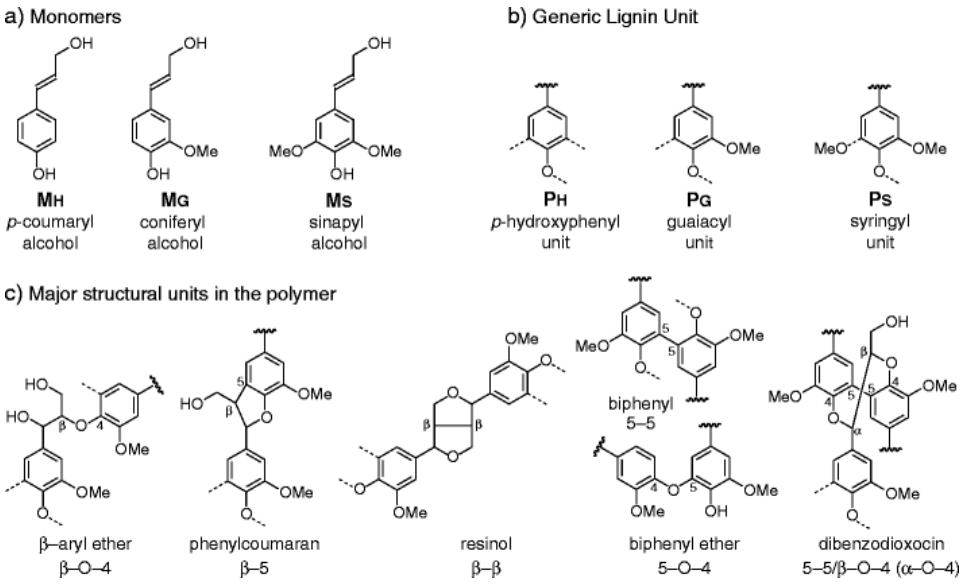

Figure 1.1 Lignin structure

a) Primary lignin monomers. (M: monolignols); b) Lignin polymer P units are denoted as generic P_H, P_G, and P_S units based on the methoxyl substitution on the aromatic ring; c) Major structural linkages in lignin molecules. Adapted from (2) with the permission of Springer.

To enhance energy recovery efficiency, enable cost-efficient biofuel production and reduce environmental impacts, urgent need has been called for lignin valorization to value-added bioproducts. The phenol-based structural nature renders lignin significantly higher energy and carbon densities than saccharides, i.e., lignin combustion can generate heat of around 22.2 to 28.5 MJ per kilogram (10). However, combined heat and power (CHP) from lignin is not considered a value-added application since the recovered value insufficiently covers the high production cost of biofuels. The flexibility of substitution on a benzene ring also makes lignin a promising feedstock to produce materials and important aromatic chemicals (as intermediates or platform chemicals), which are currently produced from the petroleum industry. Until now lignin has been studied for many applications, such as jet fuel-range hydrocarbon (11, 12), activated carbon (8), carbon fiber (13, 14), capacitor (15, 16), 3D-printer material (17, 18), as well as board binder (19, 20). Due to the complex features of lignin composition and structure, it is

difficult, even impossible, to utilize lignin directly to make high-quality products so that it has to undergo necessary modification and/or depolymerization.

Currently there are two major platforms for lignin conversion: thermochemical and biological approaches. Thermochemical processes mainly include pyrolysis (21-23), gasification (24-26), oxidation (27, 28), hydrogenation (29-32), etc. These processes typically break down large molecules of lignin by applying harsh conditions such as high-temperature, pressure and pH values (33) while catalysts are usually present. Thermochemical transformation of lignin can be carried out on a large scale with simple operation and reduced emissions of harmful gases compared to traditional incineration (34). The reaction rate and efficiency are high, but they require intensive energy input. The product matrix is generally complex due to lignin's heterogeneous composition and structure, which pose challenges for downstream separation, purification processes and final applications. On the contrary, biological platforms convert lignin into value-added products through microbial metabolism under much milder conditions (e.g., room temperature and neutral pH). Biological processes are generally slower and less efficient than thermochemical processes, while they can achieve relatively simple product matrix based on specific bio-depolymerization and metabolic mechanisms. Several classes of microorganisms have been found to possess lignin degradative capabilities, such as white rot fungi (35-37), bacteria (38, 39) and protists (40). With lignin as a carbon source, some species can synthesize valuable products [e.g., microbial lipids (41), polyhydroxyalkanoates (PHAs) (42, 43), vanillin (44), and muconic acid (45)] in which the heterogeneous portfolio of molecules produced from lignin depolymerization are converted to targeted intermediates for further conversion to fuels, chemicals, and materials. The hypothetical advantage of lignin biotransformation derives from the necessity to convert lignin into a uniform compound or a limited set of compounds that add

further metabolic value for the digesting cells. This review focuses on lignin bioconversion to produce value-added products, including depolymerization mechanisms, metabolic pathways of aromatics from depolymerization and exemplary applications of lignin biotransformation. The major pathways of lignin biodegradation are illustrated for different microorganisms, under different environmental conditions, and for various products that can be acquired through lignin fermentation.

2. Mechanisms of Lignin Bio-depolymerization

Lignin, an aromatic polymer, is composed of three types of subunits, namely guaiacyl (G), syringyl (S) and *p*-hydroxyphenyl (H). The biosynthesis of lignin is achieved through the free radical coupling of lignin precursors (1). The generated lignin chains cross-link with each other to form massive networks thus providing mechanical support for the cell wall. Those structures benefit the plants by keeping them stable and safe from external stress. Usually, complex lignin polymers need to be depolymerized and decomposed into smaller fragments prior to further applications (46, 47). In thermochemical process, lignin depolymerization is often achieved through thermal treatment with or without solvents, chemical additives or catalysts (33, 34, 47). Biological depolymerization processes are typically catalyzed by multiple ligninolytic enzymes. In nature several types of microorganisms have been identified to be able to depolymerize and degrade lignin using diverse mechanisms, which are mainly fungal and bacterial species (48).

2.1 Fungal lignin depolymerization

Fungi, white rot basidiomycetes in particular, have been reported to be the most powerful microorganisms in lignin degradation (48). Lignin degradation by white rot fungi depends on extracellular ligninolytic enzyme systems such as heme peroxidase-based [lignin peroxidase

(LiP), manganese peroxidase (MnP), versatile peroxidase (VP)] and phenol oxidase-based (laccase) (49). The bio-depolymerization of lignin is basically an enzyme-catalyzed oxidative process. LiP can catalyze the oxidation of aromatic non-phenolic lignin structures to produce aryl-cation radicals (50). Unlike LiP that directly acts on lignin molecules, MnP functions through the oxidation of Mn^{2+} to Mn^{3+} in the presence of hydrogen peroxide (51). The generated Mn^{3+} can then catalyze alkyl-aryl cleavage and α-carbon oxidation in lignin (52), and it can also form other radicals when oxidizing some organic sulfur compounds and unsaturated fatty acids to sustain the lignin degradation process (53, 54). As an attractive ligninolytic enzyme group, VP exhibits oxidative abilities on both phenolic and non-phenolic aromatic compounds as well as Mn^{2+} through a similar mechanism to LiP and MnP, though VP distinctly oxidizes substrates that span a wide range of redox potentials (49). The molecular structure of VP can provide multiple binding sites for different substrates, which can bind and oxidize substrates efficiently even in the absence of mediators (55). Laccase is a copper-containing enzyme different from heme peroxidase in that its function does not require the presence of H_2O_2. Laccase can generate reactive radicals with O_2 as a final electron acceptor to catalyze ring cleavage of aromatic compounds (56). For degradation of complex polymers, small molecules (e.g. veratryl alcohol, 3-hydroxy-anthranilic acid and manganese) can be oxidized and activated by laccase to serve as mediators and facilitate binding between laccase and polymers (57). *Phanerochaete chrysosporium* has been reported to extensively mineralize lignin to CO_2 and H_2O in pure culture, since it can secrete LiP and MnP to attack both side chain and aromatic ring of lignin molecules in a non-specific oxidative way (58). Other white rot fungal species, such as *Trametes versicolor* (59), *Ceriporiopsis subvermispora* (60), and *Dichomitus squalen*s (61) can produce laccase for lignin oxidation and decomposition. In addition to white rot fungi, brown rot fungi

[e.g., *Gloeophyllum trabeum* (62) and *Postia placenta* (63)] are also able to depolymerize lignin in which Fenton oxidation chemistry produces hydroxyl radicals that attack lignin structure. In this process, the ion acquisition and transition between Fe^{3+}/Fe^{2+} is coupled with the lignin degradation process to achieve redox cycling (62).

Given their superior ability of lignin depolymerization, fungi have been widely applied in biopulping, forage upgrading and bioremediation of soil and wastewater contaminated by lignin analogous pollutants (64-66). In addition to fungal cultures, the extracellular ligninolytic enzymes of fungi have also been isolated and utilized to synergize with other microorganisms. Salvachúa et al. (67) collected the secretome of *Pleurotus eryngii*, which exhibited the highest laccase activity in previous screening, and they incubated DMR-EH (deacetylation, mechanical refining, and enzymatic hydrolysis) lignin from corn stover with the secretome and aromatic-catabolic microbe *Pseudomonas putida* KT2440 successively. The generated low-molecular-weight lignin fragments were effectively consumed by bacteria which prevented repolymerization and pushed the reaction equilibrium toward the direction of depolymerization (67). During kraft lignin fermentation by oleaginous *Rhodococcus opacus* PD630, Zhao et al. (68) supplemented the culture with external laccase from *Trametes versicolor* to significantly enhance lignin utilization, cell growth and lipid accumulation.

2.2 Bacterial lignin depolymerization

A number of bacterial strains, such as *Rhodoccocus jostii* (69), *Pseudomonas putida* (69), *Bacillus* sp. (70), *Novosphingobium* sp. (71) and *Citrobacter freundii* (72), have also demonstrated lignin degradation ability. A special set of bacterial peroxidase, dye-decoloring peroxidase (DyP) was identified as responsible for oxidative degradation of lignin, aromatic dye and other aromatic xenobiotics (73, 74). As a heme-containing peroxidase, DyP was observed to

primarily function on lignin dimers and trimers, which are simpler and more reactive than higher molecular weight lignins, because Dyp has relatively lower oxidizing power than fungal peroxidases (74). In addition to DyP, bacteria have other oxidative enzymes that are capable of decomposing lignin by hydroxylation or demethylation, such as cytochrome P450s, non-heme iron enzymes, or Mn/Cu-containing oxidases (73, 74). For instance, laccase has been identified and studied in several bacterial species, especially the two-domain laccase from *Streptomyces* species (75), the three-domain laccase from *Pantoea ananatis* (76) and thermo-alkali-stable laccase from *Bacillus* species (77). Glutathione-dependent β-etherase has been discovered to reductively cleave β-ethyl bonds, which are highly abundant in natural lignin molecules (78, 79). The applications of bacteria for lignin conversion have mainly focused on *Rhodoccocus* and *Pseudomona* species, which can utilize both technical and native lignins for the production of microbial lipids and polyhydroxyalkanoates (PHA)s (41, 69, 80).

3. Biodegradation Pathways of Lignin-derived Aromatic Compounds

Lignin-derived aromatic compounds are usually toxic and inhibitory for most microorganisms, while species capable of aromatic anabolism are able to utilize those aromatics as carbon sources for cell growth, maintenance and bioproduct accumulation. The biodegradation of aromatic compounds typically takes multiple steps before carbon can enter central metabolism and becomes available for both microbial growth and bioproduct synthesis. A general pathway is shared by most natural lignin degraders (**Figure 1.2**), while differences occur in some metabolic steps and under specific environmental conditions.

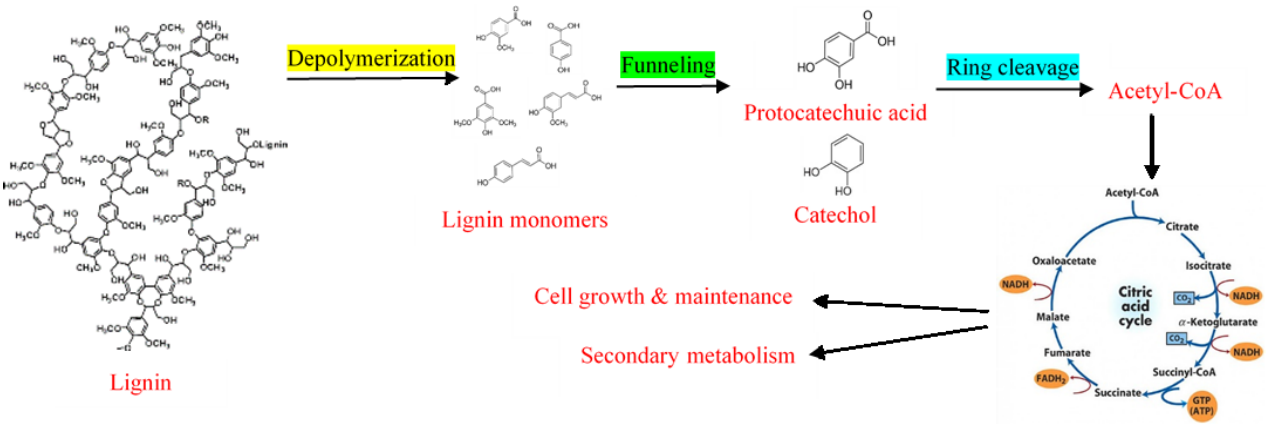

Figure 1.2 Scheme of lignin degradation under aerobic condition.
(Citric acid cycle source: https://www.westburg.eu/products/cell-biology/assays/energy-metabolism-assays/krebs-tca-cycle, accessed on 2019-03-20).

3.1 Biological funneling of aromatic compounds

After depolymerization, the diverse released lignin monomers would be converted into certain types of phenolic compounds before further microbial conversion and metabolism, i.e. the "biological funneling process." Those certain phenolic compounds serve as "central intermediates." The biological funneling process is usually the important rate- and efficiency-limiting step in the lignin bioconversion process (81). The funneling process may take several steps determined by specific structure of lignin monomers and specific environmental conditions, with involvement of diverse enzymes such as acryl-CoA synthetase, acryl-CoA hydratase, dehydrogenase, decarboxylases and O-demethylase system (82). Under aerobic conditions (**Figure 1.3**), different lignin monomers are converted with molecular oxygen as an oxidant and generate protocatechuate in most cases, which has been characterized in *Pseudomonas putida* (83) and *Sphingomonas paucimobilis* (84). Based on the structure, lignin monomers can be classified into 3 categories, H, G and S-type differing according to the number of methoxy groups on the aromatic ring. H-type compounds (e.g. 4-coumarate) are ultimately converted into 4-hydroxybenzoate, while different pathways such as the CoA-dependent β-oxidation pathway, the CoA-dependent non-β-oxidation pathway, and the CoA-independent pathway have been

identified (85). The generated 4-hydroxybenzoate is then hydroxylated to protocatechuate via 4-hydroxybenzoate-3-hydroxylase (**Figure 1.3A**). In addition to the protocatechuate pathway, Fairley et al. (86) identified that a novel haloarchaeal strain, *Haloarcula* sp. strain D1, can metabolize 4-hydroxybenzoate via the gentisate pathway. Genomic analysis also indicated the presence of the gentisate pathway in *Bacillus ligniniphilus* L1 (87) and *Candida parapsilosis* (88). For G-type compounds (e.g., ferulic acid) with one methoxy group on the aromatic ring, the funneling process is similar to H-type compounds, except the intermediate prior to protocatechuate is vanillic acid, which is finally transformed into protocatechuate through demethylation catalyzed by vanillate demethylase (**Figure 1.3A**). Distinctly, S-type compounds (**Figure 1.3B**) have two methoxy groups which make their degradation and conversion more difficult and thusly prone to requiring more studies. Complex S-type compounds (e.g., sinapate) are first funneled into syringate, and the demethylation at 3' position converts syringate into 3-O-methylgallate (3MGA) by a tetrahydrofolate-dependent O-demethylase. 3MGA can be further demethylated to form gallate, and the intermediates of S-type compound funneling (3MGA or gallate) would enter the 4,5-cleavage pathway for aromatic ring cleavage. Other aromatic compounds, such as benzene, phenol and cinnamate, are usually funneled to catechol (89).

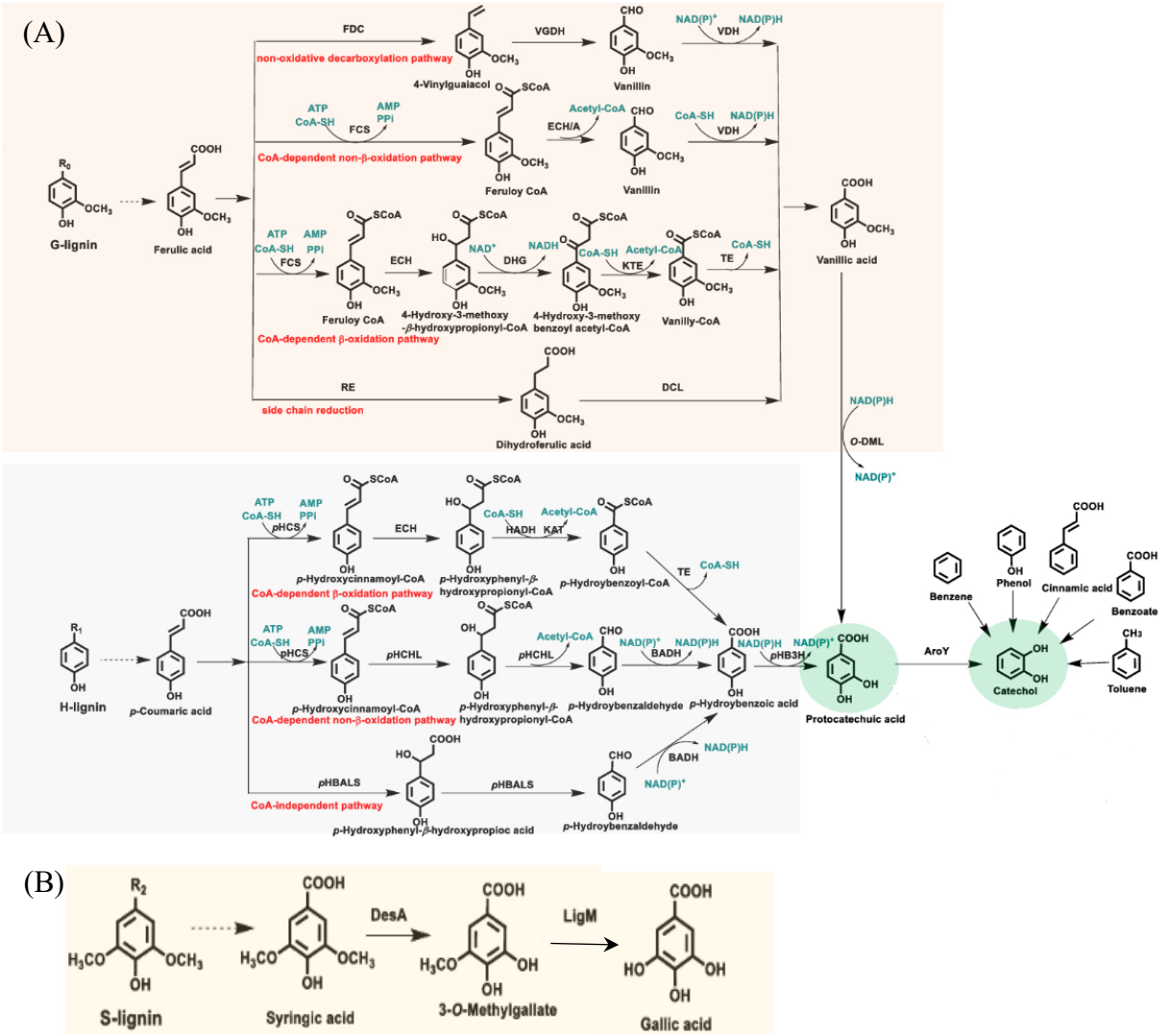

Figure 1.3 Aromatic compounds funneling pathway under aerobic conditions
(A) funneling of G and H-type aromatic compounds; (B) funneling of S-type aromatic compounds. Adapted from (85) published by Springer, under the permission of Creative Common License (http://creativecommons.org/licenses/by/4.0/).

Under anaerobic conditions, the absence of molecular oxygen necessitates the development of novel strategies for the funneling process. Special enzymes have been identified to ensure the normal function of the funneling process with no need of oxygen, such as tetrahydrofolate-dependent aromatic *O*-demethylase in anaerobic bacteria, which can achieve demethylation of vanillate through methoxy group transfer (90, 91). On the other hand, different reactions are adopted, such as reduction of benzene ring to benzoyl-CoA, 3-hydroxybenzoyl-CoA, resorcinol or phloroglucinol as central intermediates (89).

3.2 Aromatic ring cleavage

Upon the completion of lignin monomer funneling, the produced central intermediates will enter the aromatic ring cleavage process, which is the very first step to incorporate the carbon from lignin molecules into the cellular activities. As the mainstream pathway, aromatic ring ortho-cleavage is widely adopted by bacteria and fungi, and the complete pathway has been elucidated step-by-step with the aid of system analysis and gene mutation (92). The ortho-cleavage of catechol and protocatechuate are catalyzed by O_2-dependet dioxygenase generate *cis*, *cis*-muconate and 3-carboxy-*cis*, *cis*-muconate, respectively (**Figure 1.4A**). Those two types of muconate are further converted into β-ketoadipate as a characteristic product of ortho-cleavage pathway. The generated β-ketoadipate then reacts with succinyl-CoA, producing succinate and β-ketoadipyl-CoA. One molecule of acetyl-CoA will be released for the regeneration of succinyl-CoA from β-ketoadipyl-CoA. In addition to ortho-cleavage, the aromatic ring can be cleaved at meta-position (**Figure 1.4A**). For protocatechuate, cleavage at different position would generate different products, such as 2-hydroxy-4-carboxymuconic semialdehyde from 4,5 meta-cleavage and 2-hydroxy-5-carboxymuconic semialdehyde from 2,3 meta-cleavage (93). The 4,5 meta-cleavage would finally yield two pyruvate molecules and 2,3 meta-cleavage yields pyruvate and acetyl-CoA instead (94). For catechol, meta-cleavage would only produce 2-hydroxymuconic semialdehyde because of its structural symmetry and finally yield pyruvate and acetaldehyde (89). Both succinate and acetyl-CoA can enter central metabolism (e.g. citric acid cycle) directly and be used for cellular anabolism, while pyruvate needs to be further converted into acetyl-CoA.

Under anaerobic conditions, after formation of benzoyl-CoA, certain types of reductases can catalyze the further reduction of benzoyl-CoA step by step and finally cleave the ring into

acetyl-CoA (**Figure 1.4B**). That process can be completed with or without ATP as a driving force, depending on the types of microbes (89).

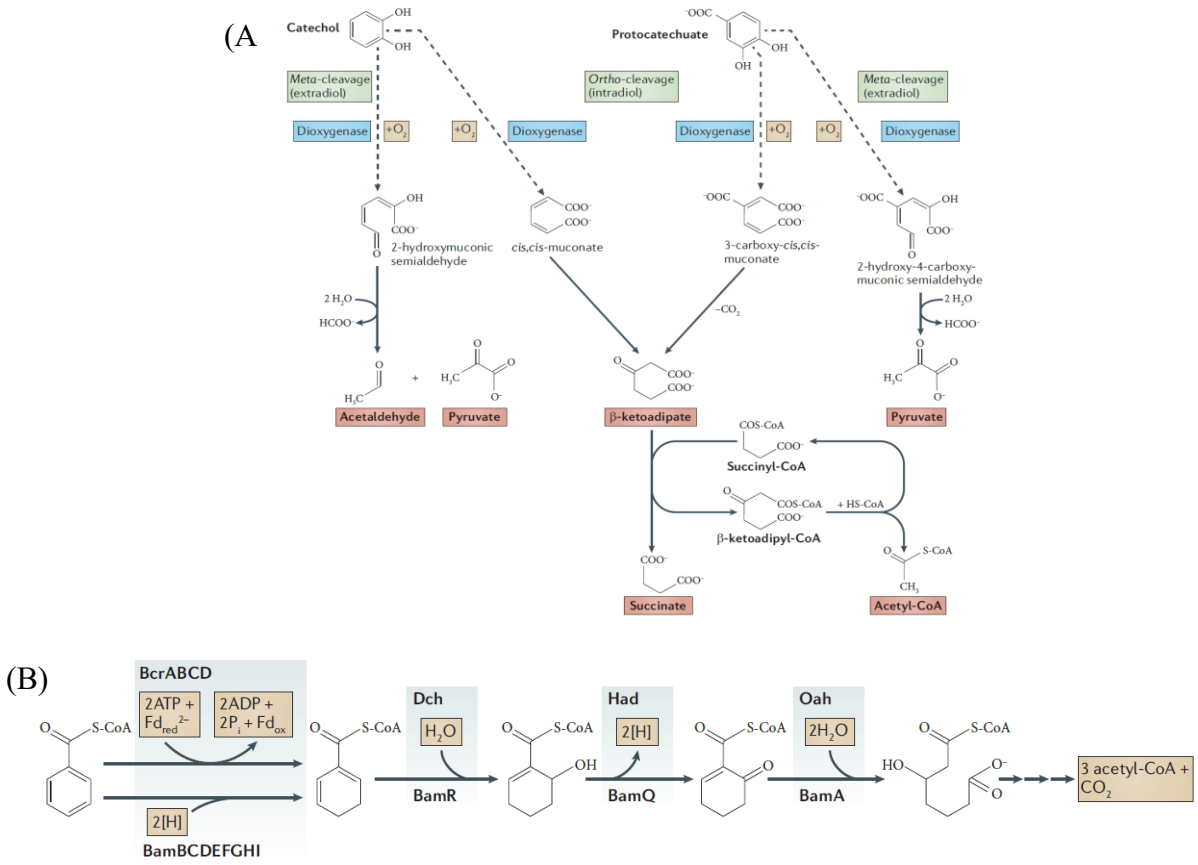

Figure 1.4 Aromatic compounds degradation pathways
(A) Degradation of catechol and protocatuchuate via ortho- and meta-cleavage of aromatic ring under aerobic condition; (B) Anaerobic degradation of benzoyl-CoA. Upper pathway: ATP-dependent; lower pathway: ATP-independent. Both adapted from (89) with the permission of Springer Nature (**Figure B.1** in **Appendix B**).

3.3 Microbial anabolism and bioproduct synthesis

After ring cleavage, the carbon from aromatic compounds enters the central metabolism process (e.g., citric acid cycle) to grow cells, maintain itself and accumulate bioproducts. Different microorganisms produce distinct products such as fatty acids and PHAs, through various metabolic pathways (**Figure 1.5**).

In oleaginous species, which can achieve lipid accumulation, the biosynthesis of fatty acids starts from acetyl-CoA which is continuously formed from citrate of citric acid cycle by ATP-citrate lysase. Acetyl-CoA carboxylase firstly converts acetyl-CoA to malonyl-CoA which

is then combined with another acetyl-CoA, and fatty acid synthase (FAS) catalyzes successive addition of more malonyl-CoA for fatty aryl chain elongation (95). During that process, a reaction system (e.g. malate oxidation by malate dehydrogenase) integrated with fatty acids synthesizing machinery provides NADPH, the major supplier of reducing power (96). The saturated products (primarily C16 and C18) from FAS are further modified with a sequence of desaturases and elongases to acquire diverse unsaturated fatty acids. Depending on the position of the final double bond nearest the terminal methyl group, those unsaturated fatty acids can be classified into two major groups, n-3 and n-6, respectively (**Figure 1.5A**).

As a kind of polyesters, PHAs can be synthesized by microorganisms from either structurally related carbon sources (e.g. fatty acids) or structurally unrelated carbon sources (e.g. glucose, aromatics) (97). Intermediates from microbial metabolism can be directed into PHA monomers and polymerized via PHA synthase. In microbial lipid metabolism, the β-oxidation pathway would both catabolize fatty acids to generate reducing power and energy and also antecedently generate shortened fatty acids for medium chain length PHA. Pyruvate generated from metabolism of glucose or aromatics can be used for synthesis of short chain length PHA. With other structurally unrelated carbon sources, diverse pathways derived from fatty acids biosynthesis can also produce medium chain length PHA. Intermediates from fatty acids biosynthesis are shunted towards PHA synthesis mainly under the action of thioesterase (**Figure 1.5B**).

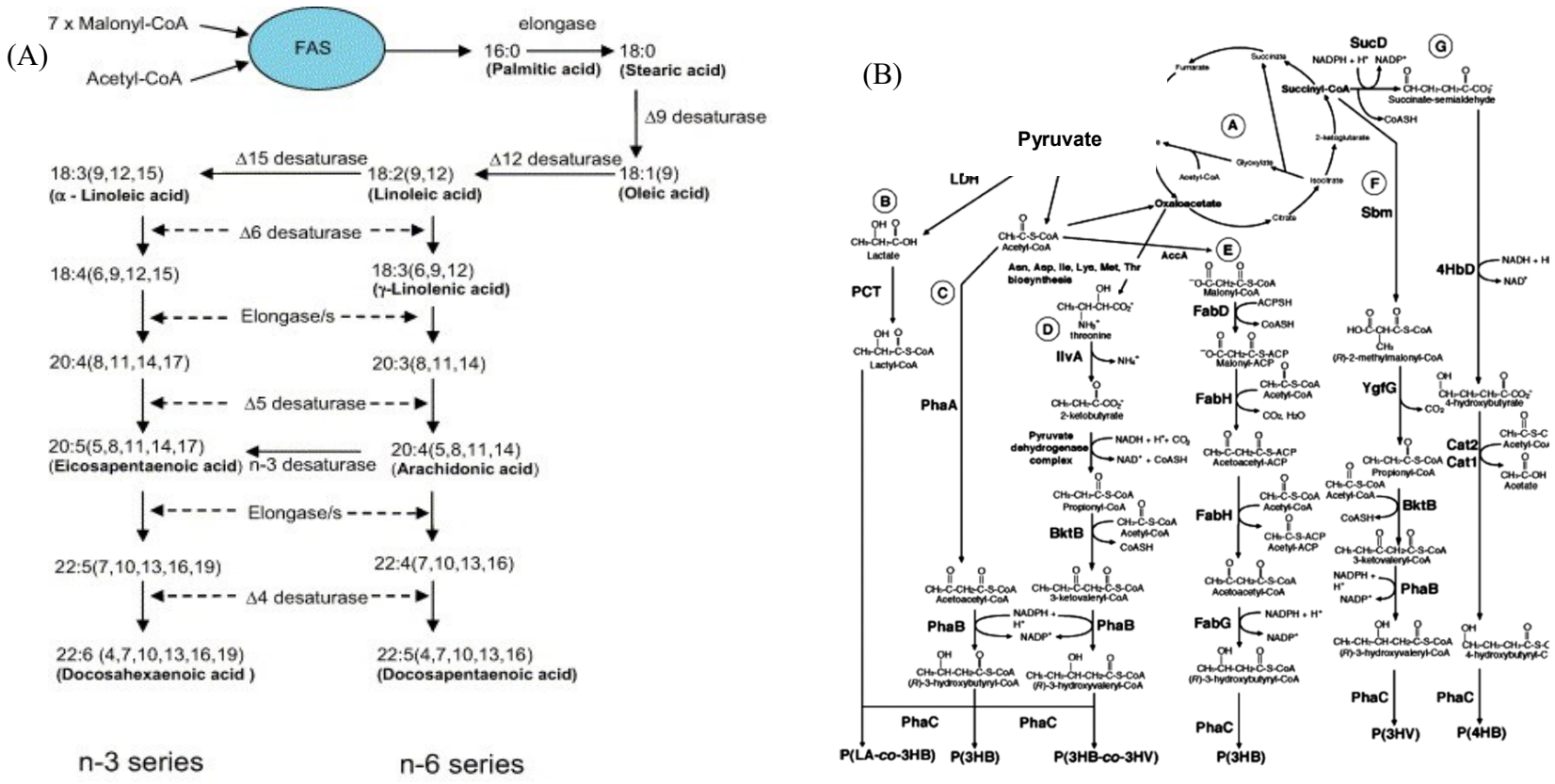

Figure 1.5 Biosynthesis pathway of microbial products

(A) Pathways of fatty acids biosynthesis, adapted from (95) under the permission of Elsevier (**Figure B.2** in **Appendix B**); (B) Pathways of PHA biosynthesis, adapted from (97) with the permission of Taylor & Francis. A. citric acid cycle; B. Synthetic pathway for the production of lactyl-CoA monomers; C. 3-hydroxybutyrl-CoA (3HB-CoA) production pathway; D. 3-hydroxyvaleryl-CoA (3HV-CoA) production pathway; E. 3HB-CoA production pathway from fatty acids biosynthesis; F. Alternative 3HV synthetic pathway; G. 4-hydroxybutyryl-CoA production pathway

Table 1.1 Bioconversion of lignin to value-added bioproducts

Product	Substrate	Microorganism	Results	Ref.
Microbial lipids	4-HBA (0.5% w/v); VanA (0.5% w/v)	*Rhodococcus opacus* DSM 1069; *R. opacus* PD630	Under nitrogen limitation, DSM 1069 accumulated fatty acids at 16.8% of dry cell weight (DCW) with 4-HBA, 8.7% with VanA within 24 h; PD630 accumulated fatty acids at 20.3% with 4-HBA, 14.6% with VanA within 48 h.	(98)
	Kraft lignin (0.5% w/v)	*R. opacus* PD 630	Laccase treatment increased lipid accumulation by 17-fold to 0.15 g/L	(68)
	Kraft lignin (6% w/v)	*R. opacus* PD 630	Laccase-HBT system significantly increased lipid accumulation to 1.02 g/L and 36.6% of DCW.	(99)
	Kraft lignin (0.75% w/v)	*R. opacus* DSM 1069	With O_2 pretreatment, the maximum lipid accumulation was 0.067 g/L and 14.21% of DCW after 36 h of growth.	(41)
	AL from CS (1% w/v)	*R. opacus* PD 630; *R. jostii* RHA1 VanA−	The co-fermentation of two strains accumulated lipid at 29% of DCW with 39.6% lignin degradation after 5 d.	(100)
	EOL from softwood (0.3% w/v)	*R. opacus* DSM 1069	The fatty acids content=0.66% of DCW and lipid yield=0.00056 g/g EOL after 9-day fermentation	(101)
	APL from CS	*R. opacus* PD 630; *R. opacus* DSM 1069; *R. jostii* DSM 44719	*R. opacus* PD 630 achieved the maximum total fatty acids at 1.3 g/L and 42.1% of DCW after 48 h; *R. jostii* DSM 44719 accumulated fatty acids at 1.05 g/L and 23.3%; *R. opacus* DSM 1069 accumulated fatty acids at 0.36 g/L and 12.6%.	(102)
	CPL from CS	*R. opacus* PD 630	Detoxification of lignin stream by heating increased lipid concentration by 2.9–9.7%; treatment by laccase and adoption of fed-batch strategy achieved the highest lipid concentration of 1.83 g/L, corresponding to 18.1% of DCW.	(103)
	4-HBAD (0.1% w/v)	*Trichosporon cutaneum*	Under fed batch mode, lipid was accumulated to 0.85 g/L and 16.6% of DCW after 480 h.	(104)

PHAs	Lignin derivatives and HBAs (2% w/v)	*Pseudomonas putida* Gpo1 and JCM 13063; *Ralstonia eutropha* H16	*R. eutropha* accumulated P(3HB) from 3-HBA and 4-HBA with a content of 65 and 63% of DCW, respectively; *P. putida* JCM 13063 Gpo1 only accumulated PHA in trace amount (less than 1%)	(81)
	Kraft lignin (1% w/v)	*P. putida* A514	With genetic and metabolic engineering strategies, the PHA content reached 73% of DCW under nitrogen starvation.	(43)
	Kraft lignin (0.5% w/v)	*Cupriavidus basilensis B-8*	The production of PHA was 128 mg/L and 17.4% of DCW after 5-day fermentation. Fed-batch fermentation improved PHA productivity to 319.4 mg/L.	(42)
	APL from CS	*P. putida* KT2440; *P. putida* mt-2; *C. necator;* *R. jostii*	The maximum PHA accumulation was 52, 60, 168 and 288 mg/L for *P. putida* KT2440, *P. putida* mt-2, *C. necator* and *R. jostii*, respectively.	(69)
	APL from CS	*P. putida* KT2440	The production of PHA was 0.252 g/L at 32% of DCW within 48-h fermentation with alkaline pretreatment liquor.	(105)
	CPL from RS	*P. putida* KT2440	After 18 h, the highest PHA content reached 19% of DCW by fermenting lignin from pretreated RS with 1% H_2SO_4 and 1% NaOH, corresponding to 0.48 g/L. Fed-batch mode further increased PHA concentration to 1 g/L	(106)
	RS	*C. basilensis* B-8	Co-pretreatment with *C. basilensis* B-8 and NaOH significantly promoted the digestibility of the rice straw by delignification. A demonstrated concentration of PHA (482.7 mg/L) was obtained from the conversion of the removed lignin.	(107)
Vanillin	Ferulic acid	*Amycolatopsis* sp. ATCC 39116	The *vdh*-deleted strain transformed ferulic acid to vanillin and the highest vanillin concentration was achieved 1.07 g/L at 18 h using fed-batch cultivation.	(108)

	APL from OPEFB	*Aspergillus niger* ATCC 6257 *P. chrysosporium*	*A, niger* ATCC 6257 converted ferulic acid in the hydrolysate to VanA with a 41% molar yield conversion; *P. chrysosporium* further converted the generated VanA to vanillin at 1.3 mg/L within 42 h, indicating a 39% molar yield conversion.	(109)
	APL from PS	*A. niger* ATCC 16404 and *P.chrysosporium* ATCC 24725	A 50% molar yield from ferulic acid released from paddy straw was achieved by *A. niger*, while only 12% molar yield from VanA to vanillin was achieved by *P.chrysosporium* generating 0.085 g/L vanillin.	(110)
	Wheat straw (2.5% w/v)	*R. jostii* RHA1	Supplemented with 0.05% glucose, the *vdh* deleted strain of *R. jostii* RHA1 accumulate vanillin to 96 mg/L after 144 h, together with smaller amount of ferulic acid and 4-HBAD.	(44)
	Coconut husk	*P. chrysosporium*	Using solid-state fermentation, the production of vanillin at 52.5 µg/g support was achieved within 24 h.	(111)
	Maize bran (10% w/v)	*A. niger* and *Pycnoporus cinnabarinus*	The sequential inoculation of *A. niger* and *P. cinnabarinus* on autoclaved maize bran produced 767 mg/L vanillin, and the supplementation of *A. niger* culture filtrate to *P. cinnabarinus* culture also achieved biotransformation of ferulic acid from maize bran to vanillin at 584 mg/L	(112)
	Sugar beet pulp	*A. niger* I-1472 and *P. chrysosporium* MUCL 39532	An optimum VanA production was obtained by *A. niger* on day 6 with 357 mg/L corresponding to a molar yield of 50%. Vanillin production by *P.chrysosporium* with VanA -rich medium from *A. niger* culture reached 105 mg/L with a molar yield of 80% after 2-day incubation.	(113)
Dicarboxylic acids	Guaiacol (0.06% w/v); HPL from pine lignin	*Amycolatopsis* sp. ATCC 39116	The mutant strain, *Amycolatopsis* sp MA-2, generated from muconate cycloisomerases gene deletion, accumulated 3.1 g/L muconic acid from guaiacol within 24 h, achieving a yield of 96%; MA-2 also produced 1.0 mM muconic acid from pine lignin hydrolysate within 10 h with a molar yield of 72%.	(45)

Benzoate	*P. putida* KT2440-JD1	The mutant strain was generated to co-metabolized benzoate to cis, cis-muconate during growth on glucose. During the fed-batch process, 18.5 g/L cis, cis-muconate was accumulated with a molar product yield of close to 100%.	(114, 115)
Vanillin (0.015%, w/v)	Engineered *Escherichia coli*	The production of muconate from vanillin was constructed with aroY from *Klebsiella pneumoniae* A170-40 and other required genes from Pseudomonas putida KT2440. The incorporation of kpdB enhanced the activity of protocatechuate decarboxylase and improved final muconic acid concentration from 0.6 mM to 0.8 mM.	(116)
Kraft lignin; Engineered tobacco	Engineered *E. coli*	Kraft lignin was chemically depolymerized into vanillin which was further converted into cis, cis-muconic acid using engineered *E. coli*. Tobacco was engineered to accumulate protocatechuate which was extracted and converted into muconic acid using engineered *E. coli*. The final concentration of muconic acid from both routes was 100~350 mg/L.	(117)
Vanillin, VanA and SYR; Extract of Kraft lignin, Japanese cedar and birch	*P.putida* PDHV85	With this transgenic strain, aromatic compounds can be converted to 2-pyrone-4,6-dicarboxylic acid at 3~208 mg, determined by initial aromatic compound loading.	(118)
Aromatic compounds; ACL-poplar treated by AHP-Cu and oxidation	*N. aromaticivorans* DSM12444	The *ligI* and *des*CD deleted strain was able to produce 2-pyrone-4,6-dicarboxylic acid from H, G or S type aromatic compounds when co-cultured with glucose; with chemically depolymerized lignin, 2-pyrone-4,6-dicarboxylic acid was accumulated to 0.49 mM with a molar yield of 59%; the fed-batch cultivation with vanillin, VanA and glucose reached a maximum concentration of 26.7 mM (4.9 g/L) after 48-h incubation.	(119)

Wheat straw (1% w/v)	*R. jostii* RHA1	The protocatechuate metabolism redesign resulted in generation of pyridine 2,4-dicarboxylic acid or pyridine 2,5-dicarboxylic acid in yield of 80~125 mg/L.	(120)

Note: 3-HBA-3-hydroxybenzoic acid; 4-HBA-4-hydroxybenzoic acid; 4-HBAD-4-hydroxybenzaldehyde; AL-alkali extracted lignin; AHP-Cu-copper alkaline hydrogen peroxidase treatment; APL-alkaline pretreatment liquor; CPL-combinational pretreatment liquor; CS-corn stover; EOL-ethanol extracted organosolv lignin; HPL-hydrothermal pretreatment liquor; OPEFB-oil palm empty fruit bunch; P(3HB)-poly(3-hydroxybutyrate); PHA- polyhydroxyalkanoates; PS-paddy straw; RS-rice straw; SYR-syringaldehyde; *vdh*-vanillin dehydrogenase gene; VanA -vanillic acid.

4. Lignin Bioconversion to Value-added Bioproducts

Even though many species of fungi and bacteria are able to degrade lignin, not all of them can produce bioproducts with potential industrial value. For instance, white rot fungi are highly efficient in lignin degradation, but they usually do not produce value-added bioproducts except for CO_2 and H_2O through mineralization. The mechanisms and pathways of lignin metabolism of fungi and bacteria have been utilized and/or manipulated to produce value-added bioproducts, such as lipids, dicarboxylic acids, PHAs, and so on (**Table 1.1**).

4.1 Microbial lipids

By means of aromatic catabolism, oleaginous species produce microbial lipids, one of the most common bioproducts of lignin bioconversion. Extensive studies have proven that *Rhodococcus* species can grow with lignin materials, including aromatic compounds, technical lignin and lignocellulose, and accumulate lipid (121). Kosa and Ragauskas (98) explored two strains of *R. opacus* DSM 1069 and *R. opacus* PD 630 on their ability to use lignin model compounds and showed that those two strains were able to grow on 4-hydroxybenzoic acid and vanillic acid at the concentration 0.5% (w/v) after a 20~30 h lag phase. Under nitrogen limiting condition (C/N ratio=10:1), triacylglycerols were accumulated to above 20% of dry cell weight (DCW). In addition to simple aromatic compounds, various isolated technical lignins have also been used as carbon sources for the fermentation of *Rhodococcus* species due to their lignin depolymerization capability. In the study of Wei et al. (41), *R. opacus* DSM 1069 exhibited poor growth when kraft lignin from black liquor was used as a substrate directly, while oxygen pretreatment of kraft lignin enhanced the degradability of lignin so that the cell mass reached 0.43 mg/mL and the maximum lipid accumulation was 14.21% (0.067 mg/mL) after 36-h incubation. Palmitic (C16:0) and stearic acid (C18:0) were identified as major components,

counting for 46.9 and 42.7% of total lipid, respectively. A decrease of lignin molecular weight and some types of linkages indicated the decomposition of lignin fragments by *R. opacus* DSM 1069, and a preference toward the removal of aliphatic-OH and G type-OH was observed as their contents decreased by 56.07 and 25.81%, respectively during fermentation (41). Cell growth and lipid accumulation have also been observed with different types of technical lignins, such as dilute alkali extracted lignin from corn stover (100) and ethanol organosolv softwood lignin (101).

Since the bacterial enzyme systems for lignin depolymerization are not as powerful as fungal enzymes, the lignin biodegradation by bacteria is usually slower, less efficient and more lignin-structure dependent. Different strategies have been developed to overcome these drawbacks. For instance, corn stover lignin in the alkaline pretreatment liquor was directly used in the fermentation of three *Rhodococcus* species (*R. opacus* PD 630, *R. opacus* DSM 1069 and *R. jostii* DSM 44719) without lignin isolation and purification (102). Those researchers found both low-molecular-weight lignin (70-300 g/mol) and solubilized glucose in pretreatment liquor served as carbon sources to support cell growth and lipid accumulation, and *R. opacus* PD 630 achieved the highest lipid yield of 1.3 g/L and cellular lipid content of 42.1% of CDW after 48-h fermentation. Liu et al. (103) used a combinational pretreatment on corn stover. In step 1, 1% sulfuric acid or liquid hot water was used, and 1% NaOH was used with or without 50% ethanol in step 2. The combinational pretreatment attacked lignin molecules with higher intensity than single pretreatment, releasing more aromatic monomers and leaving residual lignin with more vulnerable structure in pretreatment liquid stream. With lignin-rich liquid streams from different combinational pretreatments, a final lipid content of 15-25% of CDW was achieved by *R. opacus* PD 630. As a powerful ligninolytic enzyme, laccase was utilized synergistically with bacterial

lignin fermentation to improve depolymerization of kraft lignin (68, 99). With *R. opacus* PD 630 alone, only β-5 condensed phenolic OH and carboxylic OH groups were substantially degraded, and other functional groups were barely affected. Synergism with laccase caused decomposition of more lignin structures, such as aliphatic OH and guaiacyl phenolic OH groups (68). Improved degradation of lignin provided more available carbon sources and therefore increased both cell growth and lipid accumulation.

Similar to *Rhodococcus* species, some other oleaginous microorganisms were also found to have catabolic capacity of aromatics, which makes them promising candidates for lignin bioconversion to lipid. With different phenolic aldehydes being used as carbon sources, *Trichosporon cutaneum* was able to grow on 4-hydroxybenzaldehyde and accumulate lipid, while vanillin and syringaldehyde were only converted to less toxic phenolic alcohols and acids instead of lipid (104). Using fed-batch fermentation of *T. cutaneum*, those researchers increased the cell density from 2.4 to 5.1 g/L and the final lipid concentration reached 0.85 g/L compared to 0.4 g/L in batch mode (104).

4.2 PHAs

Polyhydroxyalkanoates (PHAs) are polyesters produced by microorganisms as a secondary metabolite that also serves as energy and carbon sinks responding to stress. PHAs can be used for the production of bioplastics, bring with them advantages of biodegradability, UV stability and low water permeability. In nature many kinds of microorganisms can accumulate PHA, among which *P. putida* is the most known for its lignin degradation ability. Tomizawa et al. (81) screened 11 PHA-accumulating strains on 18 kinds of lignin model compounds and identified two strains of *P. putida*, Gpo1 and JCM 13063, which were able to grow on central intermediates such as protocatechuic acid, or compounds close to central intermediates such as 4-

hydroxybenzoic acid and vanillic acid. The poor growth on other lignin compounds indicated that the funneling process, i.e. the conversion of lignin compounds to those central intermediates, was the major bottleneck in lignin compound metabolism. Using alkaline pretreatment liquor from corn stover as a substrate, Salvachúa et al. (69) demonstrated that *P. putida* KT2440 and mt-2 strains accumulated medium chain PHA while *Cupriavidus necator* produced primarily short chain PHA.

To quantify the production of PHA from lignin and improve the process efficiency, Lin et al. (43) conducted a system biology-guided biodesign for kraft lignin bioconversion by *P. putida* A514 and developed several effective strategies. They identified that that strain was utilizing a DyP-based enzymatic system for lignin depolymerization and using a variety of peripheral and central catabolism pathways to metabolize aromatic compounds. Based on those results, an effective multifunctional DyP from *Amycolatopsis* sp. 75iv2 was introduced via genetic engineering so as to improve cell growth by 2.1 fold in colony-forming unit (CFU). By overexpressing the key enzymes of aromatic compound funneling, the monomers from lignin depolymerization were used more efficiently by the engineered *P. putida* A514 while the cell grew faster and achieved higher cell mass concentration. To maximize carbon flux into PHA synthesis, the biosynthesis of fatty acids was down-regulated and the β-oxidation of fatty acids was up-regulated, which remarkably increased PHA content to 73.5% of DCW under nitrogen limitation (43).

In addition to conversion of isolated lignin, another natural strain, *C. basilensis* B-8, was employed for biological pretreatment (i.e., delignification) of rice straw (107). The combination of alkaline and bacterial pretreatment significantly promoted the digestibility of the rice straw and achieved almost complete carbohydrate conversion. Specifically, pretreatment by *C.*

basilensis B-8 further removed residual lignin in rice straw after alkaline pretreatment by consuming lignin as a carbon source for cell growth and PHA synthesis. A PHA concentration of 32.7 mg/L (6.76 % of DCW) was produced with alkaline pretreated rice straw at the solid loading of 2.88 %. The lignin-rich alkaline pretreatment liquor was also utilized for PHA production by *C. basilensis* B-8, yielding final PHA concentration of 450.0 mg/L (11.27% of DCW) (107). Liu et al. (106) employed *P. putida* KT2440 for fermentation of lignin-rich liquid stream from combinational chemical pretreatment (e.g., $NaOH+H_2SO_4$) of corn stover, achieving PHA concentration of 1.0 g/L.

4.3 Platform chemicals

In addition to microbial storage compounds, some intermediates during lignin degradation are also important platform chemicals of industrial interest. By redirecting metabolic pathways, certain chemicals can be accumulated as end-products that can serve as an alternative source to their petroleum-based counterparts.

Vanillin is the primary component of the extract of the vanilla bean and has been widely applied in flavoring agents, perfumes, cleaning products and livestock foods. It is also an important platform chemical for the production of pharmaceuticals, cosmetics and fine chemicals. The production of vanillin is mainly through chemical routes using lignosulfonate or petroleum-based guaiacol as feedstocks (122, 123). The negative environmental impact of the chemical synthesis processes have prompted the emergence of biological platforms for vanillin production with lignin as a renewable feedstock. Genetic and metabolic engineering strategies have been developed for this purpose. During lignin metabolism, vanillin can be directly released from lignin polymers through depolymerization or generated from ferulic acid transformation. Vanillin dehydrogenase can degrade vanillin and convert it into vanillic acid. It has been

reported that deletion of the vanillin dehydrogenase gene in *Amycolatopsis* sp. ACTT 39116 can achieve vanillin production from ferulic acid biotransformation (108). The absence of vanillin dehydrogenase prevented vanillin from further conversion to vanillic acid. The engineered strain grew on 2 mM ferulic acid and accumulated 6.5 mM (0.99 g/L) of vanillin after 30-h incubation, whereas in the first 15 h, the wild strain produced vanillin that was then further converted to vanillic acid (108).

With lignocellulose as feedstock, Sainsbury et al. (44) engineered another bacterial strain, *R. jostii* RHA1 by deleting the vanillin dehydrogenase gene to improve vanillin yield. When cultivated in a medium containing 2.5% wheat straw supplemented with 0.05% glucose, the modified strain accumulated vanillin up to 96 mg/L after 144 h of fermentation, along with small amounts of ferulic acid and 4-hydroxybenzaldehyde. That strain was found to secrete DyP for lignin oxidation and depolymerization. The breakdown of β-aryl ether and biphenyl components of lignin generated vanillin, and the blockage of lignin metabolism flux caused by gene deletion resulted in the accumulation of vanillin as a valuable bioproduct (44). Zuklarnain et al. (109) performed a two-step fermentation to valorize alkaline hydrolysate of oil palm empty fruit bunch (OPEFB) to vanillin, i.e., phenolic compounds in OPEFB were converted to vanillic acid in the first step by *A. niger* ATCC6257, and the produced vanillic acid was then reduced to vanillin by *P. chrysosporium* in the second step. The highest vanillin concentration reached 1.3 mg/L in 42 h of fermentation, which was equivalent to 39% molar yield based on the vanillic acid produced from the first step and 16% molar yield based on the initial phenolic compounds (primarily ferulic acid) in the alkaline hydrolysate of OPEFB (109). Different lignocellulosic biomass such as maize bran (112), paddy straw (110) and sugar beet pulp (113) have been used in a similar

two-step conversion, and the final vanillin concentration was observed to be directly related to the initial ferulic acid concentration in alkaline hydrolysate.

Muconic acid is a dicarboxylic acid mainly used for the production of bio-based polymers, including nylon, polyurethane and polyethylene terephthalate (PET) (124). Similar to vanillin, muconic acid has been conventionally produced through chemical synthesis with the utilization of corrosive catalysts. That process also generates toxic intermediates, which necessitates the development of sustainable production of bio-based muconic acid from lignocellulosic biomass (125). In biomanufacturing, muconic acid can be directly produced during the degradation of aromatic compounds, while the intermediates from glucose metabolism (e.g., 3-dehydroshikimate) can also be directed into muconic acid synthesis with genetic modification (124, 126, 127). Therefore, lignin, an aromatic-based polymer, was used as a promising feedstock for biosynthesis of muconic acid. Barton et al. (45) modified *Aspergillus* sp. ATCC 39116 by deleting two putative muconate cycloisomerases. The engineered strain was able to metabolize various lignin-based aromatic compounds and produce muconic acid and its derivatives. With guaiacol as a substrate, the final concentration of muconic acid reached 3.1 g/L within 24 h, while muconic acid of 0.26 g/L was acquired with a yield of 0.72 mol/mol aromatics in pine hydrolysate in 10 h when the guaiacol-rich lignin hydrolysate from hydrothermal pretreatment of pine was used as a substrate (45). *P. putida* KT2440 has also been modified through N-methyl-N'-nitro-N-nitrosoguanidine (NTG)-mutagenesis and exposed to 3-fluorobenzoate (3-FB), and the generated mutant was able to metabolize benzoate to muconic acid with a high specific production rate (114, 115). The biosynthesis pathway of muconic acid has also been established in *Escherichia coli* given its fast growth and high adaptability (117, 128). For example, Sonoki et al.(116) introduced a protocatechuate decarboxylase encoding

gene, *aroY*, from *Klebsiella pneumonia* A140-40 and other required genes from *P. putida* KT 2440 (e.g., *vdh* encoding vanillin dehydrogenase, *vanA* and *vanB* encoding α- and β-subunits respectively of vanillate demethylase, and *catA* encoding catechol dioxygenase) into the genome of *E. coli* so that the modified *E. coli* can produce muconic acid from vanillin. However the decarboxylation reaction of protocatechuate remained a bottleneck and rate-limiting step as stated in previous studies (127). As such, Sonoki et al. (116) further inserted a new gene, *kpdB*, and the co-expression of *aroY* and *kpdB* generated a 14-fold higher activity of protocatechuate decarboxylase than with *aroY* alone. The resultant muconic acid concentration increased by 33% compared to the original pathway (116).

Other than muconic acid, some other dicarboxylic acids can also be produced from the bioconversion of lignin. 2-pyrone-4,6-dicarboxylic acid (PDC), a novel platform chemical that can be used to produce a variety of bio-based polymers, can be synthesized by a transgenic strain of *P. putida* PDHV85 from vanillin, vanillic acid and syringaldehyde (118). Another bacterial strain, *N. aromaticivorans* DSM12444, has also been modified genetically to produce PDC from lignin-derived aromatic compounds (119). When growing on a medium that contained aromatic compounds and glucose, both substrates were consumed as glucose supported cell growth and aromatic compounds were converted into PDC. Molar yield ranging from 60 to 80% was acquired from H, G or S-type compounds. With oxidatively depolymerized poplar lignin, major aromatic compounds (e.g., vanillin, vanillic acid, 4-hydroxybenzoic acid, syringic acid, etc.) were utilized and a final PDC concentration of 0.49 mM was achieved (119). Industrial lignin sources, such as kraft lignin, lignin-rich extract of Japanese cedar and birch have also been tested as substrates for microbial fermentation so as to produce PDC (118). In the study by Mycroft et al. (120), *R. jostii* RHA1 was identified as a producer for aromatic dicarboxylic acids through re-

routing of the aromatic degradation pathway. Rather than normal ortho-cleavage to the β-ketoadipate pathway, the metabolism of protocetachuate was redesigned as meta-cleavage by gene recombination to acquire pyridine 2,4-dicarboxylic acid or pyridine 2,5-dicarboxylic acid. When the engineered *R. jostii* RHA1 grew on minimal media containing 1% wheat straw, the final yields of those two dicarboxylic acids were in the range of 80~125 mg/L. Those aromatic dicarboxylic acids are analogous to terephthalic acid which can be used for synthesis of polyester thermoplastic polymers such as PET and polybutyrate adipate terephthalate (PBAT) (129).

5. Advanced Techniques in Lignin Bioconversion Research

5.1 System analysis to investigate lignin degradation mechanisms

To illustrate the details and metabolic pathways of lignin bioconversion, system analysis involving multi-level omics analysis has been extensively applied. For relatively novel strains with limited study on lignin degradation, genomics analysis can reveal the putative genes related to lignin metabolism, the potential pathways and responsible enzymes. For example, the draft genome sequence of *Pandoraea* sp. ISTKB, a kind of β-proteobacterium isolated from soil, was obtained through the next-generation sequencing platform and was functionally annotated by Pfam. Among the 4,603 genes predicted, diverse lignin-degrading enzymes, such as DyP-type peroxidases, esterases, and dehydrogenases, were identified. Genes responsible for aromatic compound catabolism, including 4-hydroxybenzoate 3-monooxygenase, protocatechuate 3,4-dioxygenase and protocatechuate 4,5-dioxygenase, were also identified. Those results indicated the potential of *Pandoraea* sp. ISTKB to be applied in valorization of lignin and lignocellulosic biomass (130). In the kraft lignin bioconversion by *P. putida* A514, comparative genomics analysis with other 12 *P. putida* strains revealed its potential in lignin bioconversion. Its genome revealed genes encoding a broad range of oxido-reductases, enzymes required for aromatic

compound funneling and degradation, and a PHA biosynthetic gene cluster (43). Under different environmental conditions, the cluster of expressed genes would respond by exhibiting different profiles. To further confirm the gene function and understand the correlations between gene expression and environmental impacts, comprehensive analyses on transcriptome, proteome and metabolome are typically performed to capture the images of microbial metabolism under different conditions. When growing on a medium amended with lignin, an enhanced growth of the facultative anaerobe, *Enterobacter lignolyticus* SCF1 was observed compared to a medium unamended with lignin. Transcriptomics and proteomics analysis showed that enzymes involved in lignin degradation via 4-hydroxyphenylacetate degradation, NADH-quinone oxidoreductase and other electron transport chain proteins were upregulated. Those results suggested that lignin can be efficiently degraded and used as a carbon source, and its presence could also increase the energy production efficiency (131). With kraft lignin and vanillic acid as substrates respectively, Kumar et al. (132) analyzed the proteome of both conditions in detail and especially attended to proteins expressed with either kraft lignin or vanillic acid and protein differently expressed with kraft lignin and vanillic acid. Most of the differently expressed proteins were related to lignin depolymerization, and the expression of those proteins was upregulated with kraft lignin as a substrate. The detection of special enzymes on kraft lignin also indicated the presence of unusual pathways, such as 2-hydroxyhepta-2,4-diene-1,7-dioate isomerase of meta cleavage pathway. Lin et al. (43) conducted proteomics analysis during kraft lignin bioconversion by *P. putida* A514 in order to profile the expressed proteins involved in different cellular functional modules, and they identified that a DyP-based enzymatic system was employed by that strain for lignin depolymerization. The key enzymes for lignin compound degradation and fatty acids metabolism were also selected to serve as targets for further development of lignin metabolism process (43).

5.2 Synthetic biology to improve lignin bioconversion process

Considering the complexity of lignin molecules and difficulties of lignin utilization, various techniques of synthetic biology have been employed to enhance the lignin-degrading capability of microorganisms through manipulation of microbial metabolism. Such manipulation can aim at improving the efficiency and performance of naturally existing metabolic pathways through regulation on gene expression. For example, *vanAB*, the key enzyme of β-ketoadipate pathway in *P. putida* A514, was overexpressed through plasmid cloning and transformation, and the result was faster cell growth and higher final cell concentration. The enzymes for fatty acids β-oxidation (e.g., *phaJ* and *phaC*) were also overexpressed, which subsequently enhanced the degradation of fatty acids and maximized carbon flux to synthesis of target product, PHA. As a result, the PHA content was significantly elevated to more than 70% of DCW (43). In addition, genetic engineering strategies can also be exploited to edit or redesign the existing metabolic process. External, powerful enzymes can be introduced to overcome the intrinsic deficiency of microorganisms on lignin degradation and conversion. For instance, the DyP-coding gene from *Amycolatopsis* sp. 75iv2 was introduced into *P. putida* A514, which led to a remarkable increase of lignin degradation and therefore cell growth as well as PHA accumulation (43). Similarly, incorporating powerful protocatechuate decarboxylases from *Klebsiella pneumoniae* A170-40 into a reconstructed metabolic pathway significantly enhanced muconate production from lignin-derived aromatic compound in *E. coli*. Insertion or deletion of specific genes can construct distinct metabolic process and acquire new products. As an important intermediate during vanillic acid metabolism, vanillin can be obtained and accumulated as a fermentation product by deletion of vanillin dehydrogenase gene and disruption vanillinc acid metabolism in *R. jostii* RHA1 (**Figure 1.6**) (44). When growing on a medium with wheat straw, the gene-deleted strain

of *R. jostii* RHA1 was able to metabolize lignin component of wheat straw and accumulate vanillin up to 96 mg/L. The deletion of the vanillin dehydrogenase gene in *Amycolatopsis* sp. ACTT 39116 also successfully transformed ferulic acid to vanillin and achieved a final yield of 0.99 g/L [107]. Insertion of genes encoding 4,5-dioxygenase or 2,3-dioxygenease to *R. jostii* RHA1 both changed the protocatechuate metabolism from ortho-cleavage to meta-cleavage and also generated aromatic dicarboxylic acid, pyridine 2,4-dicarboxylic acid or pyridine 2,5-dicarboxylic acid respectively as valuable bioproducts. Production of certain dicarboxylic acids can be achieved by rerouting protocatechuate ring cleavage into the meta-pathway rather than the original ortho-pathway (120). Perez et al. (119) genetically modified a bacterial strain, *N. aromaticivorans* DSM12444, to enable its production of PDC from aromatic compounds. The targeted deletion of *ligI* and *desCD* disrupted the metabolism of H/G and S type aromatic compounds respectively and blocked degradation pathways. The important intermediate PDC became an end product and was accumulated consequently (**Figure 1.7**).

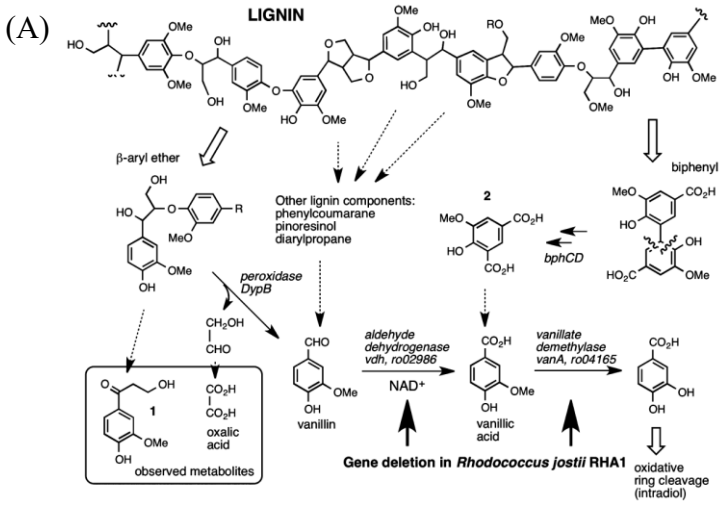

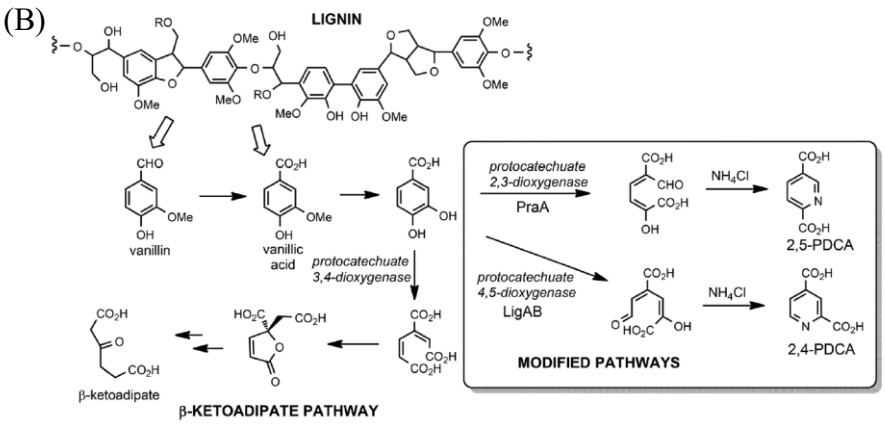

Figure 1.6 Lignin metabolism pathways in *R. jostii* RHA1

(A) Genes involved in vanillin catabolism are subjected to gene deletion, as indicated by arrows. Adapted with permission from (44). Copyright (2013) American Chemical Society (**Figure B.4** in **Appendix B**).

(B) Modified pathway for conversion of protocatechuic acid to pyridine 2,4-dicarboxylic acid (2,4-PDCA) and pyridine 2,5-dicarboxylic acid (2,5-PDCA). Adapted from (120) with the permission of Royal Society of Chemistry (**Figure B.3** in **Appendix B**).

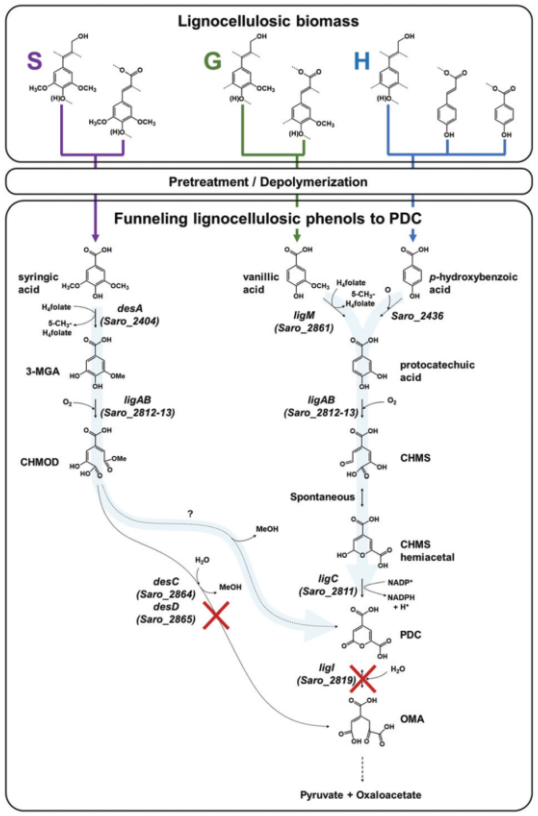

Figure 1.7 Predicted metabolic pathways of aromatic compounds in *N. aromaticivorans* DSM12444 and modification for PDC production

Target gene deletion was indicated by red X mark. 3-MGA: 3-methylgallate; CHMOD: 4-carboxy-2-hydroxy-6-methoxy-6-oxohexa-2,4-dienoate; CHMS: 4-carboxy-2-hydroxy-cis,cis-muconate-6-semialdehyde; OMA: 4-oxalomesaconate. Adapted from (119) with the permission of Royal Society of Chemistry.

Chapter 2 - A Novel Protist-based Platform for Biotransformation of Lignin to Valuable Bioproducts

1. Introduction

Lignin, one of the most abundant organic polymer on the earth, is a three-dimensional, highly branched polyphenolic molecules which can provide structural support, water transport and defense for plants (1, 133). Due to the complexity of its structure and composition, lignin is difficult to utilize and usually become part of the waste stream from the biorefinery and paper/pulping industries. However, lignin is a potentially promising feedstock for the production of biofuels and value-added chemicals and materials, and valorization of lignin would significantly improve the cost competitiveness as well as the efficiency of lignocellulosic feedstock conversion and energy utilization of biorefinery (41). Lignin can be decomposed and converted into gas, liquid oil and various types of value-added chemicals through thermochemical processes including pyrolysis, gasification, hydrogenolysis, and oxidation (47). These processes typically require harsh conditions such as high temperature (150~600 °C), high pressure, extreme pH, and chemicals (46). In addition, a variety of lignin compositions and structures results in a complex matrix of final products, making subsequent separation and utilization difficult. Bioconversion, by contrast, owns the advantages of milder reaction conditions and higher selectivity as specific metabolic pathways are involved. Currently, there are significant challenges existing in lignin utilization via biological platform due to the complexity of lignin molecules (e.g., polycyclic structure, heterogeneity of bonds and linkages, and diverse composition) (101).

In nature, several types of microorganisms have been identified to possess the ability of lignin depolymerization and degradation, including white rot fungi (e.g., *Phanerochate*

chrysosporium, *Phlebia radiate* and *Trametes versicolor*) (98) and some bacteria (e.g., *Rhodococcus opacus*, *Cupriavidus basilensis* and *Pseudomonas putida*) (1, 81). White rot fungi possess powerful enzyme systems that are able to depolymerize and degrade complex lignin structure by oxidative manners (134). They have exhibited great potential on the applications in mechanical pulping, wood surface modification, biomass pretreatment and bioremediation of aromatic pollutants (61, 135, 136). Recently, the emerging role of bacteria in lignin biodegradation and bioconversion has attracted much attention due to their excellent environmental adaptability and biochemical versatility (39). Several strains have been reported to be capable of utilizing lignin as a carbon source for growth (71, 137, 138). Moreover, some bacteria can not only depolymerize and degrade lignin but also convert the lignin-derived molecules into some value-added products. For instance, *R. opacus* can produce microbial lipids through fermentation of different lignins (41, 68). The accumulation of polyhydroxyalkanoates (PHAs) can be achieved through bioconversion of kraft lignin by *C. bailensis* (42). By screening six types of marine bacterial strains, Numata and Morisaki (139) showed that *Oceanimonas doudoroffii* was able to synthesize PHAs using lignin or lignin derivatives. They also identified the central intermediates which were sinapinic and syringic acids. Testing 11 PHA-accumulating bacterial strains on 18 lignin derivatives, Tomizawa et al. (81) found several strains that grew on lignin derivatives and synthesized PHA including *P. putida* and *Ralstonia eutropha* H16. These researchers concluded that lignin conversion into intermediates such as 4-hydroxybenzoic acid (4-HBA) and vanillic acid is the main bottleneck in the biosynthesis of PHA from lignin. As a kind of marine protist, *Thraustochytrium striatum* has been investigated for the synthesis of unsaturated long-chain fatty acids including eicosapentaenoic acid (EPA) and docosahexaenoic acid (DHA) (140-142). It also accumulates C16 and C18 fatty acids which can be utilized for

biodiesel production (143). The most distinguishing aspect is that *T. striatum* can synthesize carotenoids (e.g., astaxanthin, β-cryptoxanthin, zeaxanthin, etc.) which are valuable bioproducts with high antioxidant activity and broad applications in pharmaceutical, nutraceutical and food/feed industry (144). The capacity of *T. striatum* in simultaneous formation of various value-added products renders it a promising platform microorganism to produce bio-based products. The cultivation of *T. striatum* is usually conducted with glucose as a carbon source, while to the best of our knowledge little information is available on lignin degradation and utilization by *T. striatum*. According to Bianchi (145) and Hernes and Benner (146), lignin is one of the major terrestrially derived organic carbon sources in the coastal ocean and plays essential roles in global carbon cycling, indicating some marine microorganisms are capable of lignin decay. It is interesting to identify and understand these microorganisms about how they act to degrade and metabolize lignin and what potential products could be obtained from lignin bioconversion by these marine lignin-degrading microorganisms. Thraustochytrids are one group of marine microorganisms that are a ubiquitous component of microbial consortia in the sea, and their biomass production capability is comparable to that of bacteria (147). Due to their abundance in the marine environment, it is of intrinsic interest to investigate the applications of Thraustochytrids from the perspective of their biotechnological importance in addition to their ecological role. As such, we have been studying marine thraustochytrids (e.g., *Thraustochytrium*) including its potentials for bioconversion of lignin.

This study focused on developing a novel platform for lignin bioconversion through *T. striatum* to produce fatty acids and carotenoids. A high-biomass strain (HBS) of *T. striatum* developed in our lab was used for lignin biotransformation, with the advantages of faster growth, higher cell mass, and higher adaption to different conditions compared to the original strain.

Different types of lignin materials including lignin model compounds and technical lignins were investigated, and cell growth and product accumulation (i.e., fatty acids and carotenoids) were analyzed to evaluate the applicability of lignin as a carbon source for *T. striatum* fermentation. For lignin model compounds, fed-batch cultivation was also conducted to improve utilization of model compounds and product accumulation. For technical lignins, the potential metabolic pathway of lignin degradation was explored by identifying lignin degradation intermediates during fermentation.

2. Materials and Methods

2.1 Culture preparation

T. striatum ATCC24473 was purchased from the American Type Culture Collection (ATCC) and cultivated following the guidelines provided by the ATCC. The culture was grown in a glucose-yeast extract-peptone (GYP) medium prepared in 100% artificial seawater (ASW) at 25 °C and pH 7.0 in the dark with the agitation speed of 130 rpm, which was defined as standard conditions. The GYP medium contained 30 g/L of glucose, 6 g/L of yeast extract and 6 g/L of peptone. The ASW contained (per liter): NaCl 30 g, KCl 0.7 g, $MgCl_2 \cdot 6H_2O$ 10.8 g, $MgSO_4 \cdot 7H_2O$ 5.4 g, and $CaCl_2 \cdot 2H_2O$ 1.0 g (148). The HBS used in this study was induced by nitrogen stress which was performed in our lab. All reported cell mass in this paper is on a dry basis unless specified, otherwise. The chemicals used in this study were purchased from Fisher Scientific (PA, USA).

2.2 Fermentation of aromatic compounds

For the general screening, 15 types of aromatic compounds were selected, including 2,4-dihydroxybenzoic acid (2,4-DHBA), 3,4-dihydroxybenzoic acid (3,4-DHBA), 4-hydroxybenzoic acid (4-HBA), *p*-Coumaric acid (CMA), acetovanillone (ACE), catechol (CAT), ferulic acid

(FEA), guaiacol (GUA), p-cresol (CRE), resorcinol (RES), syringaldehyde (SYR), syringic acid (SYA), trans-cinnamic acid (TCA), vanillic acid (VAA), and vanillin (VAN). The stock solution of aromatic compounds was made by dissolving each compound in 100% ASW with the concentration of 5 g/L. NH_4Cl as the sole nitrogen source was added into each stock solution at 2 g/L. For FEA, VAA, SYA, and TCA, neutralization with 50 g/L $NaHCO_3$ was conducted first due to the low solubility of these compounds (81) and the resultant solutions were then diluted into 5 g/L. The fermentation medium for this screening study was prepared by mixing the stock solution and 100% ASW to make final concentration of each compound in the range of 0.1 to 5 g/L. The pH was maintained at 7.0 with 0.1 M Tris buffer. A positive control with glucose as a carbon source and a blank control with no carbon source were conducted simultaneously. All the media were sterilized by filtration through 0.2-μm PES membrane before inoculated with cultures prepared under standard conditions with the initial dry cell weight (DCW) concentration at around 0.6 g/L. The OD_{600} (optical density of cells at λ=600 nm) was measured daily and converted into DCW to monitor the cell growth.

After the general screening, 3,4-DHBA and 4-HBA were found to be the most digestible aromatic compounds, which were thus selected for the subsequent scale-up batch experiment by following the same conditions used in the screening experiment. Fermentation with no pH control was performed for comparison. To improve the accumulation of secondary metabolites (e.g., fatty acids and carotenoids), fed-batch cultivation was conducted with 3,4-DHBA and 4-HBA respectively whose initial concentrations were the same as batch fermentation. Cell mass and aromatic compound consumption were monitored daily, and total fatty acids (TFA) content was analyzed daily after day 4. When the concentration of aromatic compound dropped below 10% of initial value, fresh carbon source solution prepared by dissolving aromatic compound in

ASW with no nitrogen was added directly into fermentation reactors. The substrates were fed every three days for 3,4-DHBA and every two days for 4-BHA based on the changes of residual carbon source concentration until 12 days.

2.3 Simultaneous depolymerization and fermentation of technical lignins

Three types of technical lignins were used and compared in this study for fermentation of HBS, including alkali-extracted lignin from enzymatic hydrolysis residue of alkaline pretreated corn stover (AL CS) (1), organosolv (via ethanol extraction) lignin from Loblolly pine (EOL LP) and kraft pine lignin (KPL). KPL was recovered from black liquor by Sequential Liquid Lignin Recovery and Purification (SLRP) process followed by fractionation based on molecular weight via the method of Aqueous Lignin Purification with Hot acids (ALPHA) (149). The fraction with the lowest molecular weight (Mn<1,100 Da) was used as a sole carbon source. The synergy between laccase from *Agaricus bisporus* (Sigma 80498-15-3) and HBS on lignin depolymerization was studied with KPL as substrate. Different laccase loadings from 0 to 2 U/mL were used. The cultivation was conducted in 100% ASW with 1.00 g/L lignin and 0.40 g/L NH_4Cl as a nitrogen source. To monitor cell growth, samples were taken daily and lignin particles were solubilized with 0.1 M NaOH. DNA contents of samples were quantified by diphenylamine method and converted into DCW (150). Activities of three ligninolytic enzymes including lignin peroxidase (LiP), manganese peroxidase (MnP) and laccase were determined daily (151, 152). The oxidation of Azure B was carried out to evaluate LiP activity in the presence of H_2O_2. Phenol red was used as a substrate for MnP activity assay, and the absorbance at 610 nm was recorded. Laccase activity was determined by the oxidation of guaiacol, and the absorbance of product was measured at 450 nm. For LiP, one unit of enzyme activity was

defined as the amount of enzyme oxidizing 1 μmol substrate per minute. For MnP and laccase, enzyme activity was expressed as the increase of absorbance at a specific wavelength per minute.

After 7-day fermentation, the solid (mixture of cells and residual lignin) was recovered by centrifugation for characterization of products (fatty acids and carotenoids). To measure the residual lignin concentration, KPL and EOL were completely dissolved in tetrahydrofuran (THF) while ACL lignin was dissolved in 1M NaOH. After removing cell mass, lignin solution was mixed with Prussian blue reagent, and the absorbance at 700 nm was recorded (68). Lignin utilization efficiency was calculated as the following:

$$Lignin\ utilization\ efficiency = (1 - \frac{residual\ lignin\ mass}{initial\ lignin\ mass}) \times 100\%$$

2.4 Characterization of soluble lignin compounds

The consumption and conversion of aromatic compounds were analyzed by HPLC system (Agilent 1100 series) equipped with diode array detector (G1315B). Before injection, samples were filtered into HPLC vials through 0.2-μm syringe-filters. A ZORBAX Eclipse Plus C18 column (Agilent part # 959961-902) was used for separation at 30 °C. The mobile phase was mixture of acetonitrile with 0.05% formic acid and water with 0.05% formic acid at flow rate of 0.5 mL/min (**Table 2.1**).

Table 2.1 HPLC method for aromatic compounds analysis

Top: mobile phase gradient (v/v); bottom: wavelength for different compounds

Time (min)	Acetonitrile with 0.05% formic acid (%)	Water with 0.05% formic acid (%)
0.00	1.0	99.0
35.00	50.0	50.0
42.00	75.0	25.0
43.00	1.0	99.0
50.00	1.0	99.0

Compound	Wavelength (nm)
3,4-dihydroxybenzoic acid	210
Vanillic acid	225
Syringic acid	225
4-hydroxybenzoic acid	260
p-coumaric acid	325
Ferulic acid	325
Sinapic acid	325

GC-MS was used to analyze soluble compounds derived from the fermentation of technical lignins. Samples were taken from fermentation broth periodically and extracted with ethyl acetate of equal volume twice. The collected ethyl acetate layer was dried entirely with a RapidVap N_2 Dry Evaporation System (LABCONCO 7910012) at room temperature to remove the dissolved water, and the solid residue was re-dissolved in ethyl acetate. Prior to injection, the samples were derivatized with MSTFA (with 1% TMCS) at 60 °C for 45 min. The analysis was performed on Agilent 5972 GC-MS system using electron impact ionization, equipped with an Ultra 2 (5%-phenyl)-methylsiloxane column (Agilent part # 19091B-102). Helium was used as carrier gas at a constant flow rate of 1.5 mL/min. The injection volume was 1 μL with the split ratio of 20:1. The oven temperature was maintained at 80 °C for 2 min and raised to 300 °C at 10 °C/min. The mass spectrometer was operated in full scan mode.

2.5 Characterization of fermentation products

The intracellular fatty acids were first converted into fatty acid methyl esters (FAMEs) by using direct transesterification method (141) and analyzed by using GC (Shimazu GC-2010) equipped with a flame ionization detector (FID) and Rt-2560 analytical column (100 m×0.25 mm×0.2 μm). Helium was used as carrier gas with a linear flow rate of 20 cm/s, and 1 μL FAME sample was injected with a split ratio of 100:1. The oven temperature was kept at 100 °C for 5 min and then ramped to 240 °C with the rate of 4 °C/min. Supelco 37 component FAME mix

purchased from Sigma was used as the FAME standard. Pentadecane (100 μg/mL) was used as an internal standard and C13:0 (200 μg/mL) was used for recovery calculation.

DMSO was used for extraction of carotenoids (153). The freeze-dried cells were mixed with 2 mL DMSO and vortexed for 30 s in the presence of glass beads for cell disruption. The mixture was heated at 55 °C for 20 min and then centrifuged to collect the supernatant. This cycle was repeated until cell biomass became colorless. The analysis of carotenoids was also conducted on Agilent 1100 series HPLC. The mixture of acetonitrile, methanol, dichloromethane, and 1% formic acid was used as mobile phase with the flow rate of 1.5 mL/min (**Table 2.2**). The signals were recorded at λ=480 nm.

Table 2.2 HPLC mobile phase gradient (v/v) for carotenoids analysis

Time (min)	Dichloromethane (%)	Acetonitrile (%)	1% Formic acid (%)	Methanol (%)
0.00	0.0	50.0	15.0	35.0
2.00	0.0	50.0	15.0	35.0
5.00	5.0	50.0	10.0	35.0
12.00	40.0	30.0	10.0	20.0
16.00	40.0	30.0	10.0	20.0
18.00	0.0	50.0	15.0	35.0

2.6 2D ^{13}C-^{1}H HSQC and ^{31}P NMR spectroscopic analysis of lignin

To detect the alternation of lignin structure and/or composition during fermentation, the original and fermented lignin were characterized with NMR analysis at Oak Ridge National Laboratory (Oak Ridge, TN, USA). Since autoclaving as a sterilization method may also alter the structure of lignin with high temperature and pressure, autoclaved lignin without microbial fermentation was also analyzed. For HSQC analysis, the spectra were acquired on a Bruker Avance III 500-MHz spectrometer with an N_2 cryo-platform prodigy probe, and spectral processing was carried out using a Bruker Topspin 3.5 (Mac) software. About 60 mg of lignin was dissolved in 0.5 mL DMSO-d_6 in NMR tube. Heteronuclear single quantum coherence (HSQC) experiments were carried out with a Bruker pulse sequence (hsqcetgpspsi2.2) on an N_2

cryoprobe (BBO 1H&19F-5mm) with the following acquisition parameters: spectra width 12 ppm in F2 (^{1}H) dimension with 1024 data points (acquisition time 85.2 ms), 166 ppm in F1 (^{13}C) dimension with 256 increments (acquisition time 6.1 ms), a 1.0-s delay, a $^{1}J_{C–H}$ of 145 Hz, and 128 scans. The acetylation of lignin was conducted in 1 mL of 1:1 pyridine/acetic anhydride in the dark at room temperature for 24 h with magnetic stirring. The solvent/reagents were removed by co-evaporation at 45 °C with ethanol several times using a rotatory evaporator until free of acetic anhydride. The resultant acetylated lignin was dissolved in DMSO-d_6 for HSQC analysis. The central DMSO solvent peak (δ_C/δ_H at 39.5/2.49) was used for chemical shifts calibration. Assignments of non-acetylated lignin compositional subunits and inter-unit linkage were based on reported contours in HSQC spectra (149, 154). Chemical shifts of acetylated AL CS were assigned according to another publication (155). A semi-quantitative analysis of the HSQC cross-signal intensities was performed for the measurement of S, G, and side chain linkages. The $S_{2/6}$, G_2, and C_α signals were used for contour integration for S, G, and inter-unit linkages estimation.

For quantitative ^{31}P NMR, each lignin sample was phosphorylated with 2-chloro-4,4,5,5-tetramethyl-1,3,2-dioxaphospholane (TMDP) in a solvent of pyridine/$CDCl_3$ (1.6/1.0 *v/v*). In detail, 20.0 mg of lignin sample was accurately weighed into a 4-mL vial sealed with PTFE cap. A prepared stock solution of pyridine/deuterated chloroform (500 μL) including 1 mg/mL $Cr_{(acac)3}$ and 4 mg/mL internal standard (endo N-hydroxy-5-norbene-2,3-dicarboxylic acid imide) was added to dissolve lignin and 50 μL TMDP as phosphorylating reagent. Quantitative ^{31}P NMR spectra were acquired on a Bruker Avance 400 MHz spectrometer equipped with a BBO probe using an inverse-gated decoupling pulse sequence (Waltz-16), 90° pulse, 25-spulse delay with 64 scans. All chemical shifts reported are relative to the product of TMDP with water,

which has been observed to give a sharp signal in pyridine/$CDCl_3$ at 132.2 ppm. The contents of hydroxyl groups were quantitated on the basis of the amount of added internal standard.

2.7 Molecular weight analysis of lignin

The lignin samples were first acetylated with acetic anhydride in a complete homogeneous imidazolium-based ionic liquid system. In detail, 10 mg of lignin sample was added into 1 mL of $[C_4mim]^+Cl^-$ ionic liquid with magnetic stirring at 70 °C in a sand bath under the protection of nitrogen for up to 4 h until completely solvation. Acetic anhydride of 0.5 mL was injected into the solution of lignin/ionic liquid without removing the samples from the sand bath. Stirring was continued overnight to ensure the uniform acetylation. After acetylation, the homogeneous mixture solution was dropped into 100 mL deionized (DI) water, and acetylated lignin was precipitated at 4 °C overnight, centrifuged and vacuum dried at 45 °C. The average molecular weight of acetylation products was determined by using gel permeation chromatography (GPC). The products of acetylated lignin were dissolved in THF at a concentration of 1 mg/mL and fileted through 0.45-μm polytetrafluoroethylene filter before injected into GPC for molecular analysis.

2.8 Data analysis

Statistical significance was determined by analysis of variance (ANOVA, α=0.05) and Tukey's test for mean comparison using JMP Pro 12 (SAS Institute, Cary, NC, USA) with $p_{critical}$=0.05. All treatments were conducted in two replicates in this study unless specified, otherwise.

3. Results and Discussion

3.1 Fermentation of aromatic compounds

3.1.1 Aromatic compounds screening

In this study, 7 aromatic compounds including CAT, 3,4-DBHA, 4-HBA, CMA, FEA, VAA, and SYA were first screened as carbon source for the fermentation of *T. striatum* original strain. In the studied concentration range from 0.1 to 5 g/L, poor growth was observed in most cases as aromatic compounds may be inhibitory to the original strain of *T. striatum* (**Figure 2.1A**). Compared to the blank with no carbon source, growth was observed at CAT of 0.1 g/L, 4-HBA below 1 g/L, CMA below 1 g/L, and 3,4-DHBA below 2 g/L. The final cell mass concentration was around 1.0 g/L, slightly higher than 0.8 g/L from the blank, indicating the limited utilization of aromatic compounds as carbon source. The HBS was previously induced from the original strain by nitrogen stress to achieve high cell mass concentration and superior ability to adapt to adverse environmental conditions. Therefore, the HBS was also studied in the aromatic compound screening. With 3,4-DHBA at 5 g/L, the final cell mass concentration of HBS reached 2.25 g/L which was comparable with glucose as a carbon source (2.26 g/L). The cell mass concentration with 2 g/L of 4-HBA also reached a decent level of 1.89 g/L. When CAT and SYA were used, HBS was able to tolerate up to 5 g/L and grow while for FEA and VAA the upper limit concentration was 2 g/L. Based on these results, 8 more kinds of lignin model compounds were further tested and the results were summarized as a heat map (**Figure 2.1B**). A preference of HBS towards acidic compounds was observed as it was able to grow with 3,4-DHBA, 4-HBA, CMA, SYA, FEA, VAA, and TCA at most studied concentrations, with an exception of 2,4-DHBA. As for other aromatic compounds (e.g., VAN, RES, SYR, ACE, and CRE), the HBS had only slight growth at low substrate concentrations (<0.5 g/L). For most aromatic compounds, high concentration appeared to be inhibitory for cell growth, while higher concentrations of 3,4-DHBA, 4-HBA, and catechol (CAT) supported more cells. Two substrates

with best cell growth, 3,4-DHBA of 5 g/L and 4-HBA of 2 g/L, were selected for further investigation.

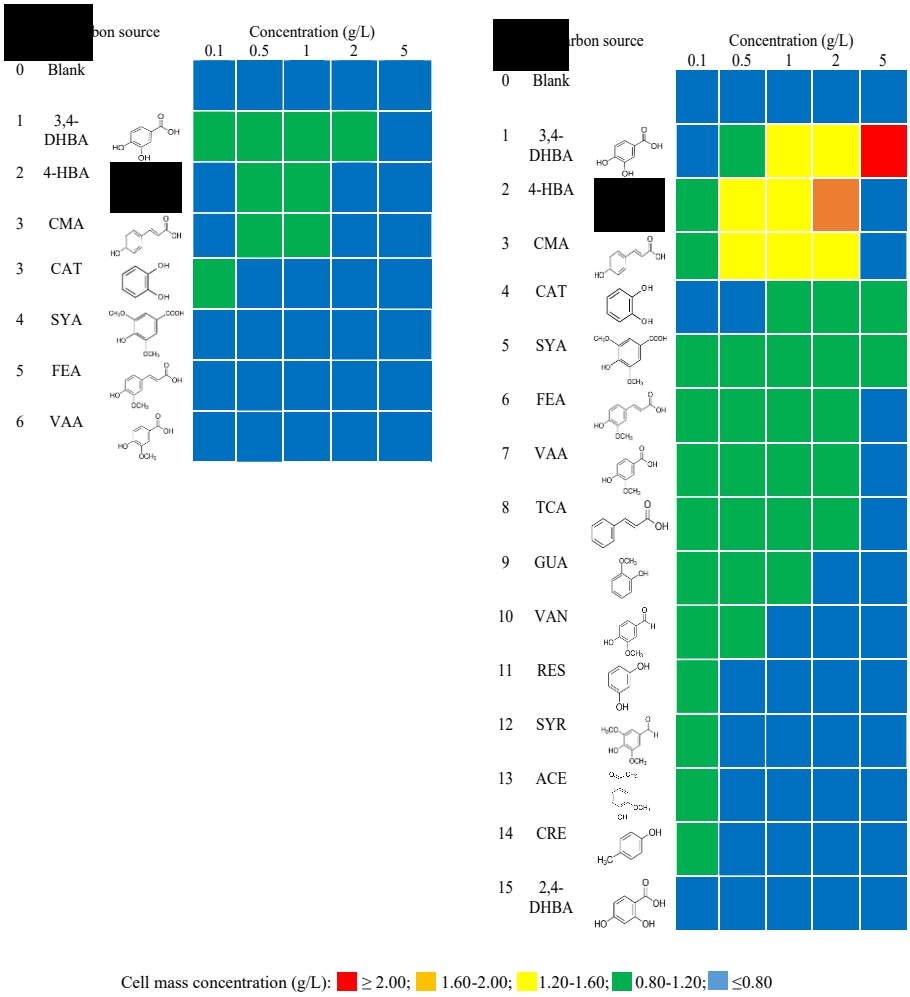

Figure 2.1 Cell mass growth with aromatic compounds at different concentrations
(A) Screening of *T. striatum* ATCC 24473 original strain; (B) Screening of *T. striatum* ATCC 24473 HBS. Aromatic compounds: (1) 3, 4-dihydroxybenzoic acid (3,4-DHBA); (2) 4-hydroxybenzoic acid (4-HBA); (3) p-Coumaric acid (CMA); (4) Catechol (CAT); (5) Syringic acid (SYA); (6) Ferulic acid (FEA); (7) Vanillic acid (VAA); (8) trans-Cinnamic acid (TCA); (9) Guaiacol (GUA); (10) Vanillin (VAN); (11) Resorcinol (RES); (12) Syringaldehyde (SYR); (13) Acetovanillone (ACE); (14) p-Cresol (CRE); (15) 2, 4-dihydroxybenzoic acid (2,4-DHBA)

3.1.2 Process analysis of aromatic compound fermentation

The fermentation of 3,4-DBHA and 4-HBA was studied in detail regarding cell growth, substrate consumption and accumulation of products. The cell growth was fast in the first two days and then leveled off after the third day, even decreased when 4-HBA was used as carbon

source. The maximum cell mass concentration reached 1.87 and 1.61 g/L for 3,4-DHBA and 4-HBA, respectively (**Figure 2.2A**). Both carbon sources were quickly utilized, i.e., 4-HBA was utterly consumed, and the concentration of 3,4-DHBA dropped to around 1 g/L after 3-day cultivation (**Figure 2.2A**). Such substrate depletion could be the reason resulting in the level-off of cell growth. *T. striatum* can synthesize both fatty acids and carotenoids when growing with aromatic compounds. The TFA content of 13% was achieved with 3,4-DHBA compared to 7% with 4-HBA (**Figure 2.2B**). The major types of fatty acids accumulated in *T. striatum* were C16 and C18, including palmitic acid (C16:0), oleic acid (C18:1) and linoleic acid (C18:2) while more species of fatty acids were synthesized with 3,4-DHBA such as heneicosanoic acid (C21:0), docosapentaenoic acid (C22:5) and lignoceric acid (C24:0). A similar level of carotenoids production was observed for both 3,4-DHBA and 4-HBA, which was about 0.1 mg/g DCW (**Figure 2.2B**). As secondary metabolites not associated with cell growth, the remarkable production and accumulation of fatty acids and carotenoids typically happened at stationary phase, which started at the 6^{th} day of cultivation for this strain. However, most carbon source has been consumed by cell mass growth and synthesis of cellular components (e.g., protein and carbohydrate) during the previous exponential phase and not much extra carbon source was still available at this time. That was possibly an essential reason for the relatively poor performance on product accumulation. Carbon flux analysis with ^{13}C labeled aromatic compounds as substrates or analysis of full metabolite flow could be a feasible strategy to illustrate this process with more details and will be conducted in the future. Fermentation with no pH control was also performed for comparison using 3,4-DHBA and 4-HBA as carbon source respectively (**Figure 2.3**). With no pH control, the solution of 3,4-DHBA and 4-HBA had initial pH as low as 3, while no significant inhibition on cell growth and product accumulation was observed. That suggested

the strong adaption of the HBS to acidic conditions and pH was therefore not controlled in the subsequent study for process simplification.

With known structure, simple aromatic compounds have been widely used to study lignin degradation pathway. In the study of Kosa and Ragauskas (98), two strains of *R. opacus*, DSM 1069 and PD630 were shown to grow with 4-HBA or VAA at 5 g/L. The growth cycle of *R. opacus* was short. A decent amount of triacylglycerols (TGA) was accumulated (15~20 % of DCW) after only 12 h. By using *p*-coumaric acid or FEA at 2 g/L, *P. putida* KT2440 was able to produce medium chain-length PHA at a comparable level with glucose (34~39% of DCW) (105). Tomizawa et al. (81) cultured 11 PHA-accumulating bacteria strains in media containing each of 18 lignin derivatives and hydroxybenzoic acids. The results showed that these strains mostly preferred 4-HBA and 3,4-HBA, and some strains were also able to grow on VAA, FEA, *p*-coumaric, and 2,5-DHBA. Among all strains, only *R. eutropha* H16 could synthesize short-chain poly-3-hydroxybutyrate (P3HB) from various hydroxybenzoic acids at a satisfactory level (65% of DCW). The authors also proposed that the conversion of lignin compounds into intermediates such as 4-HBA and 3,4-DHBA represent the major bottleneck in the synthesis of PHA (81). For lignin-derived compounds, the typical aromatic structure renders them high chemical stability and resistance to biological attack. The classic strategy of aromatic compounds degradation is well-known as the β-ketoadipate pathway. It starts from the conversion of general aromatic compounds into central intermediates such as 3,4-DHBA, 4-HBA or catechol, which is also termed as "funneling pathways" (156). Those central intermediates then undergo a ring opening process catalyzed by ring-cleaving dioxygenases and are finally catabolized (89). For the HBS in our study, the decent growth on most compounds also indicated the conversion into central intermediates might be the limiting step of lignin compound degradation.

In fed-batch cultivation, a fresh carbon source was added for the first time on the 3rd day. Subsequent feeding was conducted every three days for 3,4-DHBA and every two days for 4-HBA according to the consumption progress of substrates. The cell mass concentration reached the maximum on the 6th day and after that further growth was barely observed (**Figure 2.2C**). The subsequent consumption of substrate was mainly related to the synthesis of products. Significant improvements on TFA contents were achieved for both 3,4-DHBA and 4-HBA, from 12% and 7% on the 4th day to 22% and 14% after 12-day incubation, respectively. With 3,4-DHBA, the production of carotenoids was observed to increase gradually during the fed-batch process, from around 0.1 to 0.27 mg/g DCW, while no significant improvement exhibited with 4-HBA (**Figure 2.2D**). That is possible because the used concentration of 4-HBA was low given the tolerance of *T. striatum*, and the available carbon source cannot support the synthesis of more products. Fed-batch cultivation is an efficient strategy for processes aiming at secondary product accumulation. Its principle is to stimulate cell growth and product synthesis by varying C/N ratio (typically increasing the ratio), creating a "nitrogen starvation" condition. It has been widely applied in algae cultivation for lipid production, such as *Nannochloropsis* sp. (157), *Cheatoceros* sp. (158) and *Chlorella protothecoides* (159). The lipid content was observed to increase by around 10~20%. In this study, the availability of carbon source is the major limitation as suggested previously. The adoption of fed-batch mode provided more carbon source and increased carbon source availability for the synthesis of products, resulting in doubled TFA content for both substrates and almost tripled carotenoids content for 3,4-DHBA. As long as it is enough for basic requirements of growth and maintenance, the concentration of nitrogen source only seemed to play a minor role in product accumulation in this case.

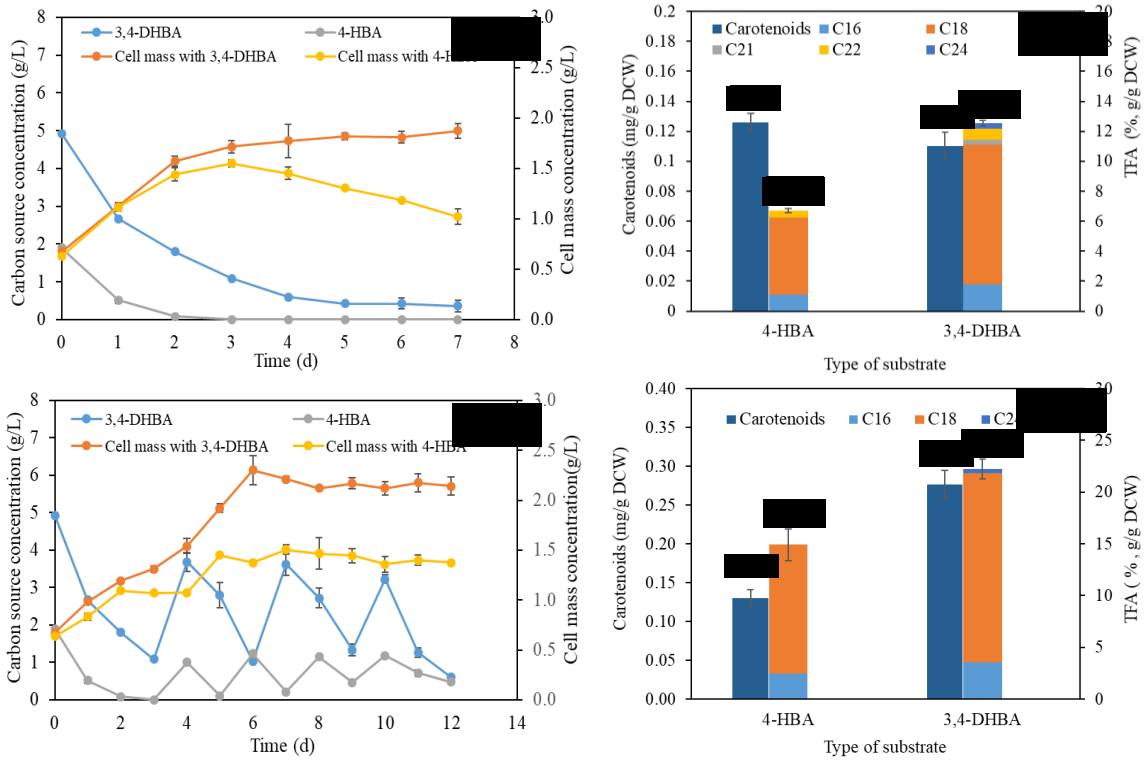

Figure 2.2 Fermentation with 3,4-DHBA (5 g/L) and 4-HBA (2 g/L)

(A)(B) Batch mode; (C)(D) Fed-batch mode; (A)(C) Cell mass growth and substrate consumption; and (B)(D) Accumulation of TFA and carotenoids. Lowercase letters and Roman numerals indicate statistical analysis results. Levels connecting with different letters/numerals are statistically different.

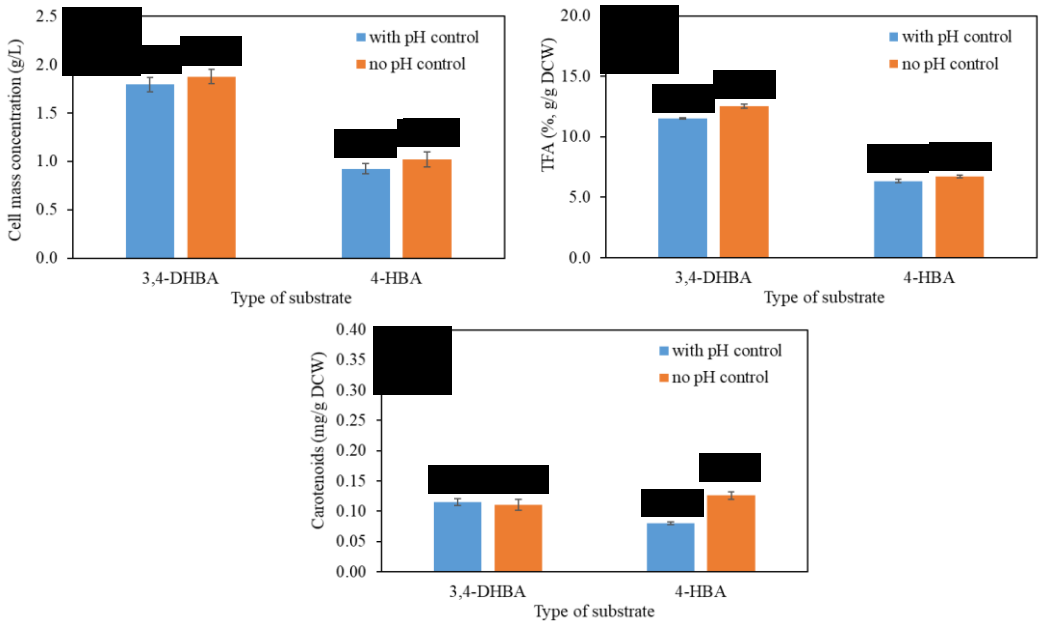

Figure 2.3 Fermentation of 3,4-DHBA and 4-HBA with/without pH control

(A) cell mass growth; (B) TFA content; (C) total carotenoids content. Lowercase letters indicates statistical analysis results. Levels connecting with different letters are statistically different.

3.2 Simultaneous depolymerization and fermentation of technical lignins

3.2.1 Cell growth and product accumulation

To further investigate the lignin-degradation ability of the HBS, three types of technical lignin, AL CS, EOL LP and KPL, were used as carbon sources respectively for fermentation. The cell growth was similar among three types of lignin, from around 0.5 to 1.3 g/L (**Figure 2.4A**). The most interesting result was about the formation of products. Fermentation of EOL LP achieved the highest carotenoids yield which was about twice of that from the fermentation of AL CS and KPL, while fermentation of AL CS generated significantly higher TFA yield, followed by KPL and EOL LP in that order (**Figure 2.4B**). The accumulation of different products is determined by the distribution of carbon source among various microbial metabolic processes, which is highly related to the features of the carbon source. The three types of lignins were acquired through different processes (organosolv and alkali extraction) from different species (corn stover and pine). Both isolation methods and biomass sources would affect molecular weight, composition, and structure of lignin samples, and subsequently affect their biodegradation. Alkali-extracted lignin was reported to be more reactive and dominant by liable β-*O*-4' linkage, while ethanol extracted lignin usually presented higher molecular weight (1). In addition, the lignin of herbaceous origin is easier to degrade, while softwood lignin (e.g., pine) is the most resistant due to the presence of stable guaiacyl units (1). Therefore, a slightly higher utilization efficiency was observed for AL CS as well as a higher concentration of TFA. Meanwhile, the degradation of pine lignin possibly generated more reactive oxidative substances (e.g., hydroxyl radicals) which would result in more oxidative stress, leading to the synthesis of more carotenoids as antioxidants for self-protection (141, 160). The correlation between the type of lignin and final products still requires further investigation.

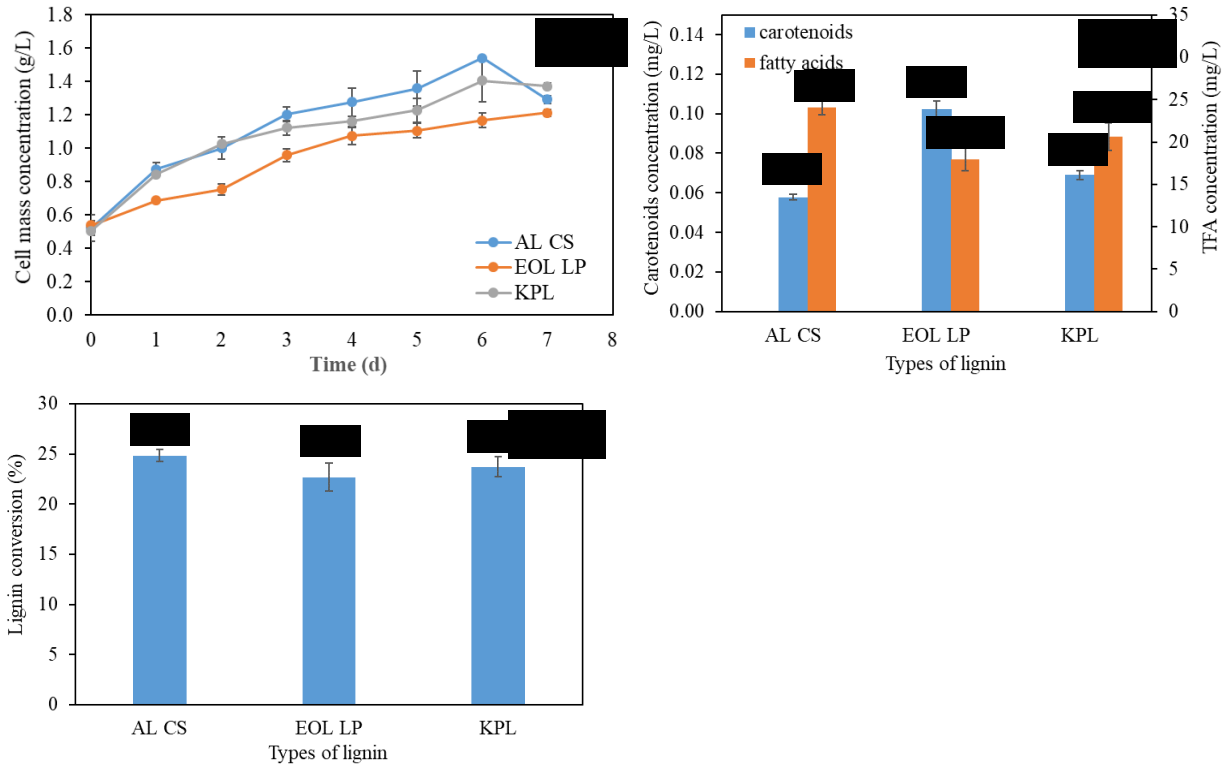

Figure 2.4 Fermentation of different types of lignin
(A) Cell mass growth; (B) Final concentrations of TFA and carotenoids in fermentation broth; (C) Total lignin conversion. Lowercase letters and Roman numerals indicate statistical analysis results. Levels connecting with different letters/numerals are statistically different.

3.2.2 Lignin utilization and modification

Upon the completion of fermentation, about 22~24% of lignin was utilized (**Figure 2.4C**), which was relatively low compared to other studies (1, 68). According to 2D-HSQC NMR analysis (**Figures 2.5A-C**), microbial fermentation did not cause significant change on lignin inter-unit linkages, for example, EOL had 3% β-5,' and 1% β-β' linkages; KPL had 0.5% β-5' and 1.4% β-β' linkages; and ACL had β-*O*-4’ linkages, which is comparable to the structure of the original lignin used. This minimal variation of lignin structure before and after fermentation may suggest the possibility that the depolymerization by the HBS on lignin polymers had no preference toward specific lignin structure or linkages. The two types of alkali lignin, KPL, and AL CS experienced a significant loss of liable β-*O*-4’ linkages during

autoclave, and simultaneously the molecular weight of AL CS remarkably dropped to one-tenth of the original value, indicating effective destruction on the network of lignin molecules. However, the molecular weight for KPL and EOL was observed to increase (**Table 2.3**), as softwood lignin (e.g., pine lignin) has higher recalcitrance toward external destruction and possibly only low-molecular-weight parts were dissolved. That was also supported by the fact that the β-β' and β-5' linkages commonly seen in the two pine lignins were not affected much. Continuing microbial fermentation further increased the molecular weight of EOL as those of lower molecular weight lignins were readily consumed by microbes so that the higher-molecular recalcitrant parts were left. On the contrary, the fermentation process caused reduction of molecular weight of KPL. The possible reason behind that was the higher reactivity of alkali lignin, which would lead to more breakdown of linkages and depolymerization.

The contents of different types of hydroxyl groups were analyzed by quantitative ^{31}P NMR (**Figure 2.5D**). Aliphatic and guaiacyl OH were observed to be the most abundant hydroxyl groups, especially in two pine lignins, EOL and KPL. Autoclave caused remarkable loss of all types of hydroxyl groups, while only slight further decrease of hydroxyl group contents was observed by subsequent microbial fermentation. For EOL the contents of all hydroxyl groups decreased to some extents after fermentation, with the most significant reduction as C5 substituted OH from 0.12 to 0.04 mmol/g. For KPL only the content of aliphatic and guaiacyl OH decreased. For AL CS the content of aliphatic OH was observed to increase compared to autoclave only, possibly due to deconstruction of other structures of lignin and leaving aliphatic OH less degraded.

Table 2.3 Relative abundances of S, G, H units, side chain linkages over total S+G+H and molecular weight of different lignins.

	S%	G%	S/G	β-*O*-4'%	β-5'%	β-β'%	M_w	M_n	M_w/M_n
EOL	0	0	0				4182	1425	2.94
EOL-a	0	100	0	ND	2.7	1.0	12388	1510	8.20
EOL-af	0	100	0	ND	2.9	1.1	15136	2191	6.90
KPL	0	100	0	2.9	0.6	1.1	2991	1307	2.29
KPL-a	0	100	0	0.3	0.7	1.2	8273	1425	5.81
KPL-af	0	100	0	0.3	0.5	1.4	4003	1201	3.34
ac-ACL	63.6	36.4	1.75	32.3	ND	ND	10399	2429	2.21
ac-ACL-a	59.9	40.1	1.50	3.6	ND	ND	1092	492	2.22
ac-ACL-af	61.2	38.8	1.58	30.3	ND	ND	1944	661	2.94

Note: a-lignin with autoclave; af-lignin with autoclave and microbial fermentation; AL CS-alkali lignin from corn stover; KPL-Kraft pine lignin; EOL-ethanol extracted lignin from loblolly pine; ND-not detected. M_w-weight-average molecular weight (g/mol); M_n-number-average molecular weight (g/mol); M_w/M_n-polydispersity. Side chain linkages percentage is based on total S+G+H of lignin.

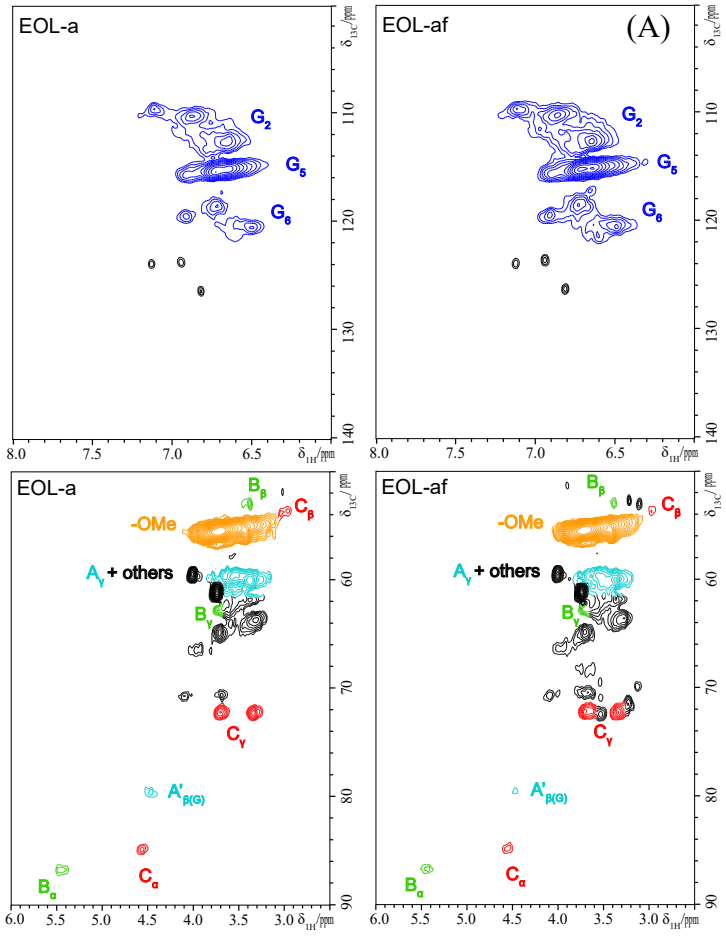

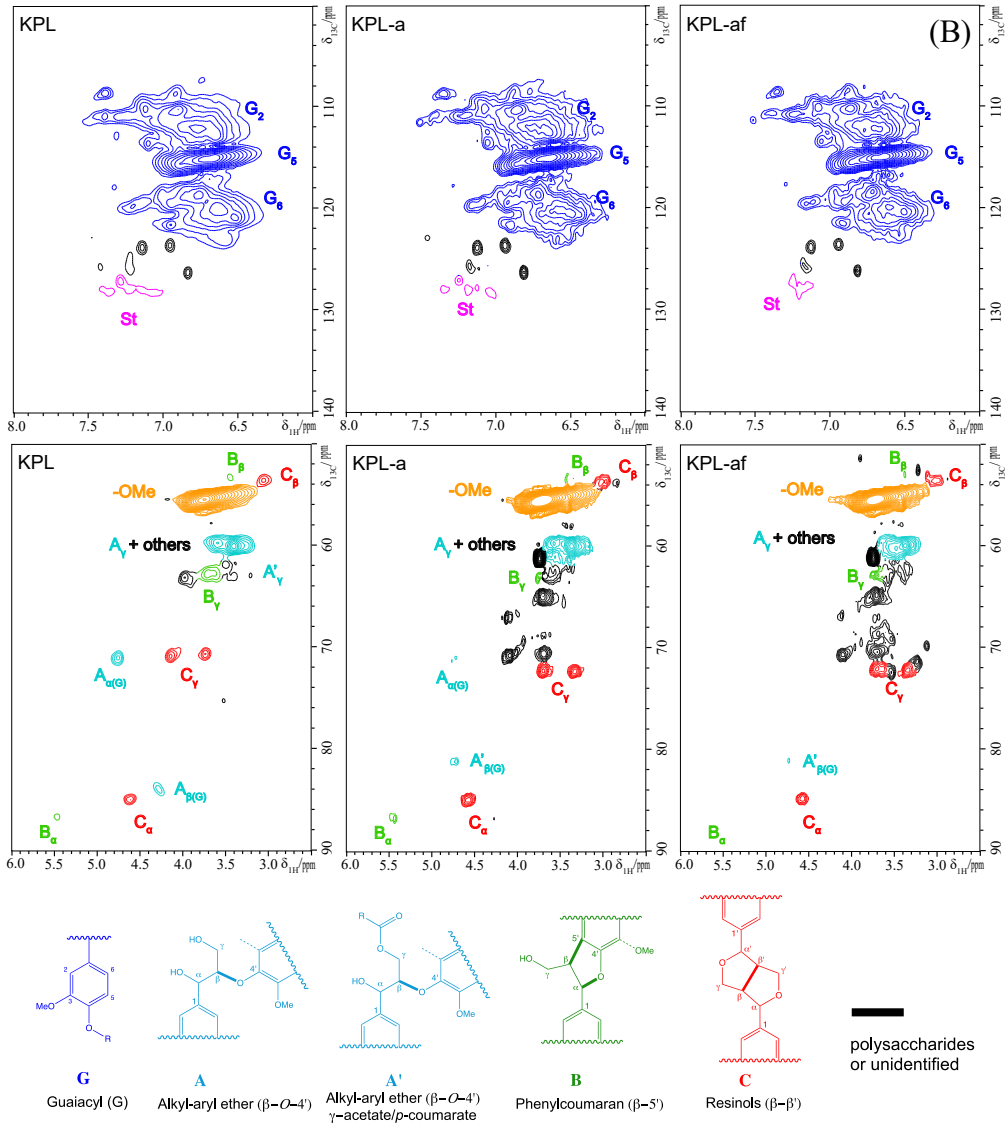
KPL
KPL-a
KPL-af
(B)
G2
G5
G6
St
-OMe
Aγ + others
A'γ
Bγ
Aα(G)
Cγ
Aβ(G)
Cα
Bβ
Cβ
Bα
A'β(G)
δ13C/ppm
δ1H/ppm
G
Guaiacyl (G)
A
Alkyl-aryl ether (β–O–4')
A'
Alkyl-aryl ether (β–O–4')
γ–acetate/p-coumarate
B
Phenylcoumaran (β–5')
C
Resinols (β–β')
polysaccharides
or unidentified

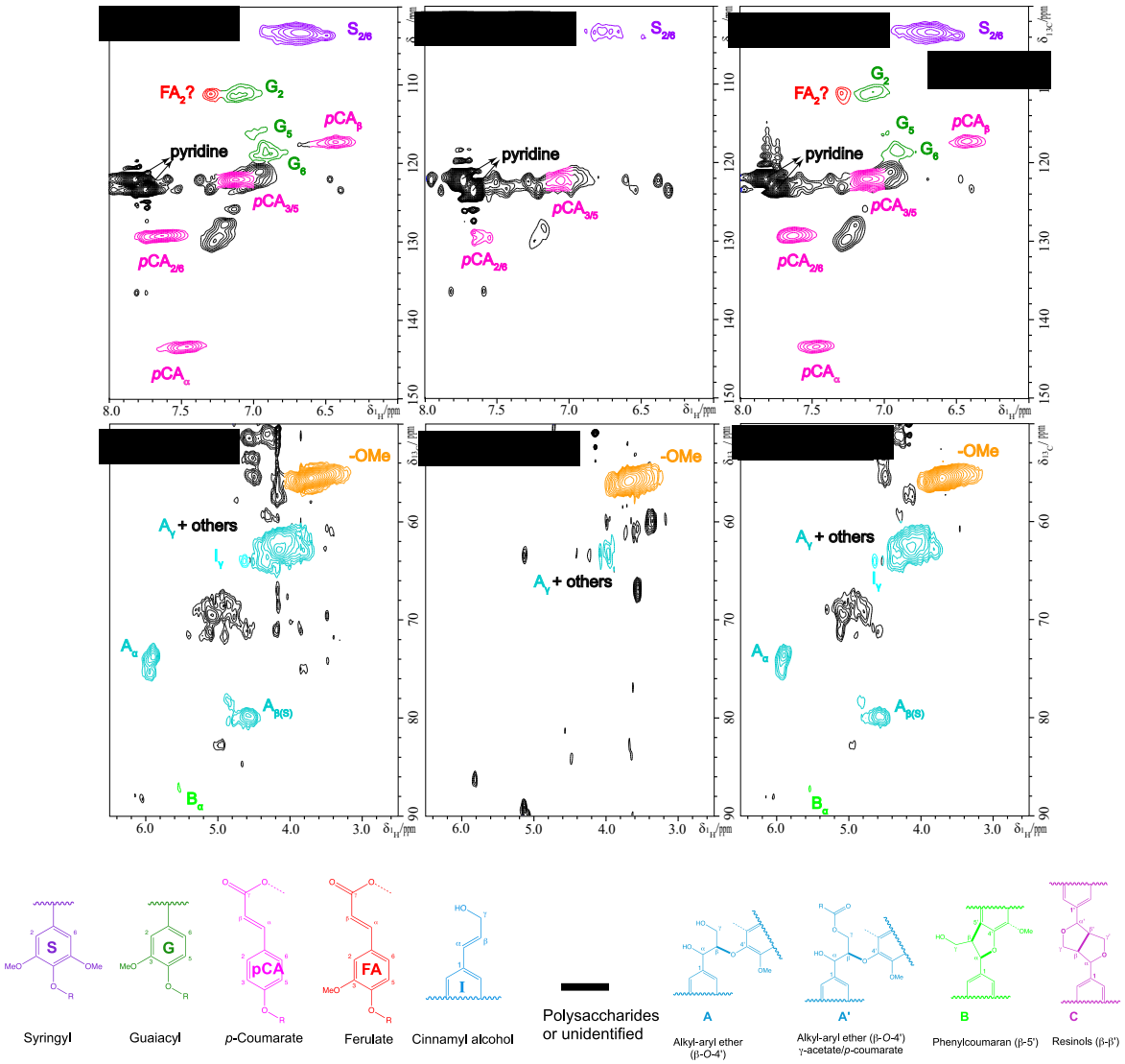
S2/6
FA2?
G2
G5
G6
pCAβ
pyridine
pCA3/5
pCA2/6
pCAα
-OMe
Aγ + others
Iγ
Aα
Aβ(S)
Bα
δH/ppm
δC/ppm
Syringyl
Guaiacyl
p-Coumarate
Ferulate
Cinnamyl alcohol
Polysaccharides or unidentified
A
Alkyl-aryl ether (β-O-4')
A'
Alkyl-aryl ether (β-O-4') γ-acetate/p-coumarate
B
Phenylcoumaran (β-5')
C
Resinols (β-β')

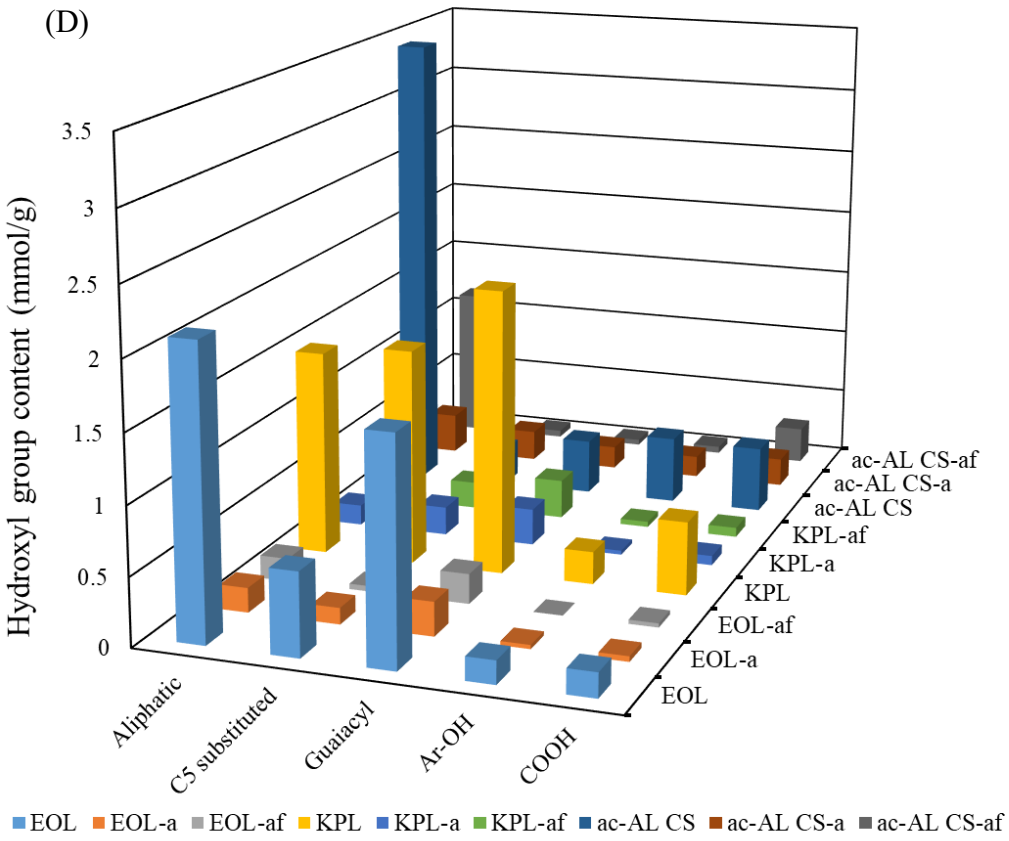

Figure 2.5 NMR analysis of lignin before and after HBS fermentation
(A)-(C) 2D ^{13}C-^{1}H HSQC analysis; (D) Hydroxyl group contents (millimole/gram) in lignin samples determined by ^{31}P NMR analysis. Ar-OH: *p*-hydroxyphenyl and other phenolic OH. COOH: carboxyl OH.
(A) EOL: aromatic (δ_C/δ_H 100-140/6.0-8.0 top) and aliphatic (δ_C/δ_H 50-90/2.5-6.0 bottom) regions. EOL NMR analysis was conducted in previous study (149); EOL-a: ethanol extracted lignin from loblolly pine with autoclave; EOL-af: ethanol extracted lignin from loblolly pine with autoclave and fermentation;
(B) KPL: aromatic (δ_C/δ_H 100-140/6.0-8.0 top) and aliphatic (δ_C/δ_H 50-90/2.5-6.0 bottom) regions. KPL-a: Kraft pine lignin with autoclave; KPL-af: Kraft pine lignin with autoclave and fermentation;
(C) AL CS: aromatic (δ_C/δ_H 100-150/6.0-8.0 top) and aliphatic (δ_C/δ_H 50-90/2.5-6.0 bottom) regions (ac-acetylated). AL CS-a: alkali lignin from corn stover with autoclave; AL CS-af: alkali lignin from corn stover with autoclave and fermentation.

3.2.3 Extracellular enzyme activity

Among the three ligninolytic enzymes evaluated, only LiP and MnP activities were detected with a relatively weak activity (**Figure 2.6**). Both of which explained the relatively poor cell growth. The change of LiP activity during fermentation process followed a similar pattern for all three types of lignins. From the 1st day, the LiP activity kept increasing, reaching the peak

value of 0.75 U/mL on the 3rd day, and then decreased gradually. Fermentation with AL CS exhibited a slightly stronger MnP activity, and its maximum value was observed on the 4th day (0.52 U/mL), while the highest MnP activity was shown on the third day for two pine lignins (around 0.4 U/mL). After that, the MnP activity declined rapidly and was hardly detected after the 6th day. Laccase was not detected among the entire fermentation process. In nature, both LiP and MnP are powerful enzymes for breakdown of recalcitrant lignin polymers, while their function requires the presence of H_2O_2 (151). The H_2O_2-generation mechanism during fermentation of this strain to support normal actions of LiP and MnP remains unknown, while it is a promising direction in the future as it may indicate the existence of novel enzymes involved in lignin degradation. In addition, since the lignin depolymerization of this strain was highly possibly peroxidase-mediated, providing more electron acceptors such as external H_2O_2 and molecular oxygen is also a feasible strategy to improve the depolymerization process.

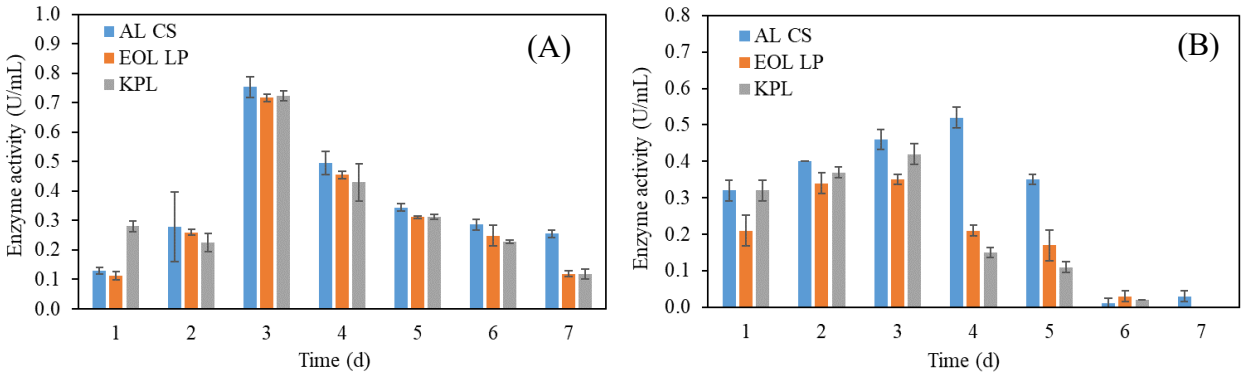

Figure 2.6 Extracellular enzymes activities during fermentation of technical lignins
(A) LiP; (B) MnP.

3.2.4 Release of soluble aromatic compounds

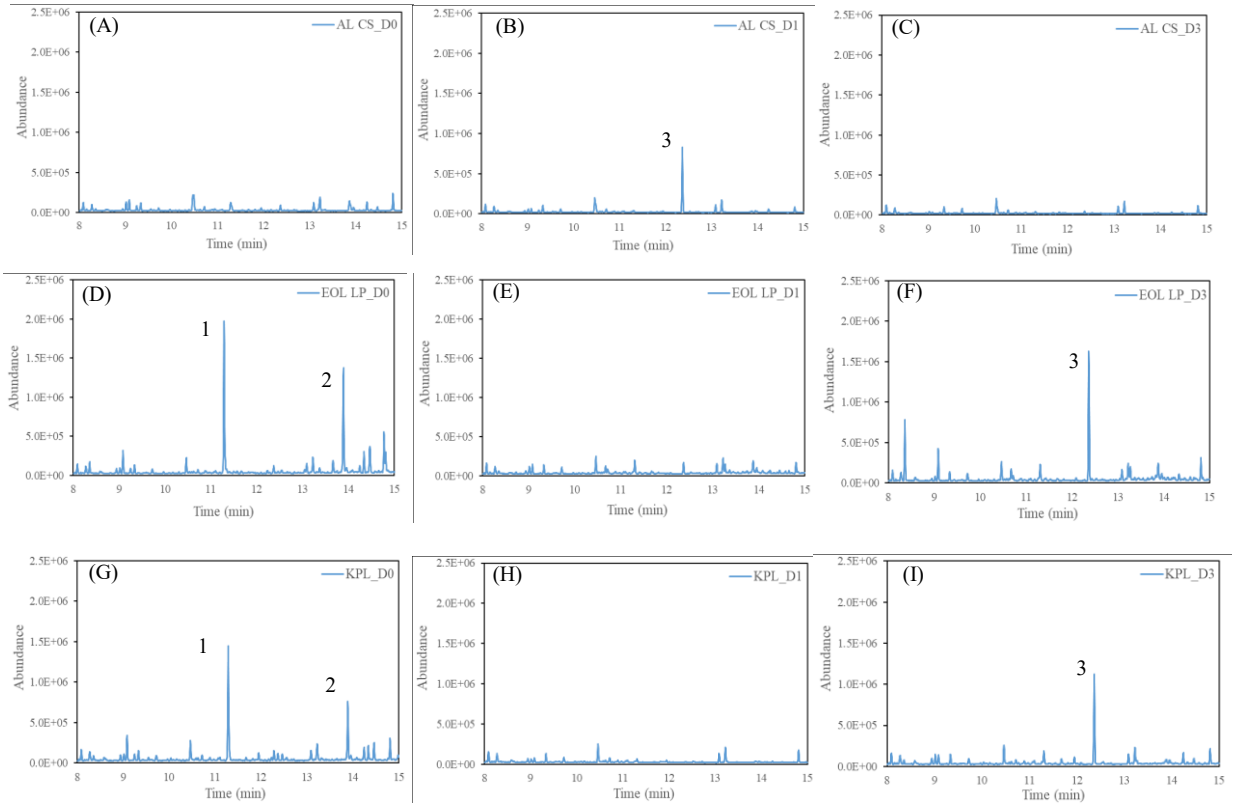

Figure 2.7 Major aromatic compounds produced during technical lignin fermentation
(A)-(C) Fermentation of AL CS; (D)-(F) Fermentation of EOL LP; (G)-(I) Fermentation of KPL. Peak 1: vanillin; peak 2: vanillic acid; peak 3: 4-hydroxybenzoic acid.

During fermentation, only a few aromatic compounds were identified through GC-MS analysis (**Figure 2.7**). The compounds present at the beginning of fermentation for the two pine lignins were believed to be released during autoclave sterilization, and only 4-HBA was detected as intermediates. The concentration of 4-HBA experienced an increase followed by gradual decrease. For AL CS, the maximum concentration of 4-HBA appeared on the 1st day while on the 3rd day for KPL and EOL due to the relatively lower recalcitrance of AL CS and therefore fast degradation of herbaceous lignin from alkali extraction process. The GC-MS results are also consistent with the change of enzyme activity. Supported by relatively higher enzyme activities during the first three days, lignin polymers were depolymerized, and the generated mono

compounds were converted into 4-HBA, resulting in significant accumulation of 4-HBA. After that enzyme activities of both LiP and MnP decreased gradually, suggesting the growth and maintenance of microorganism mainly dependent on the utilization of accumulated 4-HBA. This phenomenon suggested two possibilities. The first was that 4-HBA is a critical central intermediate during the degradation of these three types of lignin. The HBS firstly catalyzed lignin depolymerization and generated smaller fragments by the breakdown of specific linkages. Those depolymerization products were further degraded and converted into 4-HBA, which underwent ring cleavage and were used for anabolism. Since a significant accumulation was observed, the utilization of 4-HBA appeared to be the rate-limiting step. However, another possibility also holds that this HBS depolymerized lignin at specific sites and only released 4-HBA. The enzymes may only be able to function at H-type unit which has no methoxy substitute group on the aromatic ring and is much less than S or G unit and produce 4-HBA. The limited active sites of enzyme resulted in poor lignin utilization and low availability. Consequently, the cell growth and accumulation of products were low. To confirm which possibility is correct, the extracellular enzymes need to be analyzed through proteomics method to figure out the mechanism of lignin depolymerization of this strain.

3.2.5 Synergistic lignin depolymerization between laccase and HBS

Laccase is an important type of ligninolytic enzyme which is able to generate radicals under aerobic condition and depolymerize lignin macromolecules to smaller fragments (68). The self-sufficient system distinguishes laccase-based lignin depolymerization from other processes and has been widely studied on lignin biodegradation (161-164). In this study, laccase was applied with different loadings to fermentation with KPL to aid the depolymerization process. As shown in **Figure 2.8A**, the cell growth curves of all treatments followed a similar pattern with no

remarkable difference. Cell growth was observed even without the presence of laccase, suggesting that this strain can degrade lignin polymers in nature, although the ability is relatively weak compared to other species known to degrade lignin. Elevating laccase loading did not exhibit significant improvement on final cell mass concentration, although a slight increase on cell mass concentration was observed by laccase loading of 2 U/mL in the middle stage of fermentation. The products were characterized and reported as concentrations of fermentation broth rather than the content of cell mass, due to the difficulty of completely separating lignin particles from solid residues without damaging cells. The final concentration of TFA in fermentation broth was around 25 mg/L, and a trace amount of carotenoids was also identified at about 0.06 mg/L for all treatments (**Figure 2.8B**).

In previous studies, several kinds of microorganisms have been reported to be able to degrade lignin polymers. As a strain isolated from eroded bamboo slips, *Commamonas* sp. B-9 was able to degrade Kraft lignin and reduce the chemical oxygen demand (COD) of the medium by 32% after 7-day incubation, due to its high activities of MnP and laccase (137). Several other strains also exhibited the natural ability of lignin degradation, such as *Novosphingobium* sp. B-7 (71) and *Pandoraea* sp. B-6 (138). Such studies mainly usedlignin as a waste, focusing on environmental parameters rather than microbial products. In the study of Zhao et al. (68) on Kraft lignin fermentation, *R. opacus* PD630 was shown to grow very slowly while the addition of laccase significantly improved cell mass growth, lignin degradation as well as total lipid accumulation. The promotion effect by laccase is positively correlated with laccase loading. The synergy between laccase and cells was attributed to the functional group specific degradation of lignin by laccase and the efficient consumption of degradation products by cells. The laccase

from *Trametes versicolor* specifically degraded aliphatic OH and guaiacyl phenolic OH groups, generating products which were possibly compatible with the preference of *R. opacus* PD630.

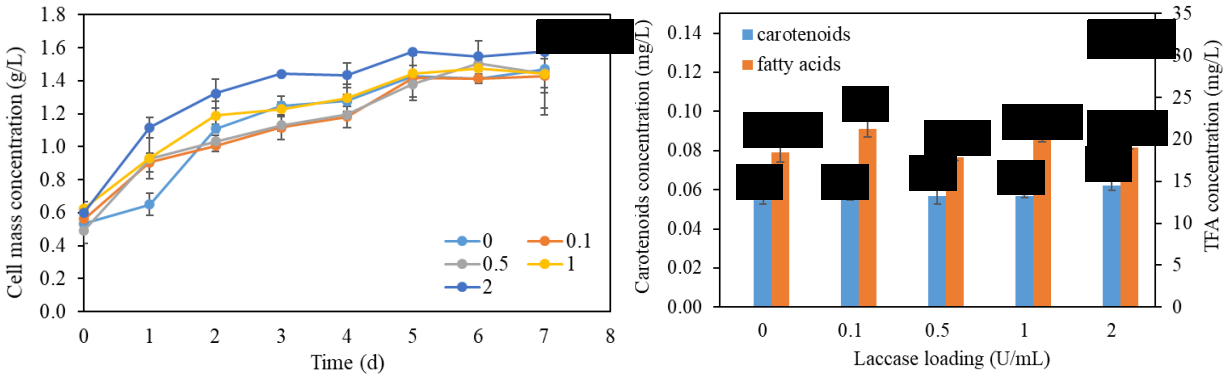

Figure 2.8 Kraft pine lignin fermentation with the aid of laccase
(A) cell mass growth; and (B) final concentration of TFA and carotenoids in the fermentation broth. Lowercase letters and Roman numerals indicate statistical analysis results. Levels connecting with different letters/numerals are statistically different.

3.3 Hypothetical pathways of lignin metabolism by *T. striatum* HBS

In the current study, *T. striatum* HBS exhibited degrading ability on lignin-derived materials including model aromatic compounds and different technical lignins. Based on analysis of metabolites from fermentation, the hypothetical pathways of lignin metabolism by HBS is proposed (**Figure 2.9**).

To degrade polymeric lignin macromolecules, extracellular ligninolytic enzymes first depolymerize lignin and produce smaller fragments and simple monomers. LiP- and MnP-type enzymes were identified to be responsible for this process while the detected enzyme activities in HBS were relatively weak and possibly only function on H-type lignin subunits. The metabolism of lignin monomers started from funneling process which converted diverse monomers into specific central intermediates. Such funneling process can be conducted in CoA-dependent β-oxidation pathway, CoA-dependent non-β-oxidation pathway or CoA-independent pathway, and different enzymes are involved for funneling of different monomers (85). G and H type

compounds are ultimately converted into protocatchuic acid (PCA, equivalent to 3,4-DHBA) while S type compound is converted 3-O-methylgallic acid (3MGA) in HBS. PCA and 3MGA then enter aromatic ring cleavage and central metabolism. The carbon and energy from lignin are utilized for cell growth as well as biosynthesis of products (i.e. fatty acids and carotenoids). To verify these pathways, a comprehensive analysis on HBS genome should be conducted in the future to identify the functional genes related to lignin degradation. An integrated multi-level omics analysis is also necessary to construct metabolic network connecting lignin metabolism, microbial central metabolism and biosynthesis of products.

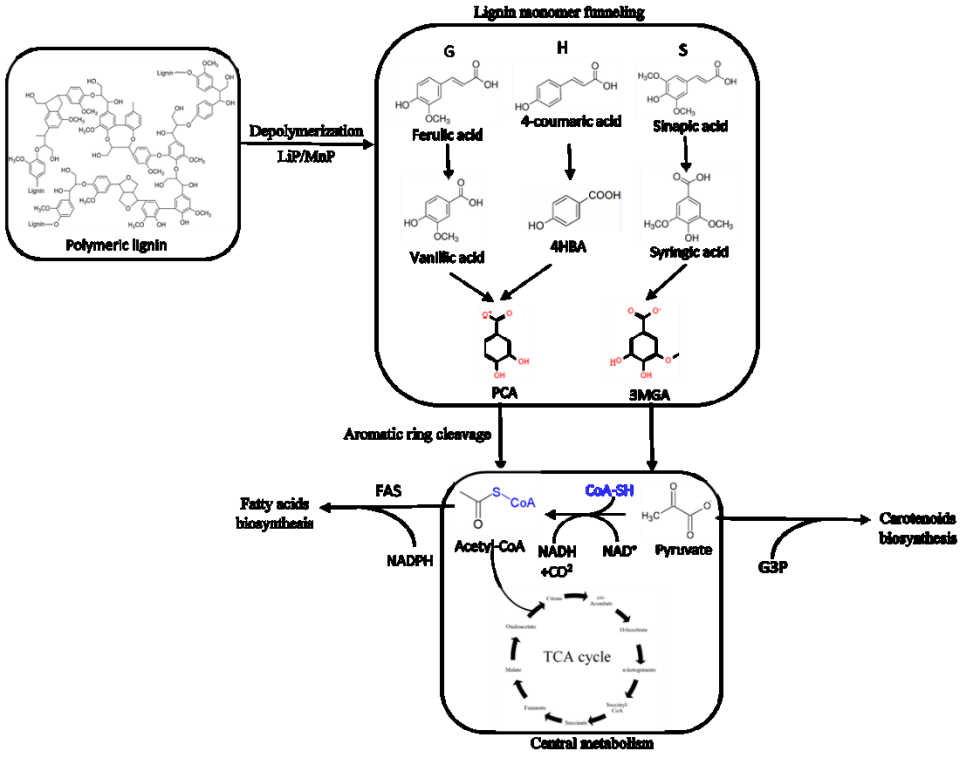

Figure 2.9 Hypothetical lignin metabolism pathways of *T. striatum* HBS
3MGA: 3-O-methylgallic acid; 4HBA: 4-hydroxybenzoic acid; FAS-fatty acid synthase; G3P-D-glyceraldehyde 3-phosphate; Lip-lignin peroxidase; MnP-manganese peroxidase; PCA-protocatchuic acid.

4. Conclusions

The HBS of *T. striatum* ATCC 24473 was proven to be able to utilize lignin-derived materials as a carbon source during the fermentation process to accumulate fatty acids and carotenoids. Among 15 kinds of lignin model compounds tested, 3,4-DHBA and 4-HBA showed the best performance on serving as a carbon source. Fed-batch cultivation mode remarkably improved the final contents of both total fatty acids and carotenoids, suggesting that the availability of carbon source is the limiting factor for product accumulation. Fermentation with three types of lignin (AL CS, EOL LP, and KPL) also proved that the HBS could degrade lignin polymer directly, although the ability is relatively weak. An increase of cell mass concentration was observed during fermentation as well as a trace number of products. The activity of two ligninolytic enzymes such as LiP and MnP were detected with apparent daily variation. NMR analysis on fermented lignin indicated that this strain possibly degraded polymeric lignin with no preference toward particular lignin structure or linkages. The GC-MS results suggest that 4-HBA may be used as a central intermediate, and other phenolic compounds need to be converted into 4-HBA firstly for further utilization, or directly released 4-HBA from lignin depolymerization. The generation and accumulation of 4-HBA mainly occurred in the first three days of fermentation, which corresponds to the relatively high enzyme activity.

Chapter 3 - Simultaneous depolymerization and fermentation of lignin by *T. striatum*

1. Introduction

Lignin, one of the most abundant naturally occurring polymers in biosphere (165), is regarded as a promising feedstock for biofuel and bioproducts. Its aromatics-based, diverse structure makes it attractive for its high energy density and flexibility in chemical transformation (166). However, the heterogeneity and high degree of cross-linking also cause enormous challenges on lignin conversion (167). Therefore depolymerization prior to downstream processing is usually necessary for efficient lignin utilization (46). Currently there are two major platforms for lignin depolymerization and conversion: thermochemical and biological. Thermochemical depolymerization employs harsh conditions (e.g., high temperature, high pressure, high alkalinity, etc.) to break down linkages between lignin subunits and release simple lignin monomers for further applications (47, 168). Such a process requires extensive energy input and uses chemicals with negative environmental impacts (33, 169). In comparison, biological depolymerization of lignin is catalyzed by ligninolytic enzymes, which function under milder conditions in a more sustainable way. Several species have been identified to have lignin depolymerization ability, especially white rot fungi which have powerful ligninolytic enzyme system (49). Bacteria, such as *Rhodococcus* (41, 100, 102) and *Pesudomonas* (43, 105) species, also degrade polymeric lignin and incorporate the released aromatic compounds into their secondary metabolism. Acquisition of value-added bioproducts can be achieved simultaneously, which would improve the cost-effectiveness of lignin bioconversion process. However, due to the relatively lower oxidizing power of bacterial enzymes (74), the ability of lignin

depolymerization in bacteria is inferior compared to fungal species, which limits the application of lignin as substrate for bacteria-based biomanufacturing process.

The previous chapter confirmed that the HBS of marine protist *T. striatum*, which was induced by high nitrogen stress, can depolymerize lignin and use the released fragments as a carbon source for cell growth and product synthesis. It was able to synthesize fatty acids and carotenoids from lignin at the same time, which is a great advantage of this strain. However, the yields of microbial product and lignin utilization efficiency were relatively low and far from practical applications. Various strategies have been developed to improve microbial fermentation performance, such as optimization of fermentation medium and fed-batch cultivation. The concept of synergy has been applied to the field of biotechnology for a long time, to utilize the advantages of diverse microbial metabolic processes. For lignin bioconversion, the powerful degradation system of fungi can couple with synthesis pathways of valuable products and improve the effectiveness of the entire process. For instance, Salvachúa et al. (67) applied fungal secretomes from *P. eryngii* for depolymerization of lignin isolated from corn stover by Deacetylation-mild alkaline treatment-followed by Mechanical Refining and Enzymatic Hydrolysis (DMR-EH). The molecular weight of lignin was reduced by 63% due to the high laccase activity, and co-incubation with *Pseudomonas putida* KT 2440 effectively prevented repolymerization via bacterial metabolism of depolymerized products (67). The addition of laccase during Kraft lignin fermentation by *R. opacus* significantly improved cell growth and the positive effects increased with higher laccase loading. At the same time, the percentage of utilized lignin elevated from approximately 15 to 30% and total lipid concentration increased by 17 folds (68). Similar results were also acquired by Xie et al. (99) and Liu et al. (103) as laccase effectively catalyzed depolymerization of lignin and produced fragments of smaller molecular

weight and simpler structure. Bacteria then utilized these fragments as carbon sources for cell growth and microbial product accumulation. The consumption of such fragments also pushed the reaction equilibrium toward the direction of depolymerization.

In this study, Kraft pine lignin (KPL) was used as sole carbon source and the fermentation process was optimized, aiming to improve lignin depolymerization and degradation by *T. striatum* HBS. Effects of different nitrogen sources and growth factors were tested and compared. KPL was also co-fermented with glucose to investigate the interactions between different types of carbon source. In addition to direct depolymerization by protist itself, three major lignin depolymerization systems in nature, peroxidase-based system, laccase-based system and Fenton reaction-based system, were added into fermentation broth. Cell growth, lignin consumption and final content of products were used to evaluate the effectiveness of synergism between external lignin depolymerization system and protist.

2. Materials & methods

2.1 Microorganism

The HBS of *T. striatum* ATCC24473 was cultured as described in **Section 2.1** in **Chapter 2**. White rot fungi, *Phanerochaete chrysosporium*, was received from the University of Kentucky and maintained on potato dextrose agar plate.

2.2 Kraft pine lignin (KPL) fermentation

In the lignin fermentation process, KPL was used as a carbon source with a loading of 1 g/L in 100% ASW. Different types of nitrogen sources [yeast extract, peptone, urea, $NaNO_3$, and NH_4Cl] were used at the concentration of 0.4 g/L and compared on fermentation performance (i.e., cell growth and lignin utilization). The effects of mineral elements and vitamins as growth factors were also studied. With KPL as a carbon source and NH_4Cl as a nitrogen source, mineral

element solution and vitamin solution were added and the fermentation performance was compared to the control (i.e., no addition of growth factors). The mineral element solution contains (per liter): 40 g $NaNO_3$, 12 g Na_2EDTA, 2 g $ZnSO_4 \cdot 7H_2O$, 1 g $Na_2MoO_4 \cdot 2H_2O$, 1 g $NaHCO_3$, 0.5 g $FeCl_3 \cdot 6H_2O$, 0.2 g $MnCl_2 \cdot 4H_2O$, and 2 mg $CoCl_2 \cdot 6H_2O$. The vitamin solution contains (per liter): 0.1 g thiamine (vitamin B_1), 0.1 g calcium pantothenate (vitamin B_5), 0.1 g biotin (vitamin B_7), 0.2 g aminobenzoate, 0.02 g vitamin B_{12}, and 0.04 g cyanocobalamin. Ten mL mineral element or vitamin solution was added (170)per liter fermentation broth. Cell growth was monitored by measurement of colony-forming unit (CFU) on day 0, 2, 4, and 7. Residual lignin was recovered by dissolving in tetrahydrofuran (THF). Lignin consumption was measured by the procedures in **Section 2.3**, **Chapter 2.**

2.3 Co-fermentation of KPL and glucose

Co-fermentation with glucose was expected to increase cell concentration and therefore improve the utilization of KPL. Different glucose concentrations, 2, 5 and 10 g/L, were applied and KPL concentration was kept at 1 g/L. To monitor cell growth, samples were taken and washed with THF to remove solid lignin followed by DDI water washing for two times to remove residual THF. OD_{600} was measured and converted into cell mass concentration (g/L) on dry basis. Lignin consumption was measured by the procedures in **Section 2.3**, **Chapter 2**. The consumption of glucose was monitored on daily basis with HPLC (Prominence LC-20AB, Shimadzu) equipped with a refractive index (RI) detector and a Shodex carbohydrate analytical column (Sugar SP0810, Showa Denko America, NY, USA). Sugars were separated at 80 °C with HPLC grade water as a mobile phase at a flow rate of 0.6 mL/min.

2.4 Preparation of fungal secretome

Enzymatic hydrolysis residue of corn stover was used as a carbon source to induce the secretion of ligninolytic enzymes in order to prepare the secretome of white rot fungi *P. chrysosporium*. The corn stover underwent alkali pretreatment at 60 °C for 2 h. The solid loading and NaOH loading were 10% and 20 g/L, respectively. Enzymatic hydrolysis of pretreated corn stover was done by following the procedure of NREL (171). The solid loading was set at 10%. CTec 2 and HTec 2 were loaded at 15 FPU/g dry biomass and 60 IU/g dry biomass, respectively. Sulfuric acid was used to adjust the initial pH to 4.8. The temperature was controlled at 50 °C and shaking speed of 150 rpm. After 72-h incubation, the hydrolysis mixture was centrifuged to collect enzymatic hydrolysis residue (EHR), which was washed with DDI to remove the attached sugars and proteins and air-dried for further use. *P. chrysosporium* was cultured in the liquid medium of Tien and Kirk (172). The basal medium contains (per liter): 2 g KH_2PO_4, 0.5 g $MgSO_4$, 0.1 g $CaCl_2$, 0.18 g $MgSO_4$, 0.03 g $MnSO_4$, 0.06 g NaCl, 0.006 g $FeSO_4•7H_2O$, 0.006 g $CoCl_2$, 0.006 g $ZnSO_4•7H_2O$, 0.006 g $CuSO_4$, 0.0006 g $AlK(SO_4)_2•12H_2O$, 0.0006 g H_3BO_3, 0.0006 g $Na_2MoO_4•2H_2O$, 0.09 g nitrilotriacetate, and 0.001 g thiamine. NH_4Cl and yeast extract were used as a nitrogen source together with a concentration of 0.87 g/L and 0.012 g/L, respectively. EHR was loaded as a carbon source at 10 g/L. As a positive control, glucose of 10 g/L was used as a carbon source supplemented with 0.4 mM veratryl alcohol for secretome preparation. Both agitated and stationary cultivation were conducted and compared on the production of ligninolytic enzymes. Tween 80 solution was added to reach the final content of 0.05% for agitated cultivation. For inoculation, spore suspension was generated from potato dextrose agar plate with OD_{650}=0.5. The liquid medium of 90 mL was inoculated with 10 mL spore suspension and cultured at 37 °C. The shaking speed of 150 rpm was applied for agitated

cultivation. After 7-day incubation, the fermentation broth was centrifuged to remove the solid phase, and supernatant was collected as fungal secretome. The activities of three major ligninolytic enzymes in fungal secretome, lignin peroxidase (LiP), manganese peroxidase (MnP) and laccase, were analyzed(173).

2.5 Simultaneous lignin depolymerization and fermentation

To improve lignin utilization, external lignin depolymerization systems were used to perform synergistic lignin depolymerization with HBS. The fermentation medium was prepared with 100% ASW and lignin was loaded at 1 g/L. NH_4Cl was used as a nitrogen source at 0.4 g/L. Three types of external lignin depolymerization systems including laccase, lignin peroxidase-dominated fungal secretome and Fenton reagent, were added to synergize with protist cells. Laccase from *Trametes versicolor* and *Rhus vernicifera* were applied at 2 U/mL. Acetate buffer (100 mM, pH=4.5) and phosphate buffer (100 mM, pH=7.0) were used to prepare the enzyme stock solution. The fungal secretome was prepared from *P. chrysosporium* under stationary conditions using EHR as a carbon source. The dominant ligninolytic enzymes in the secretome of *P. chrysosporium* was detected as LiP. The secretome loading was set at 5% (v/v) to make the final LiP loading around 2 U/mL. For the Fenton reagent, 0.2 mM $FeSO_4$ and 0.067 mM H_2O_2 were added to fermentation broth of different lignins. Cell growth and lignin reduction were measured by following procedures described previously. After fermentation, the cells were collected and freeze-dried for characterization of fermentation products (i.e., fatty acids and carotenoids).

2.6 Characterization of fermentation products

The characterization of fermentation products (i.e. fatty acids and carotenoids) followed the methods in **Section 2.5**, **Chapter 2**.

2.7 NMR analysis on residual lignin structure

2D ^{13}C-^{1}H HSQC and quantitative ^{31}P NMR spectroscopic analysis were performed to investigate lignin structure modification by fermentation, as described in **Section 2.6**, **Chapter 2**. For ^{13}C-^{1}H 2D analysis, spectra of lignin samples were acquired with the following acquisition parameters: spectra width 10 ppm in F2 (^{1}H) dimension with 2048 time of domain (acquisition time 256.1 ms), 210 ppm in F1 (^{13}C) dimension with 256 time of domain (acquisition time 6.1 ms), a 1.5-s delay, a $^{1}J_{C–H}$ of 145 Hz, and 32 scans.

2.8 Lignin molecular weight analysis

The weight-average molecular weight (M_w) and number-average molecular weight (M_n) of lignin were measured by Gel permeation chromatographic (GPC) analysis. KPL was directly dissolved in THF and size-exclusion separation was performed on an Agilent 1200 HPLC system (Agilent Technologies, Inc, Santa Clara, CA, US) equipped with Waters Styragel columns (HR1, HR2, and HR6; Waters Corporation, Milford, MA, US). An UV detector (270nm) was used for detection. THF was used as the mobile phase at a flow rate of 1.0 mL/min. Polystyrene narrow standards were used for establishing the calibration curve. The values reported below are the average of two replicates.

2.9 Data analysis

Statistical significance was determined by analysis of variance (ANOVA, α=0.05) and Tukey's test for mean comparison using JMP Pro 12 (SAS Institute, Cary, NC, USA) with $p_{critical}$=0.05. All treatments were conducted in two replicates in this study unless specified otherwise.

3. Results and discussion

3.1 Effects of nitrogen source and growth factors on KPL fermentation

For microbial fermentation, the composition of the medium -carbon source, nitrogen source, pH, salinity and trace elements- is of great importance in affecting the fermentation performance. In this study of KPL fermentation, the effects of two factors including a nitrogen source type and growth factors were tested to improve utilization of the substrate. Five types of nitrogen sources [yeast extract, peptone and urea as organic nitrogen source; $NaNO_3$ and NH_4Cl as inorganic nitrogen source] were applied (**Figures 3.1A&B**). After 7-day fermentation, the cell concentration increased from initial 1×10^7/mL to 5.5~6.5 $\times10^7$/Ml. While in fermentation with yeast extract, peptone and urea, cell growth was mainly supported by organic components in the nitrogen source. For lignin utilization, the highest percentage of lignin consumption was achieved with NH_4Cl at 17%, followed by $NaNO_3$ (7%). Less than 5% of lignin was degraded using organic nitrogen sources, which further supports that both the carbon and nitrogen required by microbial growth came from organic nitrogen sources. With the presence of a readily biodegradable carbon source, the synthesis of lignin-degrading enzymes would probably be shelved, and therefore the utilization of lignin as a carbon source would be restricted. Among inorganic nitrogen sources, NH_4Cl exhibited the best performance on both cell growth and lignin consumption. Possible reasons for this include higher nitrogen content and nitrogen in the ammonium form preferred by microorganisms. A much higher lignin degradation percentage with NH_4Cl was observed compared to cell concentration, due to the better performance on product accumulation.

In addition to carbon and nitrogen sources, growth factors including mineral elements and vitamins were also observed to affect the microbial fermentation process as important co-

factors for diverse enzymatic reactions. The addition of mineral elements has been reported to enhance the production of methane (174) and hydrogen (175) by different species. With KPL as a substrate, the addition of a mineral element solution helped improve lignin utilization from 16 to 20% (**Figure 3.1C**). No significant influence was obtained by vitamin solution alone, while some synergetic effects between mineral and vitamin solution were observed as the percentage of lignin consumed further increased to around 25%. For lignin degradation, most ligninolytic enzymes are metal-dependent, such as copper-containing laccase and heme-containing peroxidase. The presence of certain metal elements may have induction effects on enzyme production at the transcription level (176), which would consequently facilitate the depolymerization and degradation of lignin. However, even with trace elements, the improvement of lignin utilization was not remarkable, limited by the relatively weak lignin depolymerization ability of *T. striatum* HBS.

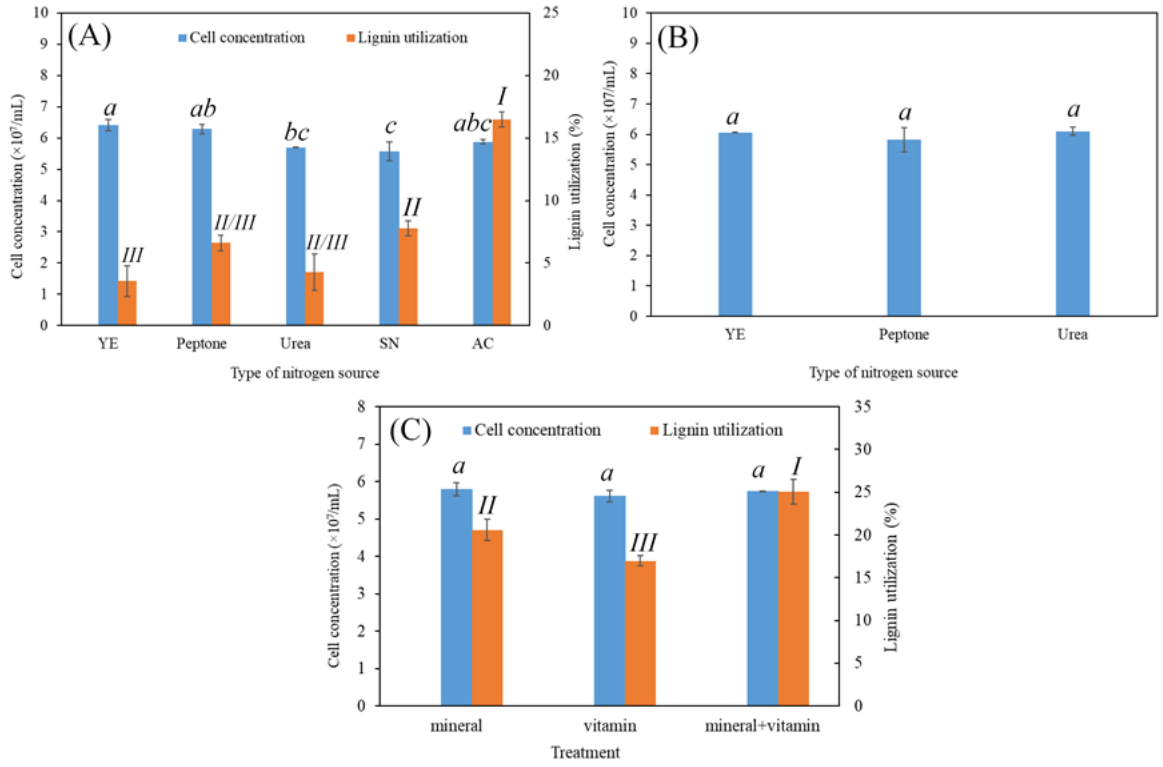

Figure 3.1 KPL fermentation optimization.

(A) Cell growth and lignin utilization with different nitrogen sources: YE-yeast extract; SN-$NaNO_3$; AC-NH_4Cl; (B) Cell growth with nitrogen source only; (C) Cell growth and lignin utilization with different growth factors. Lowercase letters and Roman numerals indicate statistical analysis results. Levels connecting with different letters/numerals are statistically different.

3.2 Co-fermentation of KPL and glucose

A co-metabolic system with glucose and lignin was also employed to improve lignin degradation. Glucose can be used as a substrate for growth and change the oxidation-reduction potential, which would create a favorable environment for microbial cell growth (177, 178). However, the effects of co-metabolism on glucose have long been ignored. In this study of KPL fermentation, glucose was supplemented at different concentrations to increase *T. striatum* HBS cell growth and therefore improve its overall ability of lignin degradation. A marginal difference inn cell mass concentration was observed between glucose only and glucose plus lignin (**Figure 3.2A**). When glucose increased from 2 to 5 g/L the final cell mass concentration also increased correspondingly, while a further increase to 10 g/L resulted in little enhancement of cell growth due to limitations of the glucose utilization ability of *T. striatum* HBS. It is noteworthy that the presence of lignin improved glucose utilization, especially at relatively higher concentrations. At 5 g/L, glucose was completely used by the third day with KPL, compared to the 5^{th} day without KPL. At 10 g/L of glucose, faster consumption and higher utilization percentage of glucose were also observed in the presence of KPL (**Figure 3.2B**). In previous studies, lignins, especially lignin-derived low-molecular-weight compounds, have been reported to boost the degradation of polysaccharides by serving as activators for redox enzymes, lytic polysaccharide monooxygenases (LPMOs) (179-181). Those compounds can provide electrons needed by the function of LPMOs and therefore aid the oxidative cleavage of glycosidic bonds (182). For this study, a similar mechanism may also exist for glucose metabolism, in which low-molecular-

weight compounds derived from KPL delivered electrons and facilitated the oxidation of glucose as well as electron transfer. As a result, KPL was also oxidized and degraded. Compared to 23.7% of lignin degradation without glucose (183), an increasing utilization efficiency of KPL was observed as the glucose concentration increased (**Figure 3.2C**).

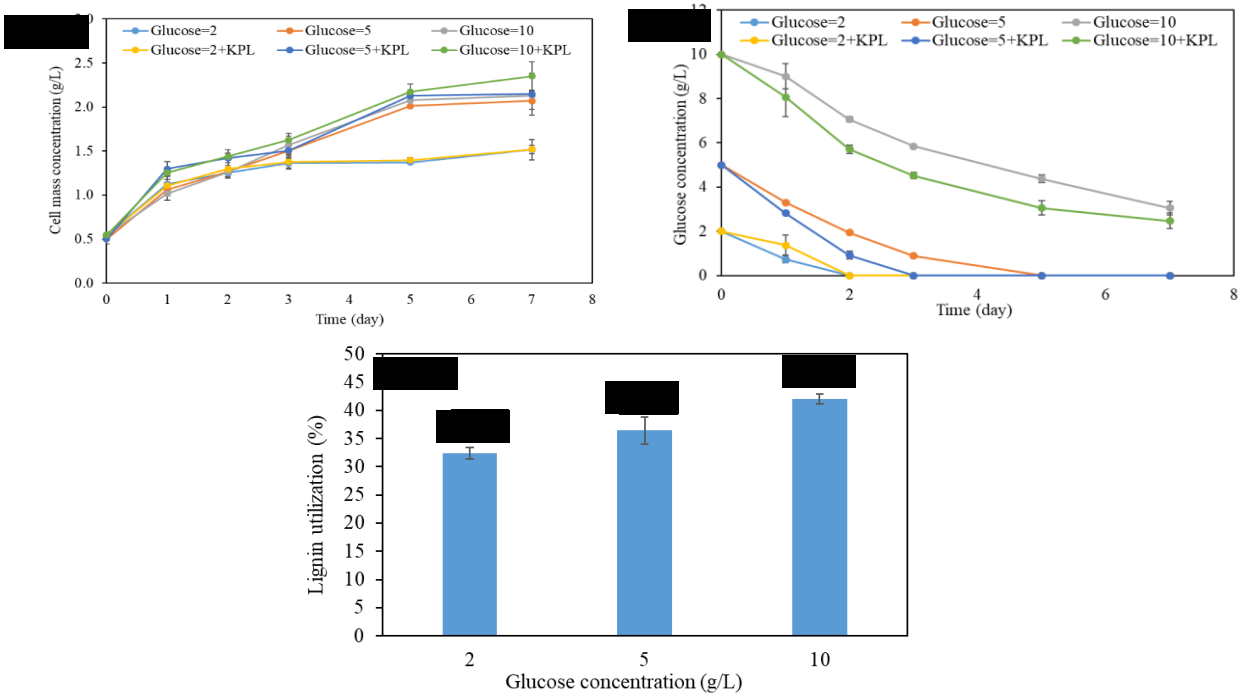

Figure 3.2 Co-fermentation of KPL and glucose of different concentrations

(A) Cell growth; (B) glucose utilization; (C) lignin utilization. Lowercase letters indicates statistical analysis results. Levels connecting with different letters are statistically different.

3.3 Secretome of white rot fungi under different fermentation conditions

In nature, white rot fungi such as *P. chrysosporium*, *T. versicolor* and *Ceriporiopsis subvermispora*, were found to be the most powerful lignin degrading microorganisms. Their secretome which contain effective ligninolytic enzymes, has also been utilized directly for degradation of lignin and lignocellulose (67, 184). In this study, fungal secretome was prepared from *P. chrysosporium* which was reported to primarily produce LiP and MnP to attack lignin structure (58). Glucose and EHR of corn stover were used as substrates. Under different

fermentation conditions, the activity of three major ligninolytic enzymes were all detected (**Figure 3.3**). With glucose as the carbon source, the activity of LiP and MnP were comparable at 8~9 U/mL and 12~13 U/mL respectively, under two cultivation conditions. Laccase showed slightly higher activity of 5 U/mL under stationary cultivation than under agitated culture (3 U/mL). The use of corn stover EHR as the carbon source significantly induced higher production of LiP, whose activity reached 40 U/mL compared to less than 10 U/mL with glucose as the carbon source. However, the activity of MnP dropped to around 5 U/mL and laccase was barely detected for both stationary and agitated cultivation. Therefore, the secretome collected from *P. chrysosporium* fermentation with enzymatic hydrolysis residue was dominantly LiP. The highest LiP activity of 48 U/mL was acquired with EHR of corn stover under stationary cultivation, which was consistent with previous studies that stationary cultivation is favorable to enzyme production and secretion (172, 185).

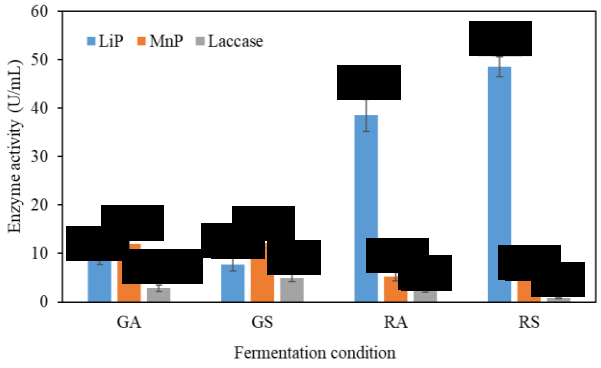

Figure 3.3 Enzyme activities of three ligninolytic enzymes from different fermentation conditions of *P. chrysosporium*.

GA-glucose, agitated; GS-glucose, stationary; RA-enzymatic hydrolysis residue, agitated; RS-enzymatic hydrolysis residue, stationary. Lowercase letters and Roman numerals indicate statistical analysis results. Levels connecting with different letters/numerals are statistically different.

3.4 Simultaneous lignin depolymerization and fermentation

The simultaneous lignin depolymerization and fermentation was performed by adding external lignin depolymerization systems into *T. striatum* HBS culture. Three naturally existing systems, laccase-based, peroxidase-based and Fenton reaction-based, were used. In comparison to the control (without treatment; data from the previous study), the addition of an external lignin depolymerization system contributed to lignin degradation and subsequent cell growth, demonstrated by the significant elevation in the final cell concentrations for all treatments (**Figure 3.4A**). The two types of laccase showed the most remarkable effect as the final cell concentration surged by hundreds of times from the initial 10^7/mL. The fungus-derived laccase from *T. versicolor* performed better than plant-derived laccase from *R. vernicifera*, exhibiting a doubled cell number. Secretome of *P. chrysosporium* and Fenton reagent also improved cell growth, and final cell concentration increased by 40-60 folds from the initial value. Lignin utilization also improved in the presence of externally enhanced depolymerization (**Figure 3.4A**). Enzymatic depolymerization resulted in 25-30% lignin degradation, slightly higher than that (22%) from Fenton reagent. Little difference in lignin reduction was observed among different treatments, which was inconsistent with cell growth results. The possible reason is that lignin depolymerization products by fungal secretome or Fenton reagent may have inhibitory effects on enzymatic reactions, cellular functions and the growth of *T. striatum* HBS. Without microbial consumption, lignin was decomposed into soluble compounds and remained in supernatant.

With more lignin degraded, the concentration of intracellular TFAs increased accordingly, especially using *R. vernicifera* laccase (**Figure 3.4B**). The highest TFA concentration was achieved with R. *vernicifera* laccase at 42 mg/L. For carotenoids, the addition

of fungal secretome and Fenton reagent resulted in higher total carotenoids concentration, possibly due to the oxidative stress caused by hydrogen peroxide (**Figure 3.4B**). As an effective antioxidant, carotenoids can be more produced by the stimulation of reactive oxidative species, such as molecular oxygen and hydrogen peroxide (186-188). During this process, the activity of β-carotene hydroxylase can be enhanced, which is the possible mechanism for oxidative stress stimulation (189). Otherwise, the improvement of lignin degradation led to a marginal increase in total carotenoids concentration. Under conditions with limited oxidative stress, the enhanced carbon flux would mostly enter the biosynthetic pathway of fatty acids as energy storage compounds, regulated by microbial metabolic system.

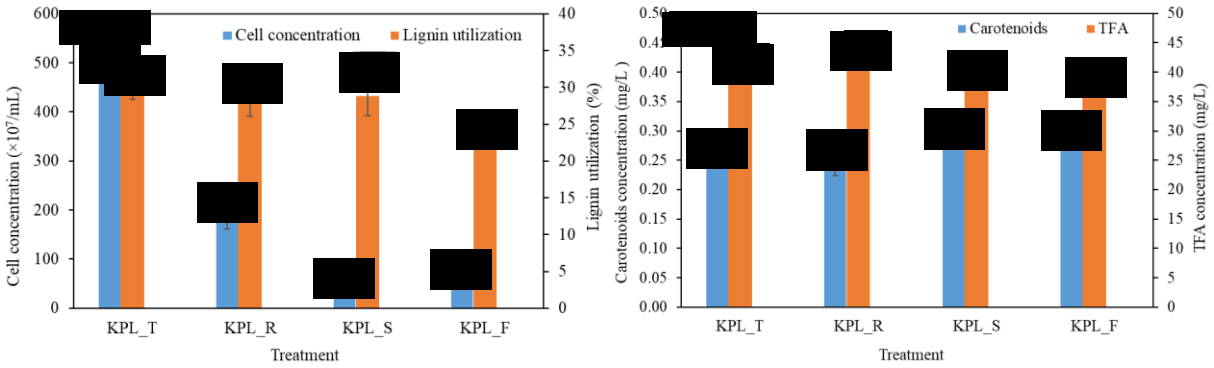

Figure 3.4 Simultaneous depolymerization and fermentation of KPL

(A) Cell concentration and lignin utilization; (B) accumulation of total fatty acids and carotenoids in fermentation broth. KPL_T: KPL fermentation with laccase from *T. versicolor*; KPL_R: KPL fermentation with laccase from *R. vernicifera*; KPL_S: KPL fermentation with secretome of *P. chrysosporium*; KPL_F: KPL fermentation with Fenton reagent. Lowercase letters and Roman numerals indicate statistical analysis results. Levels connecting with different letters/numerals are statistically different.

3.5 Structure analysis of residual lignin from KPL fermentation

After 7-day incubation, the residual lignins from the four different treatments were collected for M_w and structural analysis. Treatment with laccase from *T. versicolor* reduced lignin M_w from its initial 2991 to 2898 g/mol while all other treatments increased the M_w to various extents (**Table 3.1**). These results indicate that the consumed lignin during fermentation

was primarily low-molecular-weight fraction so consequently the average M_w increased. Additionally, *in vitro* repolymerization of depolymerized lignin fragments may occur, leading to an increase of overall M_w (190). The contents of various inter-unit linkages (reported as relative content over total aromatics unless otherwise specified) analyzed by HSQC NMR analysis showed a similar trend (**Figure 3.5A; Table 3.1**). The contents of major inter-unit linkages (e.g., β-O-4, β-β, and β-5) decreased after fermentation with *T. versicolor* laccase, which suggests that *T. versicolor* laccase was able to facilitate the breakdown of linkages in lignin molecules and therefore improve its degradation. Alternatively, the plant-derived laccase from *R. vernicifera* may mainly act on aromatic structure and catalyzed the ring opening process, which resulted in a decrease of total aromatics content and increase of inter-unit linkage contents. At the same time, higher inter-unit contents were obtained by another two treatments, specifically the fungal secretome treatment. In terms of cell growth, treatment with fungal secretome and Fenton reagent had less cell growth possibly due to the inhibition of H_2O_2, which would in turn impede the consumption of depolymerized lignin fragments. During lignin degradation, the depolymerization and repolymerization processes occur simultaneously and reach equilibrium. An effective synergism between the lignin depolymerization system and microbial lignin consumption can be developed if the microorganisms can remove lignin degradation products efficiently and force the equilibrium toward depolymerization. When the substrate utilization and cell growth of microbes were inhibited by some factors (possibly be H_2O_2 in this study), some low-molecular-weight lignin fragments can be mineralized into CO_2 and H_2O, and others may spontaneously cross-link with each other and form new linkages in neutral pH. Only a limited portion can be used to support microbial growth and activities.

A ^{31}P NMR analysis was also performed to analyze the contents of different hydroxyl groups in lignin molecules (**Figure 3.5B**). Three major OH groups, aliphatic OH, C5 substituted OH and guaiacyl OH, were degraded during fermentation. *T. versicolor* laccase was more effective on aliphatic OH, which is consistent with previous HSQC analysis results that it can function on inter-unit linkage breakdown. Additionally, as a G-type lignin, KPL has guaiacyl-OH as the dominant OH type, which was also significantly degraded with *T. versicolor* laccase. *R. vernicifera* laccase and fungal secretome attacked aromatic rings and were contributory to degradation of C5 substituted OH. However, when compared with fermentation with only HBS, the contents of the different OH groups increased, suggesting the primary mechanisms of lignin degradation by HBS was consumption of low-molecular-weight lignin fraction. The presence of external lignin depolymerization system would improve the generation of such fragments to be utilized by *T. striatum* HBS.

Table 3.1 Relative abundances of S, G, H units and side chain linkages over total aromatics.

	M_w (g/mol)	S%	G%	H%	S/G	β-*O*-4'%	β-5'%	β-β'%
Original KPL**(191)**	2991	0	100	0	0	2.9	0.6	1.1
KPL-T	2898	0	100	0	0	2.4	0.3	0.5
KPL-R	3853	0	100	0	0	3.6	0.7	2.1
KPL-S	4264	0	100	0	0	4.6	1.7	1.7
KPL-F	3952	0	100	0	0	4.0	0.2	0.8

Note: KPL_T: KPL fermentation with laccase from *T. versicolor*; KPL_R: KPL fermentation with laccase from *R. vernicifera*; KPL_S: KPL fermentation with secretome of *P. chrysosporium*; KPL_F: KPL fermentation with Fenton reagent.

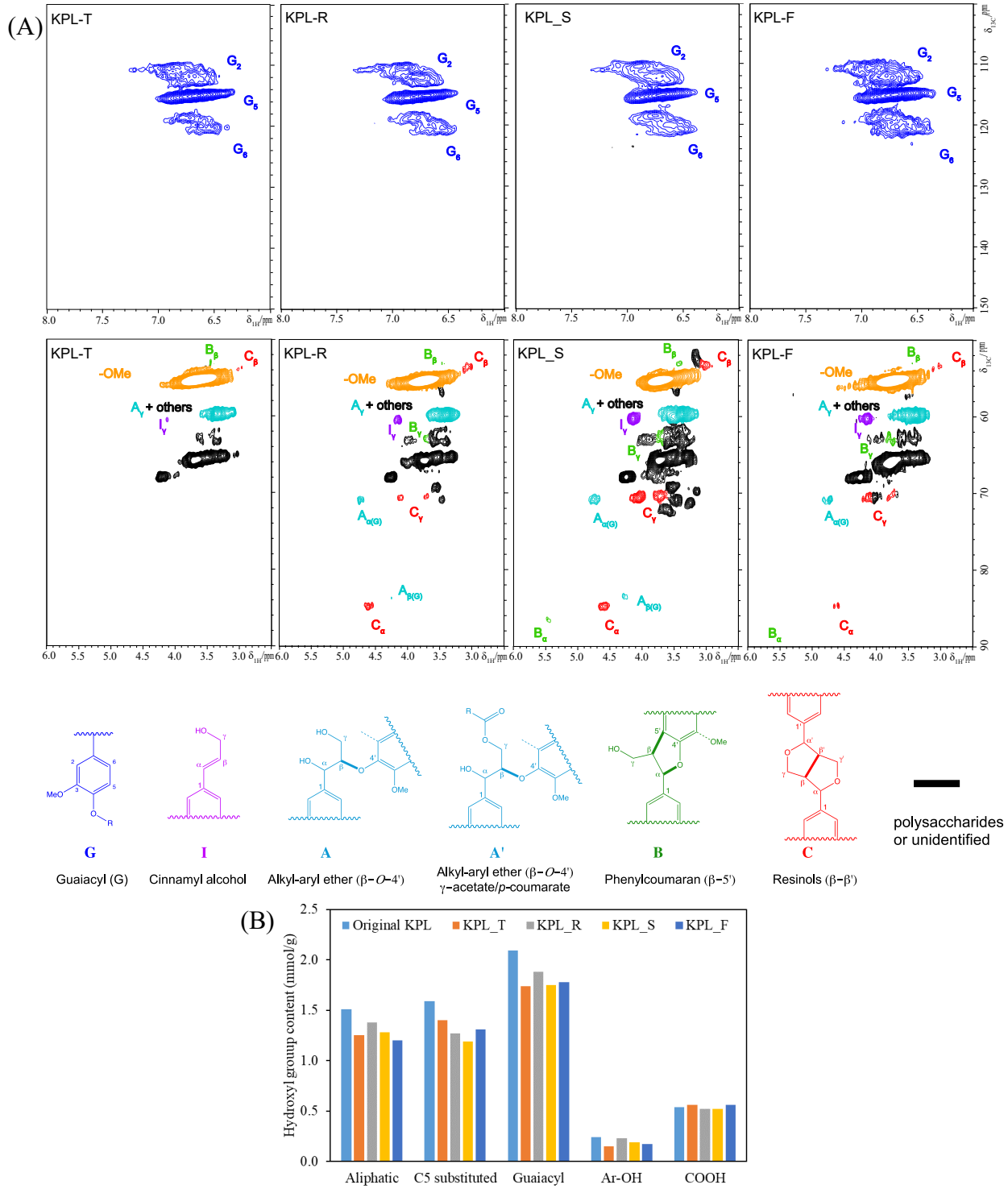

Figure 3.5 NMR analysis of residual lignin from KPL fermentation

(A) 2D HSQC spectra of aromatic (δ_C/δ_H 100-140/6.0-8.0 top) and aliphatic (δ_C/δ_H 50-90/2.5-6.0 bottom) regions; (B) ^{31}P analysis. KPL_T: KPL fermentation with laccase from *T. versicolor*; KPL_R: KPL fermentation with laccase from *R. vernicifera*; KPL_S: KPL fermentation with secretome of *P. chrysosporium*; KPL_F: KPL fermentation with Fenton reagent.

4. Conclusions

This study found that the HBS of *T. striatum* was able to degrade and utilize lignin-derived materials as carbon sources for cell growth and accumulation of intracellular bioproducts. Of the various nitrogen sources, NH_4Cl performed best on lignin degradation. The use of organic nitrogen sources (e.g. yeast extract and peptone) would impede the use of lignin, as microbes tend to obtain both carbon and nitrogen sources form organic matters instead of lignin. The addition of minerals, as important co-factors of lignolytic enzymes, was beneficial in improving lignin degradation. Three types of lignin depolymerization systems were added externally and observed to improve cell growth as well as lignin utilization. Specifically, effective synergy between two kinds of laccase and *T. striatum* HBS was observed. The fungus-derived laccase facilitated the breakdown of inter-unit linkages in lignin molecules while the plant-derived laccase attacked aromatic ring structures and generated low-molecular-weight lignin fragments. The secretome of white rot fungi and Fenton reagent were also effective on lignin degradation, while some products from lignin depolymerization appeared to have negative effects on cell growth. In addition to being a substrate, KPL was also found to facilitate glucose utilization during glucose-lignin co-fermentation. The possible mechanisms are that lignin, especially the low-molecular-weight fraction, can serve as an electron donor and contribute to electron transfer during microbial metabolism.

Chapter 4 - Application of *T. striatum* to black liquor bioconversion and investigation on metabolic mechanisms

1. Introduction

Lignin, one of the major components of lignocellulose, is an important byproduct in the pulping and biorefinery industries (192). In the treatment of biomass, cellulose and hemicellulose are generally conserved, while lignin is removed to benefit downstream processing and generate the lignin-rich waste stream, i.e., black liquor. Alkali solubilizes the constituents of biomass into black liquor, rendering black liquor extremely high chemical oxygen demand as well as strong alkalinity, high chromaticity and strong odor. Diverse compositions are contained in black liquor such as aromatic compounds, polyphenolic fragments, organic acids, sugars, and tannins (9). Black liquor has primarily been treated by incineration to serve as an energy source (i.e., combined heat and power) for the pulping process or biorefinery as well as recovery of alkali (193). Gasification (194, 195) and hydrothermal liquefaction (196, 197) have also been employed for fuel production from black liquor given its high energy content. In addition to these thermochemical strategies, detoxification of black liquor through biological treatment has attracted increasing research interest (9, 151). Both white rot fungi with their powerful extracellular enzymatic system (198, 199), and bacteria with their immense environmental adaptability and biochemical versatility (9), have been successfully applied. In the study of Chandra et al. (9), the bacterial consortium comprising *Serratia marcescens*, *Citrobacter* sp. and *Klebsiella pneumonia* was used for decolorization and detoxification of black liquor from the pulp manufacturing industry, achieving a significant reduction of COD, BOD and color by 83%, 74% and 85%, respectively. Paliwal et al. (151) investigated the potential of two indigenous bacterial strains, *Bacillus megaterium* and *Pseudomonas plecoglossicida* in black liquor

biodegradation, where effective reductions in color and lignin content were observed as well as high enzyme activities of lignin peroxidase, manganese peroxidase and laccase. Additionally, organic matters in black liquor can be potential carbon sources for the biosynthesis of microbial products. For example, sugars separated from black liquor have been used for biobutanol production (200, 201). However, due to the complexity of composition and existence of inhibitory compounds (e.g., phenolic compounds and organic acids), limited research has been done on direct utilization of whole black liquor.

In black liquor, lignin-derived aromatic components including aromatic monomers and polyphenolic compounds, account for 40~48% of solid content and contributes to above 90~95% of organic contents (9). To maximize the value of black liquor, the utilization of those aromatic components must be considered. Studies on lignin bioconversion identified several bacteria and fungi with the ability to grow with lignin-derived substrates while some species such as *Rhodococcus opacus* (41) and *Pseudomonas putida* (43) can accumulate valuable microbial products from lignin metabolism, making bioconversion more attractive and competitive compared to traditional black liquor treatment methods. The genome of these lignin-degrading microorganisms and their lignin degradation mechanisms have been extensively investigated, especially the metabolic pathways of aromatic compounds and their connections to the biosynthesis of microbial products (e.g. lipids and polyhydroxyalkanoates). With the knowledge of microbial metabolism, various strategies at the genetic or metabolic levels have been developed to improve lignin utilization efficiency or construct novel conversion pathways for target products (116, 118, 120). Numerous impressive outcomes have been acquired and provided promising directions for future development of lignin bioconversion platforms.

However, most studies were conducted under relatively simple conditions with a single carbon source. Complex lignin-rich substrates such as black liquor have been barely studied.

As a marine protist, *T. striatum* has been investigated as a biomanufacturer of long0chain polyunsaturated fatty acids such as docosahexaenoic acid (DHA) and eicosapentaenoic acid (EPA) (202), which are major components of fish oil and beneficial to human health. In addition, the *T. striatum* can synthesize a series of carotenoids of which astaxanthin has been known to be the most powerful natural antioxidant with extremely high value and fast-growing market. Previous studies in our lab have also indicated that a high biomass strain (HBS) of this species possesses lignin degradation abilities (183). The HBS induced by high nitrogen stress was able to use both aromatic compounds and technical lignins and showed high adaptability to diverse environmental conditions. Both lignin degradation mechanisms and lignin metabolic pathways remain unknown for the *T. striatum* HBS due to its position as a new class of lignin degrader. This knowledge gap resulted in tremendous challenges on development of *T. striatum* HBS as a novel biological platform for lignin conversion and upgrading. In this study, black liquor was used in fermentation with *T. striatum* HBS for the first time. The applicability of black liquor as a single carbon source for microbial growth and product accumulation was studied and optimized. The dynamic changes of black liquor composition such as aromatic compounds, polyphenolic fragments, carbohydrates, and organic acids were investigated throughout the fermentation process. The metabolic processes and interactions between different processes were also explored and analyzed by monitoring the consumption and conversion of different substrates.

2. Materials and methods

2.1 Microorganisms

In addition to HBS of *T. Striatum* ATCC24473, two more species, *Thraustochytrium* sp. ONC-T18 (PTA-6245) and *T. aureum* 34304 and *Thraustochytrium* sp. ONC-T18 (PTA-6245), were purchased from ATCC Company. The seed cultures were prepared as described in **Section 2.1** in **Chapter 2**.

2.2 Black liquor preparation and fermentation

Black liquor used in this study was prepared from alkaline pretreatment of corn stover. Corn stover was received from Idaho National Lab and milled through a 40-mesh sieve. Alkaline pretreatment was performed with a solid loading of 10% and NaOH loading of 20 g/L. The reaction was kept at 60 °C for 2 h stirring every 15 min. Upon the completion of the pretreatment process, the liquid phase (i.e., black liquor) was separated from solid residue and collected by filtration through a 150-mesh sieve, and neutralized to pH 7.0 using 37% HCl. Corresponding salts were added to bring the salinity of black liquor to 100% ASW before use. The total carbon and total nitrogen contents of black liquor were determined by Agriculture Service Laboratory of Clemson University (Clemson, SC, USA).

The suitability of black liquor as the sole carbon source was initially studied in the fermentation of three *Thraustochytrium* species. NH_4Cl was used as the nitrogen source at 12 g/L based on the total carbon content of black liquor. In addition to original black liquor, different dilution factors (2, 5 and 10) using 100% ASW were also applied to prevent the potential inhibition caused by black liquor components. During the fermentation process, samples were taken daily and centrifuged. The cell pellet was washed once with 1 M NaOH and twice with

DDI water to determine cell mass concentration at OD_{600}. The supernatant was used for measurement of total aromatics by using Prussian blue reagent (100).

Due to the superior performance of cell growth in black liquor, *T. striatum* HBS was selected for subsequent study and NH_4Cl concentration ranging from 0.5 to 16 g/L was tested to find the optimal C/N ratio. Fed-batch fermentation was also conducted and compared to the batch fermentation in terms of cell growth, total lignin consumption and accumulation of products. The feeding medium was prepared from black liquor with salinity of 100% ASW and no nitrogen. For feeding operation, the culture was firstly centrifuged at 4,300 rpm for 5 min to discard the spent medium. The cells were then harvested, washed with 100% ASW, and resuspended in the feeding medium. For fed-batch fermentation, the feeding operation was repeated every four days until 16 days.

2.3 Characterization of dynamic changes of black liquor during fermentation

2.3.1 Soluble compounds profile

Black liquor fermentation was performed for characterization of dynamic changes in black liquor composition and structure. The profile of soluble compounds in black liquor was analyzed via GC-MS. Samples taken on day 0, 3, 5, and 7 of fermentation were centrifuged at 4,300 rpm for 5 min and supernatants were collected for analysis. Prior to injection, supernatants were dried on an N-EVAP 112 nitrogen evaporation system at room temperature, and derivatized with methoxyamine hydrochloride (30 mg/mL in pyridine) at 30 °C for 2 h followed by MSTFA (with 1% TMCS) at 37 °C for 1 h. Analysis was performed on Agilent 5973 GC-MS system using electron impact ionization, equipped with an Ultra 2 (5%-phenyl)-methylsiloxane column (Agilent part # 19091B-102). Helium was used as a carrier gas at a constant flow rate of 1.0 mL/min. The injection volume was 1 μL in splitless mode. The oven temperature was maintained

at 80 °C for 5 min and raised to 300 °C at 5 °C/min. The mass spectrometer was operated in full scan mode.

2.3.2 Aromatic monomers quantification and acetic acid analysis

The major aromatic monomers identified in GC-MS were further quantified by the HPLC system (Agilent 1100 series) equipped with the diode array detector (G1315B). Samples were filtered into HPLC vials through 0.2 μm syringe-filters. The analysis of aromatic compounds followed methods described in **Section 2.4, Chapter 2**. For acetic acids, the Aminex HPX-87H Column was used at 30 °C with 50 mM sulfuric acid as the mobile phase. The flow rate was 0.6 mL/min and signals were recorded at 210 nm.

2.3.3 Composition, structure and molecular weight of solids from black liquor

Samples from black liquor fermentation were taken on day 0, 3 and 7 by centrifuge and freeze-dried for 2D ^{13}C-^{1}H HSQC and ^{31}P NMR analysis, to explore the composition and inter-unit linkages of solids from black liquor at different time points. The analysis followed procedures in **Section 2.6**, **Chapter 2** and acquisition parameters were the same as those outlined in **Section 2.7**, **Chapter 3**. The weight-average molecular weight (M_w) and number-average molecular weight (M_n) were analyzed by gel permeation chromatographic (GPC) analysis. Samples were first acetylated on a basis of ~3 mg lignin in 1 mL of pyridine/acetic anhydride (1:1 *v/v*) in the dark at room temperature for 24 h, 200 rpm as previously described (191). The solvent/reagents were removed through co-evaporation at 45°C with ethanol using a rotatory evaporator until dry. The resultant acetylated lignin was dissolved in tetrahydrofuran (THF) and the solution was filtered through 0.45 μm membrane filters before GPC analysis. Size-exclusion separation was performed as described in **Section 2.8**, **Chapter 3**.

2.4 Investigation on effects of initial pH in *T. striatum* HBS fermentation

The previous studies in **Chapter 2** exhibited the preference of *T. striatum* HBS for acidic pH and adaptation abilities under low pH conditions. Therefore, we decided to examine the effect of alkaline pH on the fermentation of black liquor with *T. striatum* HBS in this study in order to decipher if black liquor needs to be neutralized and the neutralization extent in black liquor fermentation. The initial pH was adjusted with 37% HCl to 7, 8, 9, 10, 11, 12, and 13, and black liquor with different initial pHs was used as the sole carbon source for *T. striatum* HBS fermentation. Fermentation with glucose as the carbon source with initial pH values of 3, 4, 5, 6 and 7 were conducted simultaneously to study the effects of acidic pH; alkali pH was not tested for glucose considering the alkaline degradation of glucose. Glucose concentration was set at 20 g/L, and NH_4Cl was used as nitrogen source at 2 g/L for both black liquor and glucose fermentation. Cell growth and total lignin consumption were monitored daily basis. Scanning electron microscopy (SEM) was used to characterize *T. striatum* HBS cells from fermentation with different initial pH values. Cells were mounted on a specimen stub with adhesive tape for sputter-coating with platinum in a coating machine (Hummer 6.2 Sputter System, Anatech USA, Union City, CA) under an Argon atmosphere before observation. Hitachi S-4800 analytical FE-SEM (Hitachi High-Technologies in America, CA) was operated at 5 kV to image the cell surface in response to different pH values.

2.5 Analytical methods

After 7-day incubation, cells were collected, washed and freeze-dried for characterization of fermentation products (i.e. fatty acids and carotenoids) following methods described in **Section 2.5, Chapter 2**. Glucose consumption was determined as described in **Section 2.3**, **Chapter 3**.

3. Results and discussion

3.1 Black liquor fermentation and optimization

3.1.1 Preliminary fermentation of black liquor with three *Thraustochytrium* species

As a byproduct of alkaline pretreatment and pulping industry, black liquor is typically energy-intensive and contains various kinds of components such as lignin, organic acids, aromatics, and carbohydrates(203). In this study, marine protists were investigated as a novel class of microorganisms on biodegradation of black liquor after pH adjustment and supplementation of salinity. Three species- *Thraustochytrium* sp. ONC T18, *T. aureum* and *T. striatum* (both original and HBS strains)-were used and compared. Given the possible inhibition by black liquor, different dilution factors were applied. The best performance on black liquor fermentation was acquired by *T. striatum* HBS (**Figure 4.1**). Without dilution of black liquor, the cell mass concentration increased from initial 0.6 to 2.5 g/L and a 33% reduction of total lignin from 8.2 to 5.5 g/L was observed. When black liquor was diluted, the final cell mass concentration of *T. striatum* HBS decreased as dilution factor increased due to the reduced carbon source. The other two strains were able to grow in diluted black liquor but not in the original black liquor, indicating that some components in black liquor had inhibitory effects on them. Utilization of black liquor by *T. striatum* HBS was further studied to determine whether black liquor could be used as a cheap carbon source alternative to glucose for *T. striatum* HBS fermentation.

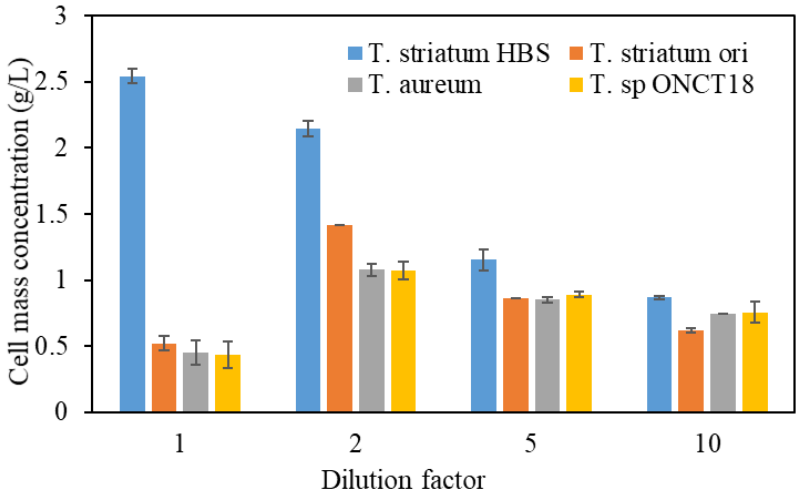

Figure 4.1 Black liquor fermentation with three species of *Thraustochytrium*
T. striatum HBS-high biomass strain of *T. striatum*; *T. striatum* ori-original strain of *T. striatum*.

3.1.2 Effect of C/N ratio on black liquor fermentation with *T. striatum* HBS

To further investigate and improve the fermentation process of black liquor as a carbon source, the fermentation process was optimized on C/N ratio (**Figure 4.2A**). When the concentration of NH_4Cl elevated from 0.5 to 2 g/L, the final concentration of cell mass increased correspondingly, and more cell growth led to higher conversion of total aromatics in black liquor. The maximum cell mass concentration (5.2 g/L) and maximum total aromatics conversion (62%) occurred at 2 g/L NH_4Cl (**Figure 4.2B**). When NH_4Cl concentration further increased, some inhibition effects on cell growth were observed and the final cell mass concentration decreased gradually. After 7-day incubation, the total fatty acids (TFA) content was around 7% at NH_4Cl of 0.5~2 g/L, which was significantly higher compared to NH_4Cl above 8 g/L. The carotenoids content was similar in the studied range of NH_4Cl concentration (**Figure 4.2C**). The optimal NH_4Cl concentration was determined to be 2 g/L and adopted in the following experiments.

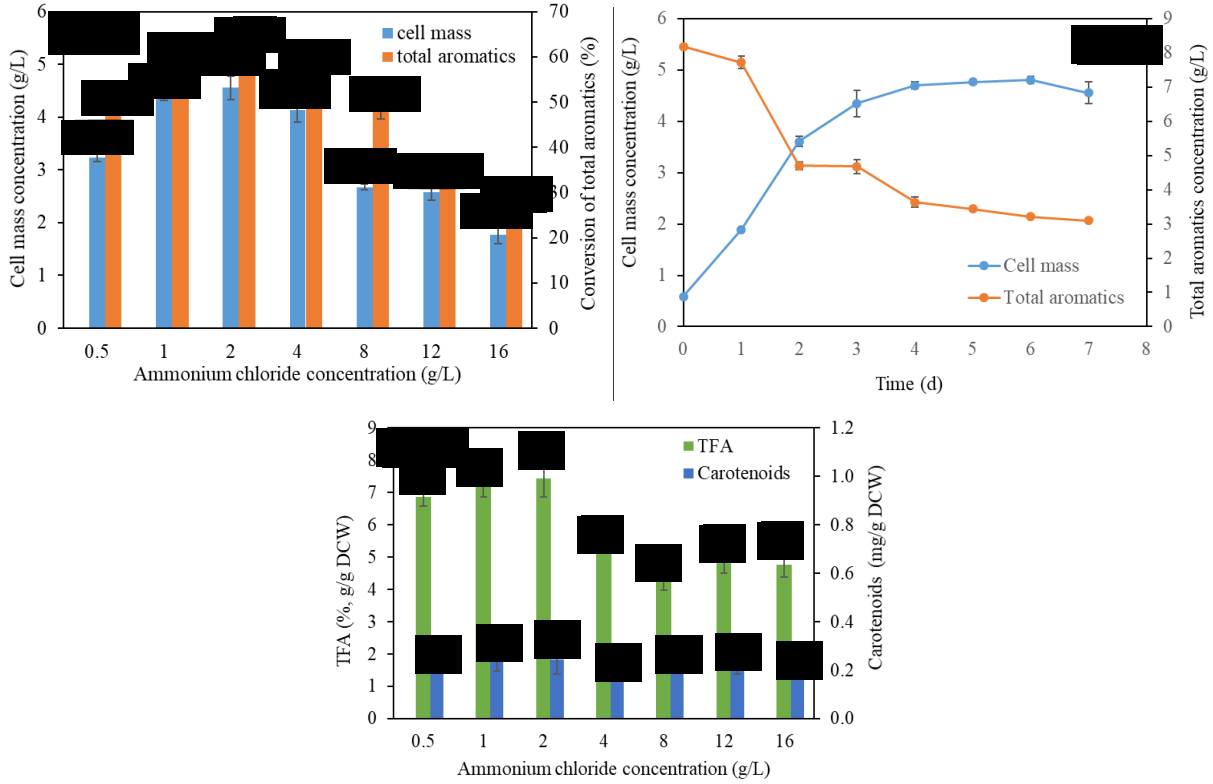

Figure 4.2 Black liquor fermentation of *T. striatum* HBS

(A) effects of C/N ratio on cell growth and total aromatics conversion; (B) fermentation at pH=7 and NH4Cl=2 g/L; (C) effects of C/N ratio on products accumulation. Lowercase letters and Roman numerals indicate statistical analysis results. Levels connecting with different letters/numerals are statistically different.

To improve the accumulation of products, the fed-batch cultivation was compared with the batch mode under optimum conditions (i.e., NH_4Cl=2 g/L without dilution of black liquor) (**Figure 4.3**). In fed-batch mode, the first feed was conducted by replacing 75% of spent medium with fresh black liquor on the 4th day and then repeated every four days. In batch mode, the highest cell mass concentration (4.3 g/L) was achieved on the 5th day. After the cells entered the decay phase, the cell mass concentration began to decrease gradually, leveling off at 2.8 g/L after the 9th day. For fed-batch mode, due to the addition of extra carbon, the cell mass kept growing and reached the final concentration of 5.2 g/L, which was significantly higher than that of batch mode. The total aromatics concentration decreased gradually as microbes consumed it as a

carbon source, and the residual 45% was believed to be compounds that could not be utilized by microbes in batch cultivation. In fed-batch mode, the addition of fresh black liquor brought the total aromatics concentration back to a relatively higher level, while microbes still consumed the added lignin and reduced the concentration to around 3.4 g/L, similar to that in batch mode. After 16-day of incubation, the TFA content of cells obtained in fed-batch mode doubled compared to that on the 8th day, and the carotenoids content slightly increased to 0.24 mg/g DCW. However, the contents of both TFA and carotenoids in batch mode decreased gradually due to cell decay and degradation of cellular components.

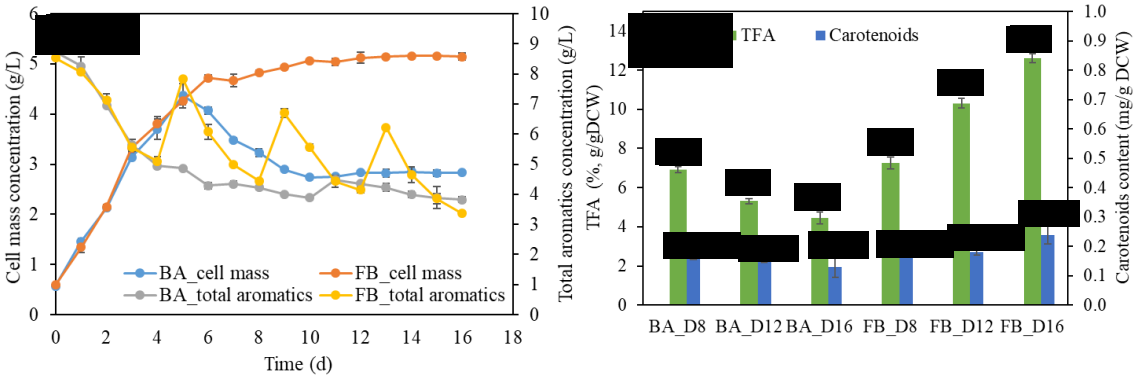

Figure 4.3 Black liquor fermentation with batch mode and fed-batch mode
(A) Cell mass growth and total lignin consumption; (B) accumulation of TFA and carotenoids. Lowercase letters and Roman numerals indicate statistical analysis results. Levels connecting with different letters/numerals are statistically different.

3.2 Characterization of dynamic changes of black liquor during fermentation

3.2.1 Soluble compounds profiling

To acquire the profile of the black liquor compositions, a comprehensive analysis of its soluble compounds was conducted on GC-MS. The consumption of those compounds and generation of new compounds were also tracked at different fermentation stages (**Table 4.1**).

Table 4.1 Variation of soluble compounds of black liquor during fermentation [a, b]

Compound	D1 (%)	D3 (%)	D7 (%)
Alcohol			
Xylitol	41.08	--	--
Erythritol	59.33	34.27	--
D-Mannitol	62.55	31.65	--
Dulcitol	--	--	--
Tyrosol	--	--	--
4-Hydroxybenzyl alcohol	--	--	--
Vanillyl alcohol	--	--	--
Sinapyl alcohol	32.43	--	--
Sugar			
Sucrose	7.24	0.10	--
Lactose	20.86	--	--
Benzyl mannose	17.86	--	--
Glucopyranose	21.54	--	--
Fructofuranose	23.79	--	--
Arabinofuranose	22.68	--	--
Arabinopyranose	19.13	--	--
Galactopyranose	20.11	--	--
Ribofuranose	14.63	--	--
Acid			
Acetic acid [c]	19.19	--	--
p-Coumaric acid	17.17	7.37	3.31
Ferulic acid	33.41	7.77	--
Quinic acid	25.59	7.32	16.74
Glyceric acid	23.91	--	--
D-Gluconic acid	10.80	9.53	--
Glycolic acid	16.40	14.27	--
2-keto-L-gulonic acid	71.86	42.66	20.85
Mannonic acid, 1,4-lactone	15.21	14.31	--
Malic acid	79.53	69.57	--
Hydracrylic acid	--	--	--
Threonic acid	--	--	--

3-Deoxytetronic acid	--	--	--
Succinic acid	45.53	19.64	2.87
Syringic acid*	207.36	414.67	--
Vanillic acid*	1556.47	4329.20	3303.53
4-Hydroxybenzoic acid*	1187.69	2312.67	--
Aldehyde			
Vanillin	--	--	--
4-Hydroxybenzaldehyde	--	--	--
Syringaldehyde	50.69	--	--
Coniferyl aldehyde	--	--	--
Sinapaldehyde	--	--	--
Others			
Acetoisovanillone	--	--	--
2,6-Dimethoxyhydroquinone	--	--	--

Note: [a] All compounds are listed in the order of peak area on D0; "--" indicated "not detected"; [b] The content of each compound at D1, D3 and D7 is expressed as the percentage of peak area on D0 and [c] acetic acid was measured by HPLC; * compounds were generated during fermentation.

Various types of compounds were detected with GC-MS analysis including aromatic compounds from lignin, sugars and sugar alcohols from cellulose and/or hemicellulose. Under alkaline conditions, the degradation of cellulose and hemicellulose produced various organic acids, such as acetic acid, glycolic acid and mannonic acid (204). Several large peaks were observed and assigned to different major compounds including xylitol, quininic acid, benzyl-D-mannose, β-D-glucopyranose, p-coumaric acid, ferulic acid, sucrose, and lactose (**Figure 4.4**). During fermentation, those compounds were typically degraded and converted. Sugars and sugar alcohols were easily biodegraded and quickly consumed in the first three days, while the degradation of most organic acids was completed in later phases of fermentation. Additionally, diverse aromatic compounds were detected including alcohols, aldehydes, acids, etc. Small amounts of both phenolic alcohols and aldehydes were identified and completely consumed within 3 days, while sinapyl alcohol and syringaldehyde were found to remain due to the difficult

conversion and degradation of S-type aromatic compounds. Notably, the content of 4-hydroxybenzoic acid, vanillic acid and syringic acid increased after 3-day incubation reflected by a larger peak, which could indicate the generation of these compounds from the degradation of other components.

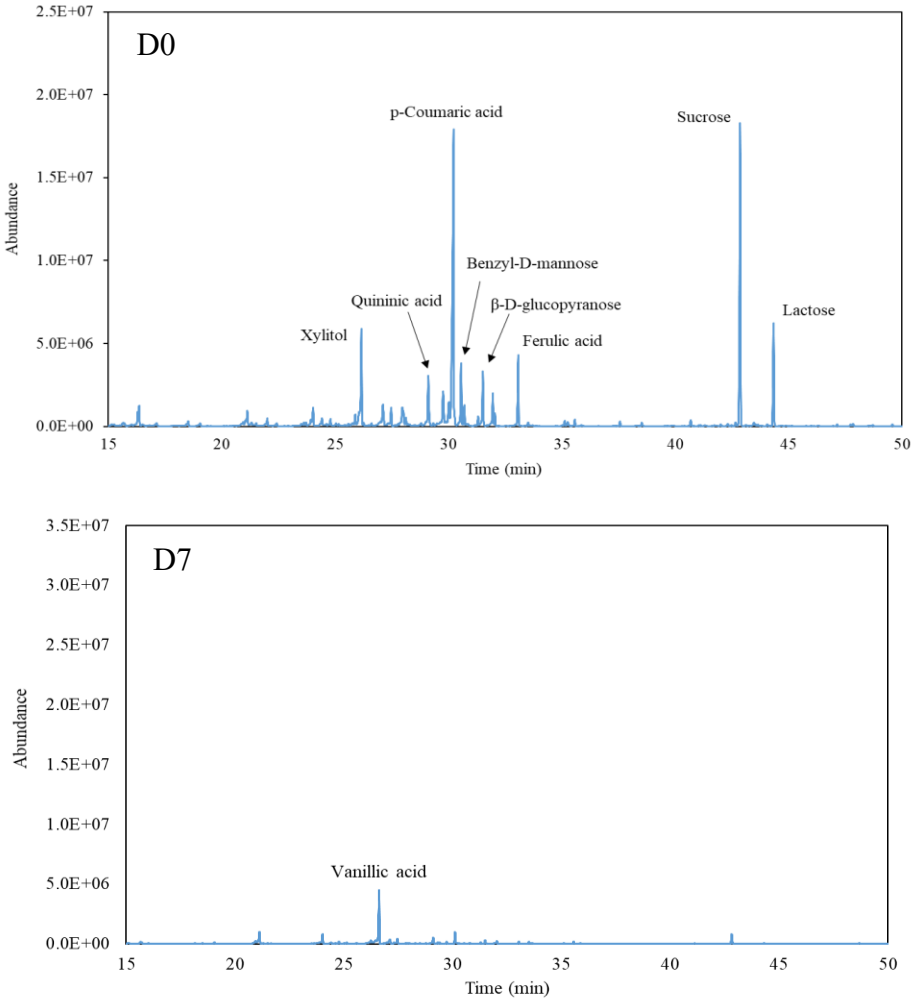

Figure 4.4 Major soluble compounds identified in black liquor with GC-MS before and after fermentation

3.2.2 Consumption and conversion of aromatic monomers

As important monomers of lignin, the degradation of cinnamic acid and its derivatives have been extensively studied, and various microorganisms share several metabolic pathways. The overall profile of soluble compounds in black liquor identified two hydroxycinnamic acids

as major monomers such as *p*-coumaric acid and ferulic acid. Their difference is the methoxyl group on the benzene ring in ferulic acid, which classified them into H- and G-type structures, respectively. These two compounds were quantitatively analyzed by HPLC daily, monitoring their degradation and conversion process. The initial concentration of *p*-coumaric acid and ferulic acid was 1.18 and 0.52 g/L, respectively, and then dropped to nearly zero after three days. Their consumption was accompanied by the production of 4-hydroxybenzoic acid and vanillic acid, whose concentration increased from initially 0.03 and 0.02 g/L to 0.25 and 0.38 g/L on Day 3, respectively. Further utilization of 4-hydroxybenzoic acid and vanillic acid supported the subsequent cell growth as well as synthesis of products. Complete consumption of 4-hydroxybenzoic acid was achieved within one day while the concentration of vanillic acid continued decreasing until the 7th day (**Figure 4.5A**). According to our previous study, *p*-coumaric acid was converted into 4-hydroxybenzoic acid and ferulic acid was converted into vanillic acid. In those reactions, the propenyl group on the side chain of both *p*-coumaric acid and ferulic acid was degraded to form a carboxylic group, which was also observed in most species with the synergism of multiple enzymes (81). Different metabolic pathways such as CoA-dependent β-oxidation pathway, CoA-dependent non β-oxidation pathway and CoA-independent pathway can be employed to achieve this process (85). The accumulation of 4-hydroxybenzoic acid and vanillic acid as degradation intermediates suggested that one or more following steps would be rate-limiting, which could be across-membrane transport, further conversion and/or ring cleavage.

3.2.3 Modifications on lignin structure

In addition to simple aromatic monomers, black liquor contained polyphenolic fragments whose degradation required depolymerization to break complex inter-unit linkages. To confirm

the presence of depolymerization and investigate the microbial modification on structure of solids in black liquor, GPC and NMR analysis were performed to characterize aromatic components of black liquor.

During fermentation, ^{1}H-^{13}C HSQC analysis results (**Figures 4.5C~E**) showed H-type compounds were significantly consumed in the first three days, dropping from 28.7 to 4.4%. The slight increase of S/G ratio indicated that degradation of G-type structures was preferred to S-type, which supports that S-type aromatic compounds are more difficult to degrade due to its two methoxy groups (85). The consumption of total aromatics by *T. striatum* HBS led to increase in the relative abundance of all inter-unit linkages, especially β-O-4 linkage as the major type of inter-unit linkages detected. However, when comparing the decrease of total lignin concentration to the increase of linkage contents, β-O-4, β-β and β-5 linkages were also found to be degraded to a moderate extent. As the result of linkage breakdown, polyphenolic fragments were decomposed into smaller pieces (e.g., dimers and trimers) and monomers, leading to a M_w decrease from 3,736 to 2,048 g/mol (**Figure 4.5B**). From D3 to D7, S/G ratio decreased slightly, suggesting more degradation of S-type lignin as biodegradable parts of G- and H-structure have been mostly consumed. The contents of linkages altered minimally, suggesting that in this period the degradation and consumption of total aromatics primarily resulted from linkage cleavage of oligomers released in the first three days. Components with larger size and more recalcitrant structure were left while low molecular weight components were consumed, resulting in an increase of overall M_w to 4,673 g/mol (**Figure 4.5B**).

Quantitative ^{31}P NMR was performed to analyze the contents of different OH groups in black liquor and their changes during the fermentation process. Results showed that major OH groups were identified as aliphatic OH and carboxyl OH, while guaiacyl-OH and phenolic OH

also existed with less amount (**Figure 4.5F**). Comparison of different samples indicated that the degradation of OH groups mainly occurred in the first three days, as the content of aliphatic OH and carboxyl OH decreased by 84% and 96%, respectively. Meanwhile, all guaiacyl-OH and phenolic OH were degraded. After D3, minimal decrease of OH content was observed.

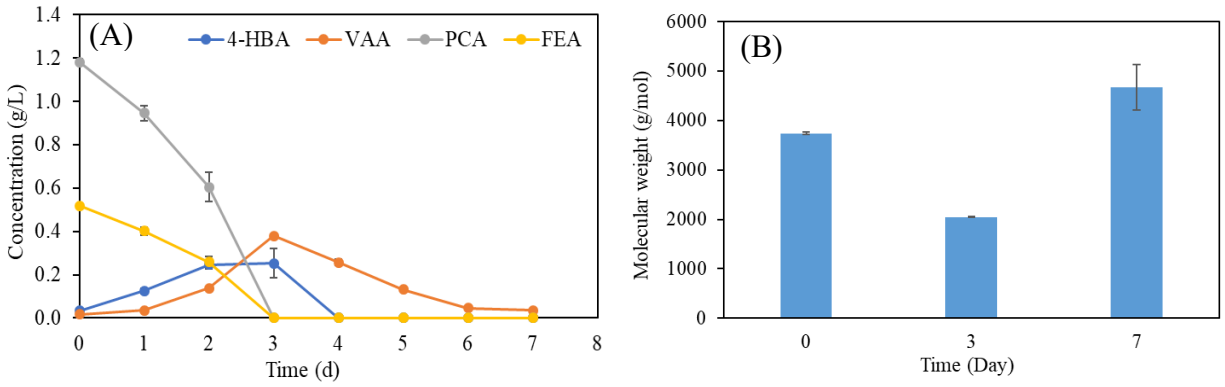

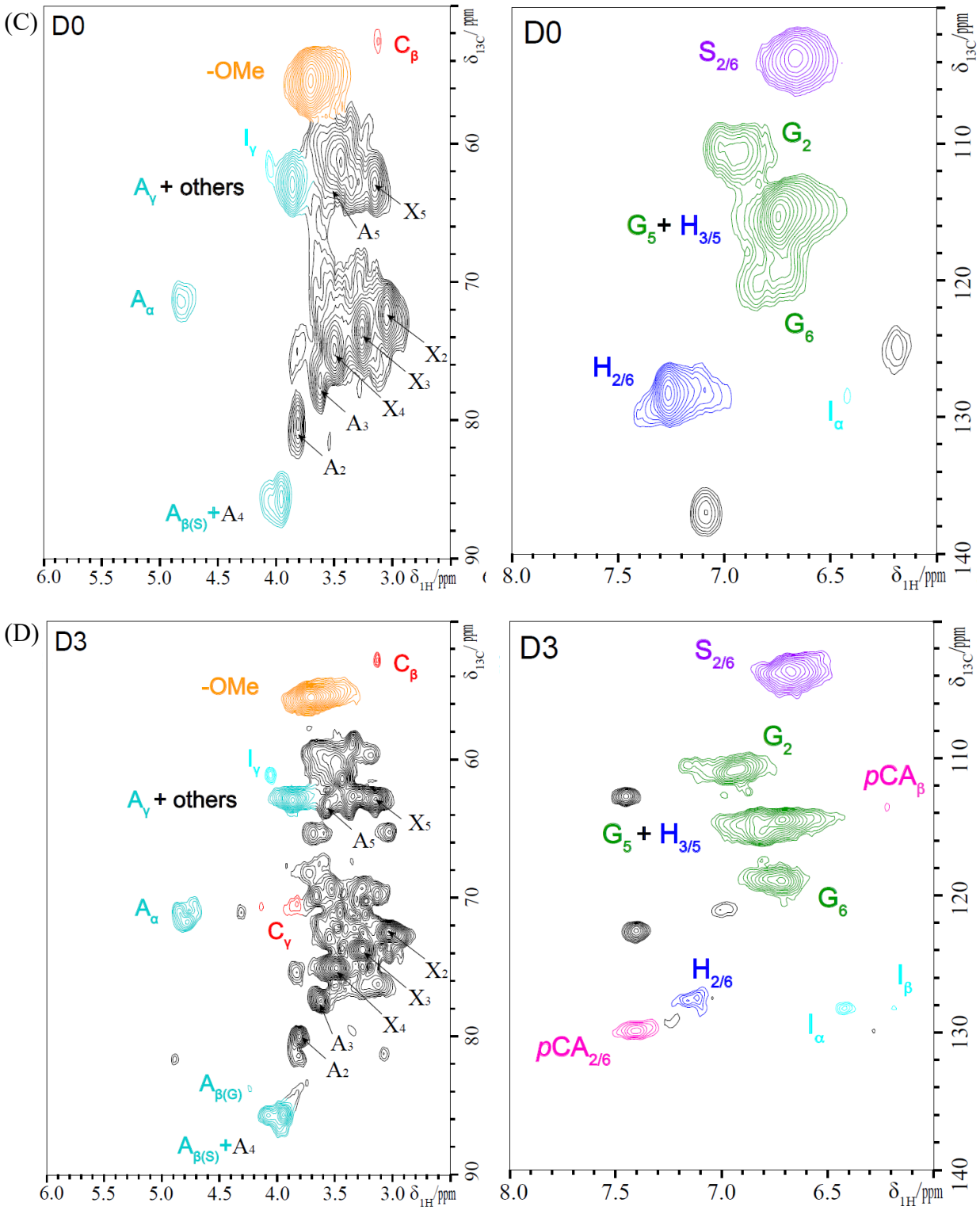
(C)
D0
-OMe
Cβ
Iγ
Aγ + others
X5
A5
Aα
X2
X3
X4
A3
A2
Aβ(S)+A4
δ13C/ppm
δ1H/ppm
D0
S2/6
G2
G5+ H3/5
G6
H2/6
Iα
(D)
D3
-OMe
Cβ
Iγ
Aγ + others
X5
A5
Aα
Cγ
X2
X3
X4
A3
A2
Aβ(G)
Aβ(S)+A4
δ13C/ppm
δ1H/ppm
D3
S2/6
G2
pCAβ
G5 + H3/5
G6
H2/6
Iβ
Iα
pCA2/6

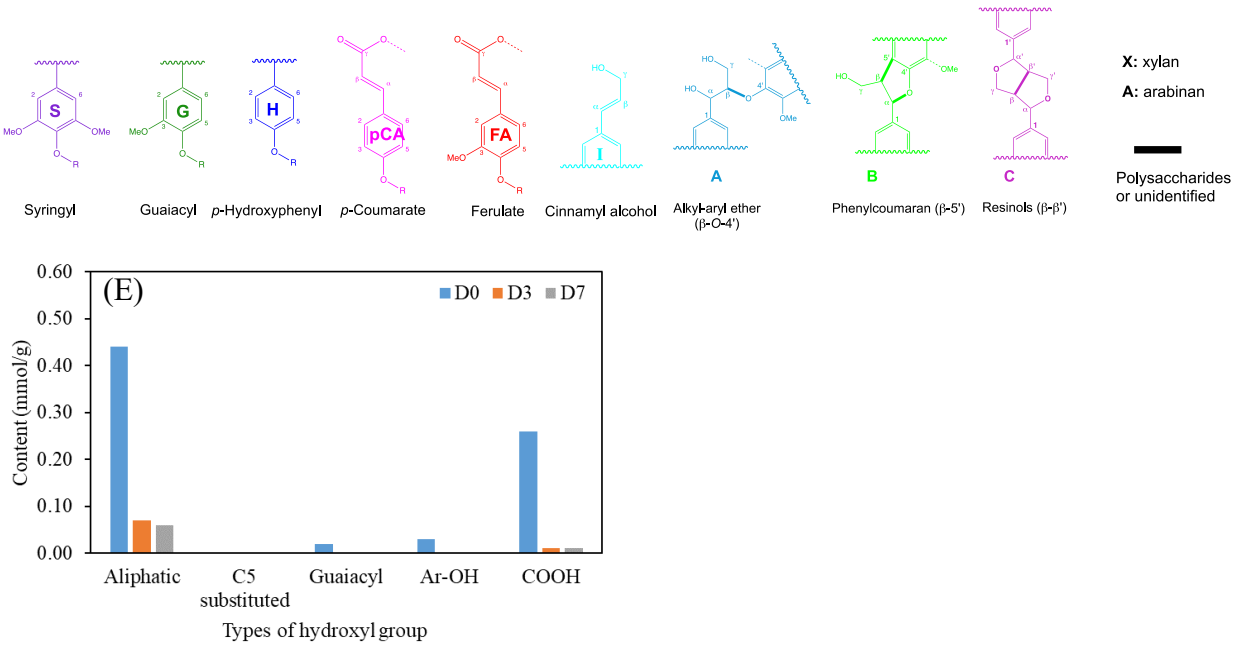

Figure 4.5 Dynamic changes of black liquor during fermentation.
(A) concentrations of major aromatic compounds; (B) molecular weight of black liquor; (C)-(D) contents of subunits and inter-units at different time: left-aliphatic regions and right-aromatic regions; (E) contents of hydroxyl groups.

3.3 Hypothetical metabolic network for black liquor fermentation

When used as the sole carbon source of microbial fermentation, various compounds in black liquor were effectively degraded, and diverse metabolic pathways were involved due to its complex composition. A hypothetical metabolic network can be constructed for black liquor fermentation by searching the detected compounds against metabolic pathway databases (MetaCyc and KEGG) (**Figure 4.6**). Sugars and sugar alcohols were primarily metabolized through glycolysis and pentose phosphate pathway, in which many organic acids were identified as important intermediates. Aromatic compounds were funneled to certain compounds and further degraded via the aromatic ring cleavage pathway. Different metabolic processes converged at critical joints, developing a complex, interactional metabolic network. During alkaline pretreatment, solubilization of cellulose and hemicellulose is the major source of sugars and sugar-derived components (e.g. sugar alcohols, sugar acids) (204), which were the most

biodegradable substrates and consumed the quickest among all detected compounds. Oligosaccharides (e.g. sucrose and lactose) need to be hydrolyzed with corresponding hydrolase (sucrose invertase and lactase) first. Glucose, fructose and galactose were generated from the hydrolysis process and subsequently entered the glycolysis process after a series of isomerization and phosphorylation. Meanwhile, pentose coming from hemicellulose (e.g. arabinose, mannose and xylose) would be directed into the pentose phosphate pathway. The degradation of sugar alcohols and sugar acids released products, which were also funneled into sugar metabolism to serve as intermediates. Pyruvate as the final product of sugar metabolism then entered central metabolism for energy release and reducing power production.

Alkaline pretreatment also caused solubilization of lignin component of biomass, and in black liquor they were present as simple aromatic monomers and polyphenolic fragments. In this study, the herbaceous corn stover containing S, G and H-type lignin subunits was used, and alkaline treatment led to release of all three types of monomers such as *p*-coumaric acid, ferulic acid and syringaldehyde. Polyphenolic components were also depolymerized by extracellular enzymes secreted by *T. striatum* HBS. Through the breakdown of inter-unit linkages such as β-O-4, β-5 and β-β linkage, more simple aromatic compounds were released. Those compounds were further converted following general patterns. Alcohols were oxidized to aldehydes and then to acids. The synergy of multiple reactions such as dehydrogenation and decarboxylation reduced the side chain on the benzene ring and generally converted methoxy group into hydroxyl group. With the above-mentioned "funneling process", G- and H-type compounds were converted to protocatechuate, and S-type compounds were converted into 3-O-methylgallate through ring cleavage. Ortho-cleavage followed by β-ketoadipate pathway was adopted as the mainstream pathway to open the ring structure of protocatechuate with various oxidoreductase

(85). For other hydroxybenzoic acids and derivatives, special cleavage pathways also possibly exist. For example, when 4-hydroxybenzoic acid was present in high concentrations, it was possibly directly cleaved rather than funneled further. After cleavage, the ring structure was converted into a 6-carbon linear structure, which can be divided into succinyl-CoA (C4) and acetyl-CoA (C2) or two pyruvates (C3) prior to entering central metabolism. The energy and reducing power released from substrate degradation would finally be used for cellular activities such as cell growth, maintenance and accumulation of microbial products.

Figure 4.6 Hypothetical metabolic pathway of compounds in black liquor
Red node: compounds detected; yellow node: compounds speculated.

3.4 Effects of initial pH on fermentation of black liquor and glucose

In our previous study, *T. striatum* HBS was observed to secrete extracellular acids which would decrease the pH of fermentation broth from initial neutral value to around three. It also suggested a strong adaptation of *T. striatum* HBS to extreme conditions, especially acidic environments. To comprehensively investigate the effects of medium pH on *T. striatum* HBS fermentation, black liquor and glucose were used as carbon sources in alkaline (pH=7-13) and acidic pH (pH=3-7) ranges, respectively (**Figure 4.7**). In black liquor fermentation, higher initial pH caused inhibition on cell growth indicated by the decreased cell mass concentration with

initial pH elevating (**Figure 4.7A**). However, significant cell growth and total aromatics consumption were observed until the initial pH of black liquor was increased to 11, suggesting that *T. striatum* HBS was able to tolerate pH as high as 11 and keep normal functions. Upon the completion of fermentation, the final medium pH values were found to decrease by around 1.0 except initial pH=7. For fermentation products, TFAs were accumulated to above 15% of DCW with initial pH 7~9, while higher initial pH disrupted the biosynthesis of fatty acids and caused low TFA contents (**Figure 4.7B**). In glucose fermentation, variations on initial pH from 3-7 resulted in limited effects on cell growth and glucose consumption. With low initial pH of three, a slightly higher glucose utilization percentage was acquired which was reflected in higher TFA content (**Figures 4.7C&D**). As the fermentation process completed, the final pH values of all treatment decreased to around three, which was consistent with our previous results.

To make black liquor fermentation and glucose fermentation comparable, the loading of glucose was decided at 20 g/L. Significantly higher cell mass concentration was obtained from black liquor fermentation even with some inhibition caused by high initial pH values, compared to around 2 g/L from all glucose fermentation. Black liquor and glucose were completely different types of carbon source with different biodegradability. When used for microbial metabolism, the efficiency of energy production was different and generated distinct profiles of metabolites. The diverse small molecule compounds existing in black liquor can be further degraded or directly used for biosynthesis of cellular components (e.g. nucleotides, amino acids and carbohydrates). Consequently, the carbon flux to bioproduct accumulation would decrease, leading to relatively lower contents.

SEM was used for cell imaging to show the effects of initial pH on cell morphology (**Figure 4.8**). Many folds and protrusion were observed on the cell surface, which may be

responsible for mass transfer, signaling and other functions connecting extracellular and intracellular environment. Compared with neutral condition, cell morphology was barely affected by low pH and exhibited little difference in surface structure and cell size (**Figures 4.8C&D**). On the contrary, extremely high pH, such as 13, caused significant size reduction of cells and the observed textures (**Figures 4.8A&B**). In response to strong alkalinity, cells tended to shrink and developed a smooth surface to reduce contact with the external environment and resist the adverse conditions. Based on the results, the mechanisms employed by *T. striatum* HBS in response to extreme pH values can be proposed. Enzymes involved in metabolic processed are present with high stability indicated by unaffected cell growth and product accumulation in pH range of 3~9. An extremely robust cell wall structure is also responsible including diverse cell surface protein with strong tolerance to environmental pH. When pH keeps increasing, cell wall with high intensity may be developed to protect intracellular components from damage under alkaline condition. Consequently, material transport and exchange would be restricted which limited substrate adsorption and therefore cellular activities. In addition to adaptation, *T. striatum* HBS also showed the ability to modify the surrounding environment. The secretion of extracellular acids and the presence of abundant extracellular polymeric substance (EPS) (205) can serve as a buffering system for self-protection as well as adjustment of the vicinal environment to desired conditions. For example, the EPS of cyanobacterium *Microcystis aeruginosa* has been proven to buffer against the biocidal effect of H_2O_2 by effectively scavenging radicals (206). EPS can also protect cells by adsorbing hazardous materials such as heavy metals (207) and antibiotics (208). Considering the strong adaptation of *T. striatum* HBS to wide range pH, it is a promising candidate for wider applications such as bioremediation of sites with pollutants such as acids and aromatics.

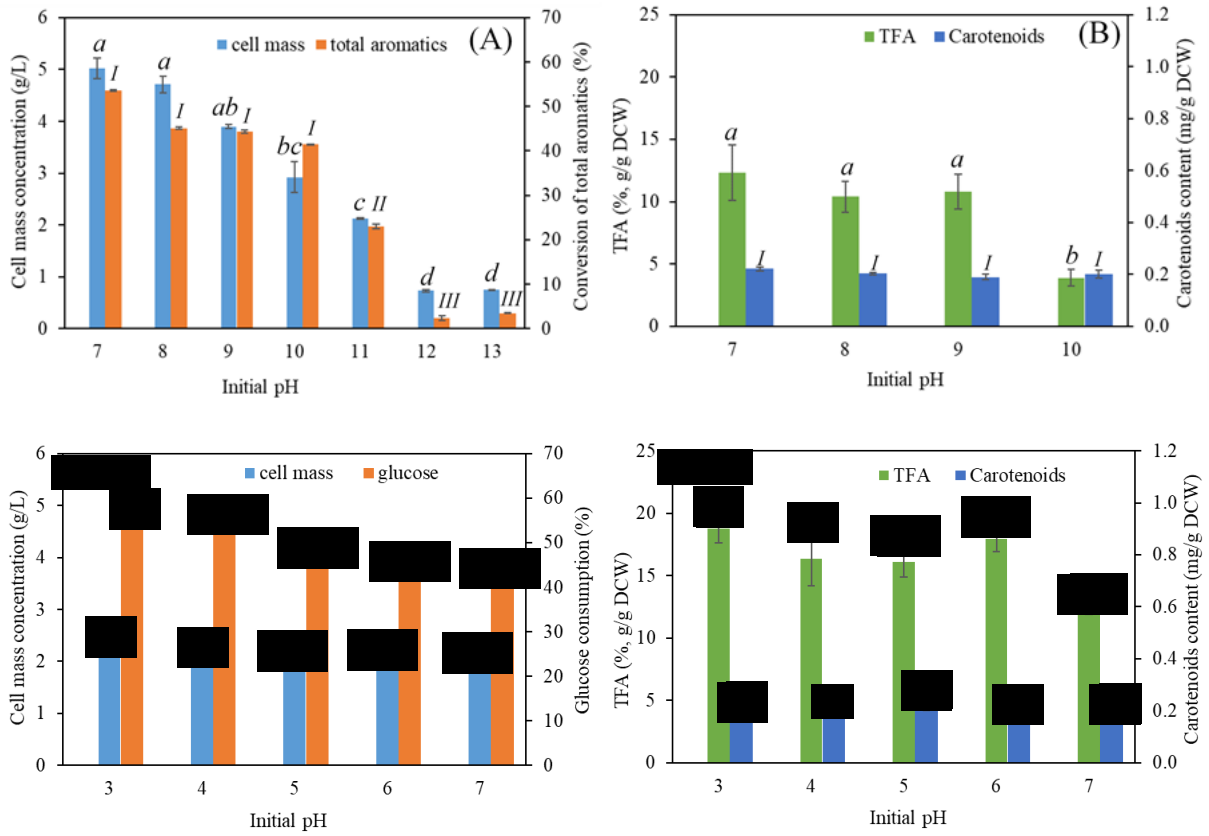

Figure 4.7 Fermentation with different initial pH values

(A) Cell growth and total lignin consumption in black liquor fermentation; (B) accumulation of TFA and carotenoids in black liquor fermentation; (C) cell growth and glucose consumption in glucose fermentation; (D) accumulation of TFA and carotenoids in glucose fermentation. Lowercase letters and Roman numerals indicate statistical analysis results. Levels connecting with different letters/numerals are statistically different.

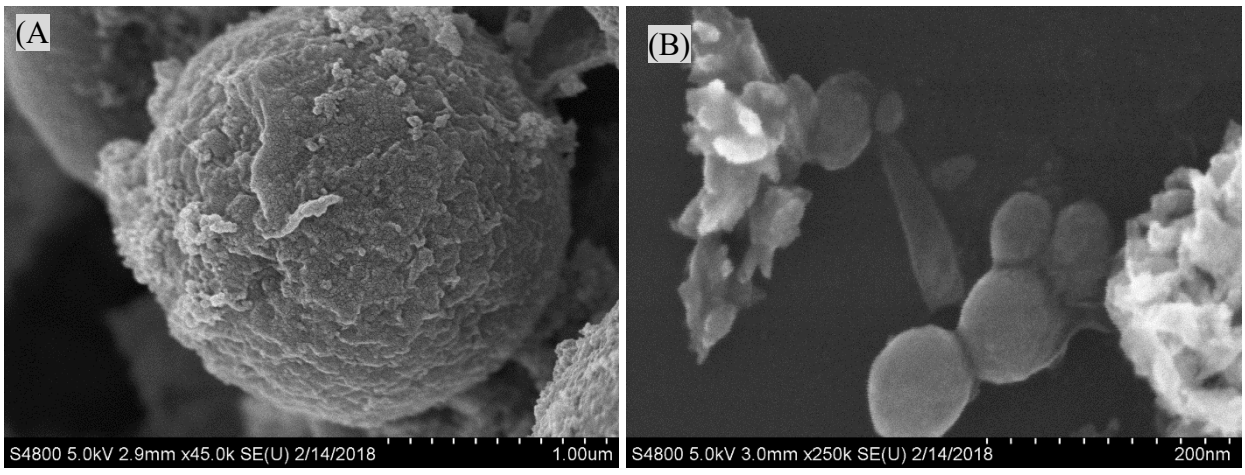

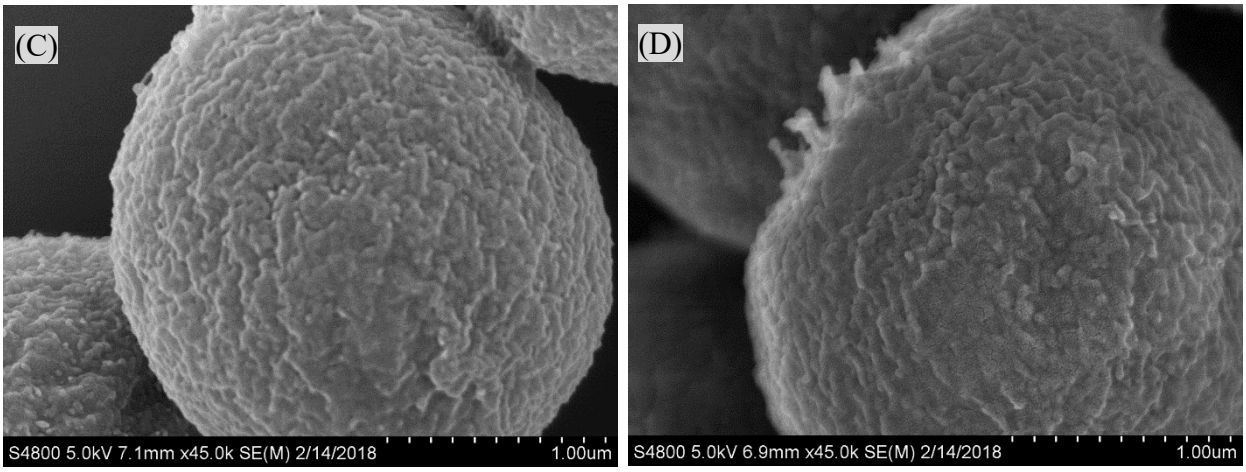

Figure 4.8 SEM images of *T. striatum* HBS cell under different fermentation conditions
(A) Black liquor fermentation with pH=7; (B) black liquor fermentation with pH=13; (C) glucose fermentation with pH=7; (D) glucose fermentation with pH=3.

4. Conclusions

Black liquor can be used as carbon and energy sources for protist fermentation. In this study, marine protist *Thraustochytrium* was studied as a novel class of lignin degrader for bioconversion of black liquor obtained from alkaline pretreatment of corn stover. Among three species tested, the HBS of *T. striatum* was found to be the most effective, which was able to utilize black liquor for cell growth and product accumulation. A general composition profile showed that various sugars, sugar alcohols and organic acids were contained in black liquor, all of which were consumed during the fermentation process. Lignin and lignin-derived aromatic compounds were identified as main substrates of *T. striatum* HBS fermentation. The *T. striatum* HBS was able to not only degrade simple aromatic monomers but also break down inter-unit linkages (e.g., β-O-4 linkage) and depolymerize polyphenolic fragments of lignin. The metabolic versatility of *T. striatum* HBS was observed in black liquor fermentation, as diverse metabolic processes were involved in degradation of various black liquor components as well as biosynthesis. A strong adaptation to a wide pH range was found for *T. striatum* HBS. It was able to grow with no inhibition under acidic conditions, and alter alkaline environments by secreting

extracellular acids. Such robust adaptive ability of the *T. striatum* HBS may result from highly stable enzymes to pH stress and EPSs as a buffering system, which makes it a promising candidate to be used for more applications under extreme conditions.

Chapter 5 - Investigation on metabolism of *T. striatum* HBS

1. Introduction

As an important component of lignocellulose, lignin has attracted increased attention for use as feedstock in producing sustainable fuels and chemicals due to its high-energy content and versatile structure. Extensive studies have been performed on lignin valorization through biological platforms. Many species in nature have been isolated with lignin modification and degradation abilities, and various bioproducts have been identified in lignin fermentation. For example, *Rhodococcus opacus*, a well-known lignin-degrading bacterium, can produce lipid from lignin, and *Pseudomonas putida* can accumulate PHA. However, the major disadvantages of biological platform for lignin conversion are slow reactions and low efficiency compared to thermochemical lignin conversion. To overcome the limitation of the biological process and better utilize the biosynthetic power of microbes, extensive research has been conducted on lignin metabolism to illustrate the detailed metabolic process of lignin and identify the key steps to improve lignin bioconversion. The understanding of lignin metabolism built a basis to develop genetic and metabolic strategies that aim to improve the efficiency of lignin degradation and carbon flux toward the target product. The pathways of lignin degradation can be redesigned to obtain more types of products, such as dicarboxylic acid and vanillin.

In our previous studies, the HBS of *T. striatum* was proven to be a promising candidate for lignin bioconversion. It can utilize various lignin-type substrates and synthesize multiple microbial products including lipid and carotenoids which are important antioxidants. This strain exhibited a strong adaptive ability to grow in black liquor from alkaline pretreatment of corn stover as shown in **Chapter 4**. Cell mass increased and product accumulation was achieved while limited inhibitory effects caused by black liquor were observed. During the process of

black liquor fermentation, lignin served as an important substrate and other components such as carbohydrates and organic acids were efficiently consumed. These findings suggested that in addition to the ability of lignin metabolism, this strain also has a powerful stress regulation system, which can maintain a stable status under extreme conditions. However, as a new lignin degrader, little information is available on its performance on lignin bioconversion and the underlying mechanisms for lignin metabolism remain unknown.

This study aims for systematical investigation on black liquor bioconversion by *T. striatum* HBS with multi-omics analysis. Metabolomics analysis was first conducted to detect intracellular metabolites generated from black liquor fermentation and illustrate the degradation of different components. A reference transcriptome was constructed by RNA sequencing to perform a comprehensive analysis of gene composition and the metabolic potential of *T. striatum* HBS. In addition to aromatics metabolism, special attention was paid to biosynthesis of microbial products (e.g. fatty acids and carotenoids). These results would be the knowledge basis to illustrate the mechanisms of both degradation and adaptation of *T. striatum* HBS, which would contribute to achieving direct utilization of lignin-rich industrial waste. Novel genes and enzymes identified would provide resources to construct promising metabolic pathways and improve the efficiency of lignin biological valorization to desired value-added bioproducts.

2. Materials and methods

2.1 Black liquor fermentation

The HBS of *T. Striatum* ATCC24473 was cultured as described in **Section 2.1**, **Chapter 2**. The black liquor preparation and fermentation followed the operation in **Section 2.2**, **Chapter 4**.

2.2 Metabolomics analysis

Samples were taken on day 3, 5 and 7 to track the profile of intracellular metabolites during black liquor fermentation. Cells were harvested from 20 mL culture by centrifugation at 4,300 rpm for 5 min and then washed with 0.1M NaOH once and DDI water twice. For metabolite extraction, 5 mL of cold 100% methanol was added, and the mixture was sonicated for 5 min (with 30% amplitude and 30 s intervals for every minute). After centrifugation at 4,300 rpm for 15 min at 4 °C, the clear supernatant was collected and dried using a nitrogen evaporator. Prior to injection into GC-MS, samples were derivatized with 50 µL methoxylamine hydrochloride (30 mg/mL in pyridine) at 30 °C for 2 h, followed by derivatization with 50 µL MSTFA in 1% TMCS at 37 °C for 1 h.

GC-MS analysis was performed on an Agilent 6890N GC coupled to an Agilent 5973N quadrupole mass selective detector equipped with an Ultra 2 (5%-phenyl)-methylsiloxane column (Agilent part # 19091B-102). Helium was used as carrier gas at a column flow rate of 1 mL/min. The injection volume was 1 µL in splitless mode. The oven temperature was initially maintained at 80 °C for 5 min and raised to 300 °C at 8 °C/min, holding for another 5 min. The mass spectrometer was operated in full scan mode from m/z =50 to 650.

2.3 Transcriptomics analysis

A reference transcriptome for *T. striatum* HBS was constructed by sequencing of mRNA from different conditions to build up a database of genes expressed during microbial activities. For total RNA extraction, samples from fermentation with different carbon sources (glucose and black liquor) were taken at different time points (day 3, 5 and 7). Cells were harvested with centrifugation at 4,300 rpm for 5 min, and then washed with cold phosphate buffered saline (PBS). Total RNA was extracted with dry ice grinding plus TRIzol reagent and then purified

with PureLink™ RNA mini kit (Invitrogen Inc., CA, USA) by following the manufacturer's instruction. Total RNA from different samples was mixed and sent to Novogene Company (Sacramento, CA) for sequencing and data analysis. For library preparation, mRNA was enriched from total RNA using oligo (dT) beads and synthesized into cDNA after fragmentation. The sequencing was performed at Illumina platform and the raw data was recorded in a FASTQ file. Reads containing adapters and reads of low quality were removed to obtain clean reads, which were used for transcriptome reconstruction by Trinity (209). Corset was used for hierarchical clustering analysis to remove redundancy (210). Contigs assembled from reads were clustered based on shared reads in which those with a low number of mapped reads were filtered out. Next, the longest transcripts from each cluster were selected as unigenes which were functionally annotated against seven databases [Gene Ontology (GO) (http://www.geneontology.org/), Eukaryotic Orthologous Groups (KOG) (http://www.ncbi.nlm.nih.gov/COG/), Kyoto Encyclopedia of Genes and Genome (KEGG) (http://www.genome.jp/kegg/), NCBI non-redundant protein sequences, NCBI nucleotide sequences, Pfam (http://pfam.xfam.org), and Swiss-Prot (http://www.ebi.ac.uk/uniprot/)]. The annotated genes were then classified based on GO and KOG terms as well as the KEGG pathway.

3. Results and discussion

3.1 Intracellular metabolite profile during black liquor fermentation

During fermentation, components of black liquors were first degraded by extracellular enzymes into simple compounds and transported into cells as substrates for microbial activities. Then, those compounds were further degraded and converted, and different cellular components were synthesized, constituting an intracellular metabolome with high diversity. With GC-MS

based analysis, the detected intracellular metabolites were classified into different groups (**Table 5.1**). Three aromatic compounds, 4-hydroxybenzoic acid, vanillic acid and syringic acids, represented final products of the funneling process from H-, G- and S-type lignin subunits. They were found to be transported from extracellular environments into cells, and generation of 3,4-dihyroxybenzoic acid from those three compounds were observed prior to aromatic ring cleavage. Additionally, benzoic acid was detected and possibly synthesized by microbes as a precursor to intracellular aromatic components such as aromatic amino acids. In addition to aromatics from lignin, alkaline pretreatment also solubilized cellulose and hemicellulose which were present in black liquor as monosaccharides, oligosaccharides, sugar alcohols and acids from reactions with alkali. Those carbohydrates were assimilated by cells to serve as another type of important substrate. Oligosaccharides such as sucrose, mannobiose and cellobiose generated from hydrolysis of polysaccharides were detected, which were further degraded into monomers such as glucose and mannose. The metabolism of those sugars produced many kinds of phosphorylated sugars for electron and energy transfer.

The degradation of substrates (e.g., aromatics and sugars) would generate energy and reducing power, which would be used for various biosynthetic processes to produce cellular components (e.g., amino acids, structural carbohydrates and lipids) and energy storage compounds. New kinds of carbohydrates such as maltose were detected, possibly synthesized by cells. However, in most cases, it is hard to differentiate cell-synthesized sugars from the medium-contained sugars. Amino acids with relatively simple structures, such as alanine and serine, were detected at the beginning of black liquor fermentation due to their fast synthesis. Among those amino acids, glutamic acid and aspartic acid were the most abundant species. After 3-day fermentation, more types of amino acids were synthesized such as proline, tyrosine and

tryptophan. Their complex structure (e.g., ring structure) explained that their synthesis required more time and reactions. Ornithine, a special amino acid, was also detected, which is generally involved in protein molecules and an important intermediate for biosynthesis of other amino acids. Diverse compounds involved in the metabolism of fatty acids and lipids were detected because of *T. striatum* HBS's ability to accumulate fatty acids. Saturated fatty acids were present with different chain lengths, such as hexanoic acid (C6), myristic acid (C14), palmitic acid (C16), stearic acid (C18), and lignoceric acid (C24). Short-chain fatty acids were synthesized fast and detected in the first three days. After continuous chain elongation, more fatty acids with medium- to long-chain length were formed. Palmitic acid and stearic acid were two major types of fatty acids accumulated by *T. striatum* HBS. Primary unsaturated fatty acids detected were C18 with one or two unsaturated bonds, such as oleic acid and linoleic acid. Ergosterol which is usually a cellular membrane component, was also detected as well as stigmasterol and beta-sitosterol.

The most versatile type of compounds detected in cells were organic acids (excluding fatty acids). For many microbial metabolic processes, organic acids can function as important intermediates, carriers of electron or links between different reactions. Acids involved in citric acid cycle including succinic acid, citric acid and malic acid, were detected which serve as essential joints for the central metabolism and connect catabolism and anabolism. Other organic acids also have critical roles in different metabolic processes. For example, methylmaleic acid is involved in valine biosynthesis. Most sugar metabolism would generate pyruvic acid as important product, which could enter citric acid cycle for energy release.

Table 5.1 Intracellular metabolites during black liquor fermentation

Aromatic compounds	**Carbohydrates**
4-hydroxybenzoic acid	D-Glucose
Vanillic acid	Lactose
Syringic acid	D-Galactose
Protocatechuic acid	Sucrose
Benzoic acid	3-α-Mannobiose
Amino acid	2-D-Mannopyranose phosphate
L-Alanine	6-phosphate-D-Mannose
Glycine	6-phosphate-D-Glucose
Proline	2-D-Glucopyranose phosphate
L-Valine	3-α-Mannobiose
Threonine	D-fructose
L-Aspartic acid	2-D-Mannopyranose phosphate
L-Glutamic acid	L-(+)-Threose
L-Glutamine	D-(+)-Cellobiose
L-Serine	
Ornithine	
Tryptophan	
Tyrosine	
Fatty acids & lipids	**Organic acids**
Ergosterol	Lactic acid
Stigmasterol	Glycolic acid
β-sitosterol	Pyruvic acid
Hexanoic acid	2-Hydroxybutyric acid
Myristic acid	4-(Dimethylamino)butyric acid
Plamitic acid	2-Ketobutyric acid (enol)
Steric acid	Succinic acid
Archidic acid	Methylsuccinic acid
Behenic acid	2-ketocaproic acid
Lignoceric acid	Itaconic acid
Cerotic acid	Methylmaleic acid
Leinoleic acid	Malic acid
Oleic acid	Citric acid
Vaccenic acid	5-Hydroxyindoleacetic acid

3.2 Analysis of reference transcriptome

3.2.1 Sequencing and assembly of reference transcriptome

To construct a reference transcriptome of *T. striatum* HBS, mRNA mixture from different fermentation conditions was sequenced with Illumina platform, generating 53,140,146 raw reads. After filtering and quality check, 51,818,876 clean reads were obtained and assembled into 12,366 transcripts (**Table 2**).

Table 5.2 Statistics of sequencing and assembly results

Total reads	53,140,146
Clean reads	51,818,876
N rate	0.91%
GC content	62.14%
Total number of transcripts	12,366
Min. length	201 bp
Max. length	20194 bp
Mean length	1992 bp
N50 transcript length	2953 bp
N50 transcript length	1005 bp

3.2.2 Unigene functional annotation and classification

After assembly, the identified unigenes were annotated and mapped into different classes based on several strategies to better describe and analyze the gene composition of *T. striatum* HBS (**Figure 5.1**). Among 12,307 unigenes detected, 64.97% were annotated in GO database and assigned into 55 groups in three main GO categories: cellular component, molecular function and biological process. The largest number of annotated unigenes was related to biological process, followed by cellular component and molecular function (**Figure 5.1A**). BLAST searched against the Eukaryotic Clusters of Orthologous Groups (KOG) database was performed for unigenes and 42.13% were classified into 25 KOG groups. The cluster of general function

prediction only (12.69%) represented the largest group, followed by posttranslational modification, protein turnover, chaperones (9.97%), translation, ribosomal structure and biogenesis (7.72%) and signal transduction mechanisms (7.65%) (**Figure 5.1B**). For KEGG pathway annotation, 3,584 unigenes were classified into 32 metabolic processes, led by translation (10.05%), signal transduction (8.665%) and endocrine system (6.35%) (**Figure 5.1C**). To our interest, 150 genes and 26 genes fall into the group of lipid metabolism and metabolism of terpenoids/polyketides, respectively. These two metabolic processes were directly related to synthesis of microbial products, fatty acids and carotenoids. In the 180 genes assigned to overview of microbial metabolism, five genes were involved in the degradation of aromatic compounds.

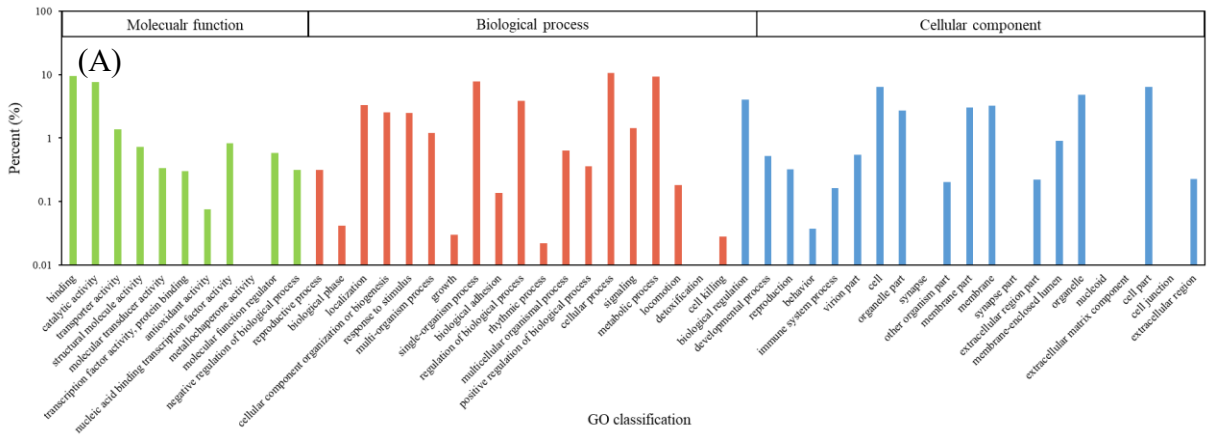

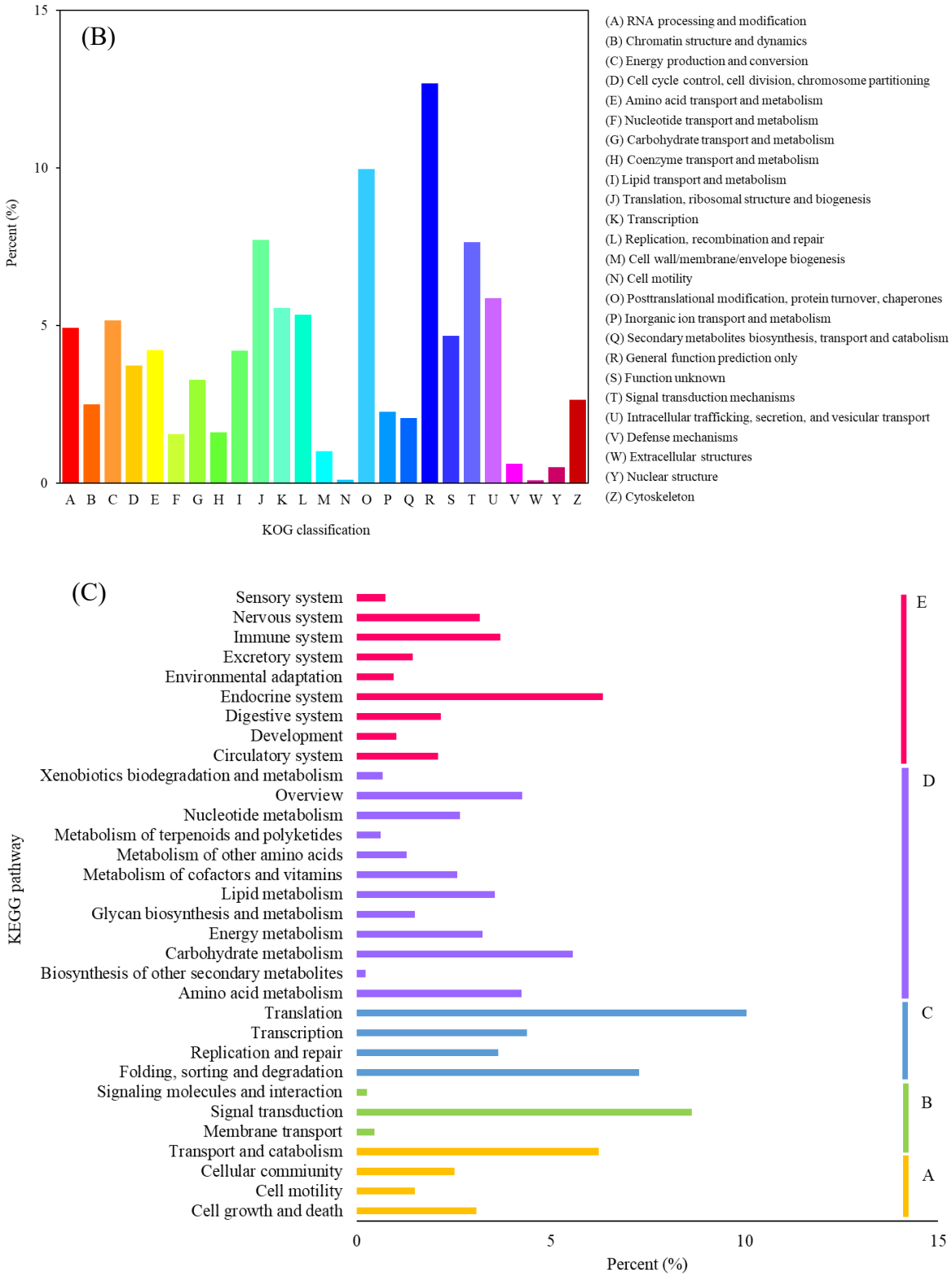

Figure 5.1 Classification of *T. striatum* HBS unigenes

(A) by GO term; (B) by KOB term and (C) by KEGG pathway. A: cellular process; B: environmental information processing; C: genetic information processing; D: metabolism; E organismal systems.

3.3 Investigation of metabolic process in *T. striatum* HBS

After classifying unigenes based on their metabolic functions, a comprehensive analysis of genes related to lignin degradation was performed, as well as biosynthesis of fatty acids and carotenoids. MetaCyc database (https://biocyc.org/) was used as a reference to construct corresponding metabolic pathways and the transcriptome of *T. striatum* HBS was searched for enzymes involved in those processes based on the annotation results with Swiss-Prot.

3.3.1 Lignin degradation

During fermentation of lignin-type substrates, *T. striatum* HBS was observed to degrade both simple aromatic compounds and technical lignin which is highly polymerized. In the transcriptome, multiple kinds of oxidase/reductase were identified, which can be responsible for the degradation process, especially the oxidative lignin depolymerization (**Table 5.3**). For example, genes having high homology with the laccase gene of two yeast species (*Cryptococcus neoformans* and *Rhodotorula glutinis*) were detected. Those enzymes have copper as ligand and oxidize polymeric phenol at diverse positions to release aromatic monomers, which were funneled into certain types of intermediates with the co-function of various enzymes, such as iron- and zinc-containing alcohol dehydrogenase, aldehyde dehydrogenase and lyase. Catechol dioxygenase-type enzymes catalyze ring cleavage at ortho position, which is the mainstream way for aromatic compound degradation. The detection of 4,5-DOPA dioxygenase extradiol, which opens cyclic ring between C4 and C5, indicated the presence of special meta cleavage pathway (211). Such a pathway can be used for direct degradation of 4-hydroxybenzoic acid and saving the step of conversion into protocatechuic acid.

- Lipid metabolism

As a marine protist, *Thraustochytrium* species have been studied as a biomanufacturer of polyunsaturated long-chain fatty acids (PULCFA), which are of great importance in pharmaceutical or nutraceutical fields. A comprehensive analysis of genome of one strain, *Thraustochytrium* sp. ATCC 26185, was performed and confirmed the biosynthesis and assembly pathways of PULCFA (212). The analysis of *T. striatum* HBS reference transcriptome has found various lipid metabolism processes, including biosynthesis of fatty acids, glycerolipid, glycerophospholipid and steroids, were contributed by different numbers of genes. Special attention was paid to the production of PULCFA, which consist of several steps from fatty acids biosynthesis, elongation and desaturation. Acetyl-CoA generally served as the starting point of fatty acid biosynthesis, and the chain length elongation was achieved through recurring addition of malonyl-CoA. After the chain length reached 16 carbon, enzymes such as reductase and desaturase mad modifications, generating unsaturated fatty acids. Among all fatty acids-relating genes, a high similarity with one yeast species, *Schizosaccharomyces pombe*, is observed.

- Carotenoids biosynthesis

Carotenoids, a type of terpenoid, are effective antioxidants and can be accumulated by *T. striatum* HBS. The biosynthesis of carotenoids started from acetyl-CoA, which was condensed into acetoacetyl-CoA and mevalonate. Then, mevalonate entered the biosynthesis of geranylgeranyl diphosphate, which was converted into lycopene. Lycopene cyclase catalyzed the production of β-carotene from lycopene. In *T. striatum* HBS, β-carotene was primarily converted by hydroxylyase into β-cryptoxanthin, an important precursor of astaxanthin. Enzymes of *T. striatum* involved in carotenoids biosynthesis share homology mostly with fungi and plants (**Table 5.3**).

Table 5.3 Selected enzymes of *T. striatum* HBS involved in aromatics degradation, fatty acids and carotenoids biosynthesis

Enzyme	Organism	Swiss-Prot E-value
Aromatics degradation		
Laccase	*Cryptococcus neoformans*	5.70E-14
	Rhodotorula glutinis	5.30E-238
Feruloyl esterase	*Neosartorya fischeri*	2.50E-14
	Aspergillus oryzae	1.8E-56
	Aspergillus terreus	1.20E-16
Alcohol dehydrogenase	*Schizosaccharomyces pombe*	1.30E-38
	Emericella nidulans	7.00E-77
	Bacillus subtilis	1.20E-40
	Aspergillus clavatus	7.00E-75
Aldehyde dehydrogenase	*Alternaria alternata*	3.40E-29
	Agaricus bisporus	9.4E-163
Aromatic peroxygenase	*Coprinellus radians*	2.10E-24
4-Coumarate-CoA ligase	*Oryza sativa*	3.80E-42
4,5-DOPA dioxygenase extradiol	*S. pombe*	7.40E-29
	Beta vulgaris	1.30E-11
Fatty acids biosynthesis		
Long chain acyl-CoA synthase	*Arabiopsis thaliana*	1.10E-118
Very-long-chain 3-oxoacyl-CoA reductase	*Coprinopsis cinerea*	4.40E-69
Acyl-CoA desaturase	*Mus musculus*	1.90E-160
Acetyl-CoA carboxylase	*S. pombe*	3.1E-130
Long-chain-fatty-acid--CoA ligase	*S. pombe*	9.80E-133
Enoyl reductase	*S. pombe*	9.50E-33
Acyl-CoA desaturase	*S. pombe*	4.10E-123
3-ketoacyl-CoA thiolase	*Yarrowia lipolytica*	4.80E-128
Acyl-CoA oxidase	*Y. lipolytica*	1.60E-160
Carotenoids biosynthesis		
3-hydroxy-3-methylglutaryl-CoA reductase	*Phycomyces blakesleeanus*	2.30E-156
Phosphomevalonate kinase	*Arabidopsis thaliana*	3.60E-45
Mevalonate diphosphate decarboxylase	*Ganoderma lucidum*	1.50E-119
Isopentenyl-diphosphate Delta-isomerase	*Phaffia rhodozyma*	2.50E-75
Farnesyl pyrophosphate synthase	*Kluyveromyces lactis*	1.70E-124
Geranylgeranyl pyrophosphate synthase	*Mucor circinelloides*	4.40E-93
phytoene synthase	*Leptosphaeria maculans*	1.20E-110

phytoene dehydrogenase	*Rhodosporidium diobovatum*	2.13E-61
phytoene desaturase	*Acyrthosiphon pisum*	559767855
Lycopene cyclase protein	*S. pombe*	1.20E-110

After a preliminary searching and screening, the conversion process of lignin as a substrate to fatty acids and carotenoids can be observed in **Figure 5.2**. Additional works need to be done to identify the rate-limiting steps and carbon distribution between different metabolic processes. Genetic and metabolic strategies can be developed to redesign the metabolic network to achieve specific objectives, e.g., improving carotenoids biosynthesis by suppressing fatty acids biosynthesis.

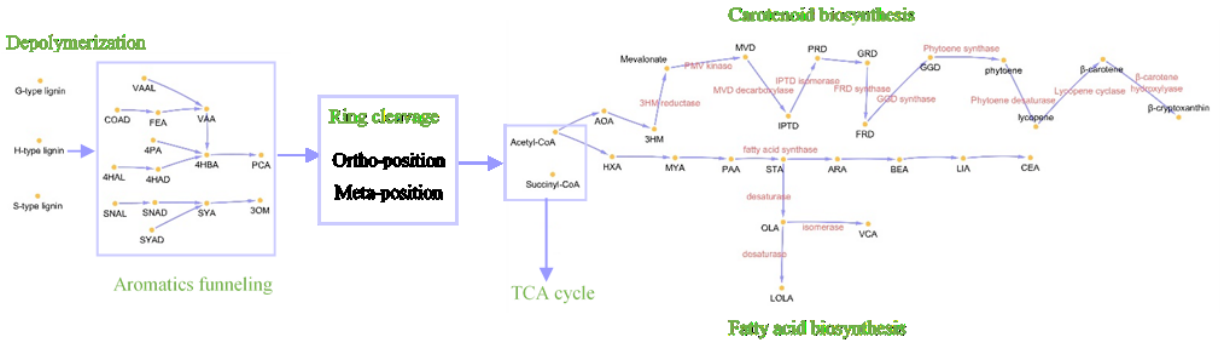

Figure 5.2 Scheme of lignin bioconversion to biosynthesis of fatty acids and carotenoids in *T. striatum* HBS.

Abbreviations: 3HM: 3-hydroxy-3-methylglutaryl-CoA; 3OM: 3-O-methylgallate; 4HAD: 4-hydroxybenzyaldehyde; 4HAL: 4-hydroxybenyl alcohol; 4HBA: 4-hydroxybenzoic acid; 4PA: 4-coumaric acid; AOA: acetoacetyl-CoA; COAD: coniferyl aldehyde; FEA: ferulic acid; FRD: farnesyl diphosphate; GGD: geranylgeranyl diphosphate; GRD: geranyl diphosphate; IPTD: isopentenyl disphosphate; MVD: mevalonate disphosphate; PCA: protocatechuic acid; PMV kinase: Phosphomevalonate kinase; PRD: prenyl diphosphate; SNAD: sinapaldehyde; SNAL: sinapyl alcohol; SYA: syringic acid; SYAD: syringaldehyde; VAA: vanillic acid; VAAL: vanillyl alchol.

4. Conclusion

The analysis of metabolites during black liquor fermentation and construction of reference transcriptome provided a basic idea of the metabolic potential of *T. striatum* HBS as well as the mechanisms of black liquor bioconversion. Both aromatics and carbohydrates in black liquor can be effectively utilized for its diverse metabolic functions. Polymeric aromatics

were first degraded by laccase and esterase and then funneled into several intermediates by enzymes such as hydrogenase and decarboxylase. Cleavage of aromatic rings can be performed on either ortho-position or meta-position, which would improve the utilization efficiency of aromatics. The carbon and energy from the substrate can be used by *T. striatum* HBS for accumulation of bioproducts. With acetyl-CoA as the initial unit, the biosynthesis of fatty acids followed a linear pattern, in which fatty acid synthase catalyzed the chain elongation while reductase and desaturase were responsible for modification of fatty acid structure. Additionally, starting with acetyl-CoA, a set of reactions were employed to generate mevalonate as important intermediates for many metabolic functions and then produced β-cryptoxanthin.

Chapter 6 - Conclusions and perspectives

1. Conclusions

As one of the most abundant materials in the biosphere, lignin has been extensively studied as feedstock for the sustainable production of fuels and chemicals. By means of the metabolic power of microorganisms, scientists have developed biological conversion into an effective platform for lignin upgrading, and they employ various species to produce valuable microbial products with lignin-type materials as a carbon source. In this project, the marine protist, *T. striatum* HBS, was used as a novel lignin degrader. The screening of 14 kinds of aromatic compounds proved that *T. striatum* HBS was able to grow with most compounds and accumulate microbial lipids as well as carotenoids. A preference toward aromatic carboxylic acids was also observed, especially 3,4-DHBA and 4-HBA. The use of fed-batch mode significantly improved the performance of product accumulation by providing more carbon source.

In addition to simple aromatic compounds, *T.striatum* HBS also exhibited the ability to depolymerize polymeric lignin. The activities of ligninolytic enzymes such as LiP and MnP were detected during fermentation of three technical lignins (AL CS, EOL LP and KPL), which can deconstruct lignin macromolecules and generate aromatic monomers and oligomers for cellular activities. However, such depolymerization ability was relatively weak compared to other lignin degraders (e.g white rot fungi), which resulted in a limited availability of the carbon source and therefore low contents of products. To improve the lignin depolymerization process, different nitrogen sources, mineral elements and vitamins were applied respectively for optimization of fermentation medium composition. Among different types of nitrogen sources, NH_4Cl showed performed best on lignin degradation, and the addition of mineral elements also facilitated lignin degradation as important co-factors of lignolytic enzymes. The externally added laccase was also able to improve cell growth as well as lignin utilization by developing an effective synergy with *T. striatum* HBS. The low-molecular-weight fragments generated from laccase degradation were consumed by *T. striatum* HBS which would shift the equilibrium between lignin depolymerization/repolymerization toward the depolymerization direction.

The lignin-rich waste stream, black liquor from alkaline pretreatment of corn stover was also studied as a carbon source for fermentation of *T. striatum* HBS. That strain efficiently utilized the various components of black liquor, such as sugars, sugar alcohols and organic acids via diverse metabolic processes. Specifically, lignin and lignin-derived aromatic compounds were identified as the main substrate for microbial fermentation. HBS was able to both degrade simple aromatic compounds and break down inter-unit linkages (e.g. β-O-4 linkage) and depolymerize polyphenolic fragments of lignin. A strong adaptation to a wide pH range was

found in HBS. It was able to grow uninhibited under acidic conditions, suggesting a powerful stress regulation system which can be used in more applications.

2. Current Challenges and Perspectives

Given the potential benefits of lignin bioconversion (e.g., mild condition, adaptation to diverse aromatic substrates, simple products, and minimal product separation/purification), extensive studies on flask- and bench-scale have been carried out on fungal and bacterial lignin conversion to lipid, platform chemicals, polymers, and so on. The biotransformation holds promise for lignin valorization to value-added bioproducts. However, many challenges still persist for process scale-up and industrial applications, which needs to be addressed in future research in the following aspects.

2.1 Improvement on lignin depolymerization process

Although various products can be obtained from bioconversion of lignin-derived aromatics, the yield and conversion efficiency are far below the level of industrial interest. One of the main barriers is the difficulty of lignin depolymerization, which significantly limits the bioavailability of lignin substrate and conversion rate. As one of the most abundant materials in the biosphere, lignin has extremely complex and diverse composition and structure, each of which renders lignin different resistance to external attack (1). Concerning the biological degradation of lignin, microorganisms show preferences toward different lignin structures. For example, *R. opacus* was observed to preferably degrade different hydroxyl groups (e.g., aliphatic OH, guaiagyl-type OH, β-5 condensed phenolic OH, and carboxylic OH groups) of kraft lignin but slight G unit and β-O-4 linkage (41, 68) while a large fraction of lignin molecules were barely changed, especially those condensed fragments. That generally resulted in a relatively slow degradation rate and a low percentage of lignin utilization.

To effectively degrade lignin and convert it into valuable bioproducts, strategies can be applied to overcome the resistance of lignin depolymerization and enhance the bioavailability of substrates. Such strategies can be either biological or thermochemical. Fungal ligninolytic enzymes with strong oxidative ability can be supplemented into lignin fermentation system to facilitate the destruction of complex lignin molecules (68, 99). Other than single enzymes, fungal secretome (i.e., enzyme mixture) was also directly added into the lignin fermentation broth, which led to a reduction of lignin molecular weight by more than 60% (67). The application of fungal secretome owns the advantages of synergy between various peroxidases and oxidases and saving the efforts on enzyme isolation and purification. With thermochemical strategies, lignin is depolymerized first during the thermochemical processes, and the generated small fragments, which are more readily metabolized by microorganisms are funneled into specific bioproducts (41, 103). Considering the preference of microorganisms toward different lignin monomers and structures, selective depolymerization can promisingly produce depolymerized lignin fragments favored by microbes and thereby increasing lignin utilization. Direct use of biomass pretreatment lignin-rich liquid stream is also feasible, as it would save the efforts of lignin isolation and other soluble compounds existing can serve as co-substrates to support microbial growth. However, since the composition of pretreatment liquid stream is generally complex and contains possible inhibitors, microorganisms with higher tolerance should be developed and applied. To monitor the degradation and conversion process, more advanced analytical techniques are also necessary.

2.2 Improvement on understanding of lignin-derived aromatics metabolism

In most cases, aromatic compounds are toxic to microorganisms on their growth and activities. For species with the lignin-degrading ability, the metabolism of lignin-derived aromatic compounds is complex and involves various process, such as aromatic compounds

degradation, shuttling to central metabolism, bioproduct synthesis, and also stress regulation system due to the inhibitory effects of aromatics. In practical applications, the loading of lignin-derived materials as a carbon source is relatively low; otherwise a long lag phase or even severe cell growth inhibition would occur. As such, a decent product concentration is typically difficult to achieve. Traditional strategies such as acclimation (213) and fed-batch operation (45) have been adopted to mitigate the inhibitory effects of aromatic compounds. However, to efficiently harness the biosynthetic processing power of microbial world, a comprehensive understanding of the entire metabolic network of lignin degradation would be indispensable.

The current understanding on microbial metabolism of lignin-derived aromatic compounds is still limited to a few bacterial species, such as *P. putida* and *S. paucimobilis*. As more and more kinds of microorganisms are involved in studies on lignin bioconversion, more research effort should be invested in understanding the principles that govern the functional properties of lignin biodegrading organisms, especially at the genomic level. Multi-omics tools of modern systems biology will need to be advanced to address the problems associated with the microbial conversion of lignin, such as the bottlenecks of lignin conversion process, carbon flux during microbial metabolism and the effects of environmental stress (e.g. pH, light and oxidative potential). Analytical techniques with higher resolving power are necessary for high throughput analysis of complex microbial samples. With a solid knowledge basis, novel platform microorganisms should be developed with novel functional capabilities, biosynthetic pathways and stress tolerance features, so they can finally be employed to acquire diverse value-added products from lignin.

2.3 Development of genetic and metabolic engineering strategies

The development of genetic and metabolic engineering has enabled the manipulation of microbial metabolism at different levels and achieved specific objectives in order to improve lignin bioconversion process. The construction and application of genetic and metabolic tools dependend on the understanding of genomic systems and metabolic processes of microorganisms. To date, those tools are mostly for bacteria. As more species become involved and fundamental research on lignin bioconversion continues to advance, the genetic toolbox should be expanded to incorporate more possible lignin degraders and more attractive biosynthetic pathways, such as marine protists which are able to utilize lignin and synthesize carotenoids as important antioxidants. Different metabolic process can be combined to maximize the advantages of different species. For example, the lignin depolymerization system of fungi and synthetic pathway of certain bioproducts can be reconstructed and expressed in model organisms (e.g., *E. coli*) which have high genomic tractability and growth rate. Such an artificial metabolic process is more defined and controllable than those embedded in complex microbial metabolic network, and it could exhibit higher efficiency than lignin bioconversion via single species.

Lignin bioconversion and upgrading to value-added products is an emerging area which has attracted increasing attention recently. Much progress has been made in elucidating lignin degradation mechanisms and aromatic compound metabolic pathways and conducting genetic/metabolic manipulation of some bacterial strains. Those strains have also been successfully applied to convert lignin-based feedstocks to microbial products (PHA and lipid) and important platform chemicals of industrial interest from lignin metabolism intermediates. Given the state of current research, further research is still needed to significantly improve the

cost-effectiveness of lignin bioconversion to value-added bioproducts. The proposed research endeavor is highly interdisciplinary, spanning multiple fields in biology, systems biology, chemical and metabolic engineering, protein engineering, bioprocessing engineering, and even computational biology. The collaboration among complementary expertise from different areas would be paramount to the success of the commercialization of bioproducts from lignin bioconversion.

References

1. Li, X. and Y. Zheng, *Lignin-enzyme interaction: Mechanism, mitigation approach, modeling, and research prospects.* Biotechnology Advances, 2017. **35**(4): p. 466-489.

2. Azarpira, A., J. Ralph, and F. Lu, *Catalytic Alkaline Oxidation of Lignin and its Model Compounds: a Pathway to Aromatic Biochemicals.* BioEnergy Research, 2014. **7**(1): p. 78-86.

3. Yoon, S.-H. and A. Van Heiningen, *Kraft pulping and papermaking properties of hot-water pre-extracted loblolly pine in an integrated forest products biorefinery.* Tappi J, 2008. **7**(7): p. 22-27.

4. Merali, Z., et al., *Characterization of cell wall components of wheat bran following hydrothermal pretreatment and fractionation.* Biotechnology for Biofuels, 2015. **8**(1): p. 23.

5. Nitsos, C.K., et al., *Optimization of Hydrothermal Pretreatment of Hardwood and Softwood Lignocellulosic Residues for Selective Hemicellulose Recovery and Improved Cellulose Enzymatic Hydrolysis.* ACS Sustainable Chemistry & Engineering, 2016. **4**(9): p. 4529-4544.

6. Saha, B.C., et al., *Biological pretreatment of corn stover with white-rot fungus for improved enzymatic hydrolysis.* International Biodeterioration & Biodegradation, 2016. **109**: p. 29-35.

7. Hu, T.Q., *Chemical modification, properties, and usage of lignin*. 2002: Springer.

8. Sangchoom, W. and R. Mokaya, *Valorization of Lignin Waste: Carbons from Hydrothermal Carbonization of Renewable Lignin as Superior Sorbents for CO2 and Hydrogen Storage.* ACS Sustainable Chemistry & Engineering, 2015. **3**(7): p. 1658-1667.

9. Chandra, R., A. Abhishek, and M. Sankhwar, *Bacterial decolorization and detoxification of black liquor from rayon grade pulp manufacturing paper industry and detection of their metabolic products.* Bioresource Technology, 2011. **102**(11): p. 6429-6436.

10. Demirbas, A., *Higher heating values of lignin types from wood and non-wood lignocellulosic biomasses.* Energy Sources, Part A: Recovery, Utilization, and Environmental Effects, 2017. **39**(6): p. 592-598.

11. Wang, H., et al., *Biomass-derived lignin to jet fuel range hydrocarbons via aqueous phase hydrodeoxygenation.* Green Chemistry, 2015. **17**(12): p. 5131-5135.

12. Wang, H., et al., *Production of Jet Fuel-Range Hydrocarbons from Hydrodeoxygenation of Lignin over Super Lewis Acid Combined with Metal Catalysts.* ChemSusChem, 2018. **11**(1): p. 285-291.

13. Oroumei, A., B. Fox, and M. Naebe, *Thermal and Rheological Characteristics of Biobased Carbon Fiber Precursor Derived from Low Molecular Weight Organosolv Lignin.* ACS Sustainable Chemistry & Engineering, 2015. **3**(4): p. 758-769.

14. Ding, R., et al., *Processing and characterization of low-cost electrospun carbon fibers from organosolv lignin/polyacrylonitrile blends.* Carbon, 2016. **100**: p. 126-136.

15. Salinas-Torres, D., et al., *Asymmetric capacitors using lignin-based hierarchical porous carbons.* Journal of Power Sources, 2016. **326**: p. 641-651.

16. You, X., et al., *Preparation of electrode for electric double layer capacitor from electrospun lignin fibers*, in *Holzforschung*. 2015. p. 1097.

17. Nguyen, N.A., C.C. Bowland, and A.K. Naskar, *A general method to improve 3D-printability and inter-layer adhesion in lignin-based composites.* Applied Materials Today, 2018. **12**: p. 138-152.

18. Sutton, J.T., et al., *Lignin-Containing Photoactive Resins for 3D Printing by Stereolithography.* ACS Applied Materials & Interfaces, 2018. **10**(42): p. 36456-36463.

19. Valkonen, S., et al., *Use of low molecular weight lignin together with lignin for the production of a phenol-formaldehyde binder composition*. 2018, Google Patents.

20. Gouveia, S., et al., *Green Binder Based on Enzymatically Polymerized Eucalypt Kraft Lignin for Fiberboard Manufacturing: A Preliminary Study.* Polymers, 2018. **10**(6): p. 642.

21. Kim, J.-Y., et al., *Catalytic pyrolysis of lignin over HZSM-5 catalysts: Effect of various parameters on the production of aromatic hydrocarbon.* Journal of Analytical and Applied Pyrolysis, 2015. **114**: p. 273-280.

22. Kalogiannis, K.G., et al., *Pyrolysis of lignin with 2DGC quantification of lignin oil: Effect of lignin type, process temperature and ZSM-5 in situ upgrading.* Journal of Analytical and Applied Pyrolysis, 2015. **115**: p. 410-418.

23. Shen, D., et al., *Production of aromatic monomers from catalytic pyrolysis of black-liquor lignin.* Journal of Analytical and Applied Pyrolysis, 2015. **111**: p. 47-54.

24. Wang, H.-m., et al., *Study on the catalytic gasification of alkali lignin over Ru/C nanotubes in supercritical water.* Journal of Fuel Chemistry and Technology, 2015. **43**(10): p. 1195-1201.

25. Pinto, F., et al., *Effects of experimental conditions and of addition of natural minerals on syngas production from lignin by oxy-gasification: Comparison of bench- and pilot scale gasification.* Fuel, 2015. **140**: p. 62-72.

26. Wei, R., et al., *Coupled biomass (lignin) gasification and iron ore reduction: A novel approach for biomass conversion and application.* Energy, 2017. **140**: p. 406-414.

27. Villar, J.C., A. Caperos, and F. García-Ochoa, *Oxidation of hardwood kraft-lignin to phenolic derivatives with oxygen as oxidant.* Wood Science and Technology, 2001. **35**(3): p. 245-255.

28. Tarabanko, V.E., D.V. Petukhov, and G.E. Selyutin, *New Mechanism for the Catalytic Oxidation of Lignin to Vanillin.* Kinetics and Catalysis, 2004. **45**(4): p. 569-577.

29. Wang, Y.-Y., L.-L. Ling, and H. Jiang, *Selective hydrogenation of lignin to produce chemical commodities by using a biochar supported Ni–Mo2C catalyst obtained from biomass.* Green Chemistry, 2016. **18**(14): p. 4032-4041.

30. Wang, J., et al., *Liquefaction of kraft lignin by hydrocracking with simultaneous use of a novel dual acid-base catalyst and a hydrogenation catalyst.* Bioresource Technology, 2017. **243**: p. 100-106.

31. Yi, J., et al., *High Efficient Hydrogenation of Lignin-Derived Monophenols to Cyclohexanols over Pd/γ-Al2O3 under Mild Conditions.* Catalysts, 2016. **6**(1): p. 12.

32. Chen, W., et al., *Low temperature hydrogenation of pyrolytic lignin over Ru/TiO2: 2D HSQC and 13C NMR study of reactants and products.* Green Chemistry, 2016. **18**(1): p. 271-281.

33. Xu, C., et al., *Lignin depolymerisation strategies: towards valuable chemicals and fuels.* Chemical Society Reviews, 2014. **43**(22): p. 7485-7500.

34. Liu, W.-J., H. Jiang, and H.-Q. Yu, *Thermochemical conversion of lignin to functional materials: a review and future directions.* Green Chemistry, 2015. **17**(11): p. 4888-4907.

35. Liew, C.Y., et al., *Lignin biodegradation and ligninolytic enzyme studies during biopulping of Acacia mangium wood chips by tropical white rot fungi.* World Journal of Microbiology and Biotechnology, 2011. **27**(6): p. 1457-1468.

36. Yang, X., et al., *Structure alteration of lignin in corn stover degraded by white-rot fungus Irpex lacteus CD2.* International Biodeterioration & Biodegradation, 2010. **64**(2): p. 119-123.

37. Su, Y., et al., *Biodegradation of lignin and nicotine with white rot fungi for the delignification and detoxification of tobacco stalk.* BMC Biotechnology, 2016. **16**(1): p. 81.

38. Wang, Y., et al., *A novel lignin degradation bacterial consortium for efficient pulping.* Bioresource Technology, 2013. **139**: p. 113-119.

39. Bugg, T.D.H., et al., *The emerging role for bacteria in lignin degradation and bio-product formation.* Current Opinion in Biotechnology, 2011. **22**(3): p. 394-400.

40. Li, X., et al. *A Novel Platform for Bioupgrading of Lignin to Valuable Nutraceuticals and Pharmaceuticals*. in *2018 ASABE Annual International Meeting*. 2018. American Society of Agricultural and Biological Engineers.

41. Wei, Z., et al., *Bioconversion of oxygen-pretreated Kraft lignin to microbial lipid with oleaginous Rhodococcus opacus DSM 1069.* Green Chemistry, 2015. **17**(5): p. 2784-2789.

42. Shi, Y., et al., *Directed bioconversion of Kraft lignin to polyhydroxyalkanoate by Cupriavidus basilensis B-8 without any pretreatment.* Process Biochemistry, 2017. **52**: p. 238-242.

43. Lin, L., et al., *Systems biology-guided biodesign of consolidated lignin conversion.* Green Chemistry, 2016. **18**(20): p. 5536-5547.

44. Sainsbury, P.D., et al., *Breaking Down Lignin to High-Value Chemicals: The Conversion of Lignocellulose to Vanillin in a Gene Deletion Mutant of Rhodococcus jostii RHA1.* ACS Chemical Biology, 2013. **8**(10): p. 2151-2156.

45. Barton, N., et al., *Enabling the valorization of guaiacol-based lignin: Integrated chemical and biochemical production of cis,cis-muconic acid using metabolically engineered Amycolatopsis sp ATCC 39116.* Metabolic Engineering, 2018. **45**: p. 200-210.

46. Wang, H., M. Tucker, and Y. Ji, *Recent Development in Chemical Depolymerization of Lignin: A Review.* Journal of Applied Chemistry, 2013. **2013**: p. 9.

47. Pandey, M.P. and C.S. Kim, *Lignin Depolymerization and Conversion: A Review of Thermochemical Methods.* Chemical Engineering & Technology, 2011. **34**(1): p. 29-41.

48. Ahmad, M., et al., *Development of novel assays for lignin degradation: comparative analysis of bacterial and fungal lignin degraders.* Molecular BioSystems, 2010. **6**(5): p. 815-821.

49. Dashtban, M., et al., *Fungal biodegradation and enzymatic modification of lignin.* International journal of biochemistry and molecular biology, 2010. **1**(1): p. 36-50.

50. Vrsanska, M., et al., *Induction of Laccase, Lignin Peroxidase and Manganese Peroxidase Activities in White-Rot Fungi Using Copper Complexes.* Molecules, 2016. **21**(11): p. 1553.

51. Forrester, I.T., et al., *Manganese, Mn-dependent peroxidases, and the biodegradation of lignin.* Biochemical and biophysical research communications, 1988. **157**(3): p. 992-999.

52. Tuor, U., et al., *Oxidation of phenolic arylglycerol. beta.-aryl ether lignin model compounds by manganese peroxidase from Phanerochaete chrysosporium: oxidative*

cleavage of an. alpha.-carbonyl model compound. Biochemistry, 1992. **31**(21): p. 4986-4995.

53. Wariishi, H., et al., *Thiol-mediated oxidation of nonphenolic lignin model compounds by manganese peroxidase of Phanerochaete chrysosporium.* Journal of Biological Chemistry, 1989. **264**(24): p. 14185-14191.

54. Kapich, A.N., K.A. Jensen, and K.E. Hammel, *Peroxyl radicals are potential agents of lignin biodegradation.* FEBS letters, 1999. **461**(1-2): p. 115-119.

55. Camarero, S., et al., *Description of a Versatile Peroxidase Involved in the Natural Degradation of Lignin That Has Both Manganese Peroxidase and Lignin Peroxidase Substrate Interaction Sites.* Journal of Biological Chemistry, 1999. **274**(15): p. 10324-10330.

56. Munk, L., et al., *Can laccases catalyze bond cleavage in lignin?* Biotechnology Advances, 2015. **33**(1): p. 13-24.

57. Claus, H., *Laccases: structure, reactions, distribution.* Micron, 2004. **35**(1-2): p. 93-96.

58. Gold, M.H. and M. Alic, *Molecular biology of the lignin-degrading basidiomycete Phanerochaete chrysosporium.* Microbiological reviews, 1993. **57**(3): p. 605-622.

59. Bourbonnais, R., et al., *Lignin oxidation by laccase isozymes from Trametes versicolor and role of the mediator 2,2'-azinobis(3-ethylbenzthiazoline-6-sulfonate) in kraft lignin depolymerization.* Applied and Environmental Microbiology, 1995. **61**(5): p. 1876-1880.

60. Guerra, A., et al., *Structural Characterization of Lignin during Pinus taeda Wood Treatment with Ceriporiopsis subvermispora*. Applied and Environmental Microbiology, 2004. **70**(7): p. 4073-4078.

61. Fackler, K., et al., *Lignin degradation by white rot fungi on spruce wood shavings during short-time solid-state fermentations monitored by near infrared spectroscopy.* Enzyme and Microbial Technology, 2006. **39**(7): p. 1476-1483.

62. Jensen, K.A., et al., *Pathways for Extracellular Fenton Chemistry in the Brown Rot Basidiomycete Gloeophyllum trabeum*. Applied and Environmental Microbiology, 2001. **67**(6): p. 2705-2711.

63. Vanden Wymelenberg, A., et al., *Comparative Transcriptome and Secretome Analysis of Wood Decay Fungi Postia placenta and Phanerochaete chrysosporium*. Applied and Environmental Microbiology, 2010. **76**(11): p. 3599-3610.

64. Winquist, E., et al., *Production of lignin modifying enzymes on industrial waste material by solid-state cultivation of fungi.* Biochemical Engineering Journal, 2008. **42**(2): p. 128-

132.

65. Wesenberg, D., I. Kyriakides, and S.N. Agathos, *White-rot fungi and their enzymes for the treatment of industrial dye effluents.* Biotechnology Advances, 2003. **22**(1): p. 161-187.

66. Wan, C. and Y. Li, *Fungal pretreatment of lignocellulosic biomass.* Biotechnology Advances, 2012. **30**(6): p. 1447-1457.

67. Salvachúa, D., et al., *Lignin depolymerization by fungal secretomes and a microbial sink.* Green Chemistry, 2016. **18**(22): p. 6046-6062.

68. Zhao, C., et al., *Synergistic enzymatic and microbial lignin conversion.* Green Chemistry, 2016. **18**(5): p. 1306-1312.

69. Salvachúa, D., et al., *Towards lignin consolidated bioprocessing: simultaneous lignin depolymerization and product generation by bacteria.* Green Chemistry, 2015. **17**(11): p. 4951-4967.

70. Abd-Elsalam, H.E. and A.A. El-Hanafy, *Lignin biodegradation with ligninolytic bacterial strain and comparison of Bacillus subtilis and Bacillus sp. isolated from Egyptian soil.* Am Eurasian J Agric Environ Sci, 2009. **5**(1): p. 39-44.

71. Chen, Y., et al., *Kraft lignin biodegradation by Novosphingobium sp. B-7 and analysis of the degradation process.* Bioresource Technology, 2012. **123**: p. 682-685.

72. Chandra, R. and R.N. Bharagava, *Bacterial degradation of synthetic and kraft lignin by axenic and mixed culture and their metabolic products.* Journal of environmental biology, 2013. **34**(6): p. 991.

73. Brown, M.E. and M.C.Y. Chang, *Exploring bacterial lignin degradation.* Current Opinion in Chemical Biology, 2014. **19**: p. 1-7.

74. de Gonzalo, G., et al., *Bacterial enzymes involved in lignin degradation.* Journal of Biotechnology, 2016. **236**: p. 110-119.

75. Fernandes, T.A.R., et al., *Laccases from Actinobacteria—what we have and what to expect.* Advances in Microbiology, 2014. **4**(06): p. 285.

76. Xiong, X.Q., et al., *Isolation of a rice endophytic bacterium, Pantoea sp. Sd-1, with ligninolytic activity and characterization of its rice straw degradation ability.* Letters in Applied Microbiology, 2014. **58**(2): p. 123-129.

77. Sondhi, S., et al., *An extracellular thermo-alkali-stable laccase from Bacillus tequilensis SN4, with a potential to biobleach softwood pulp.* 3 Biotech, 2015. **5**(2): p. 175-185.

78. Sato, Y., et al., *Identification of Three Alcohol Dehydrogenase Genes Involved in the*

Stereospecific Catabolism of Arylglycerol-β-Aryl Ether by Sphingobium sp. Strain SYK-6. Applied and Environmental Microbiology, 2009. **75**(16): p. 5195-5201.

79. Pereira, J.H., et al., *Structural and Biochemical Characterization of the Early and Late Enzymes in the Lignin β-aryl Ether Cleavage Pathway from Sphingobium sp SYK-6.* Journal of Biological Chemistry, 2016.

80. Wells, T., Z. Wei, and A. Ragauskas, *Bioconversion of lignocellulosic pretreatment effluent via oleaginous Rhodococcus opacus DSM 1069.* Biomass and Bioenergy, 2015. **72**: p. 200-205.

81. Tomizawa, S., et al., *Understanding the Limitations in the Biosynthesis of Polyhydroxyalkanoate (PHA) from Lignin Derivatives.* ACS Sustainable Chemistry & Engineering, 2014. **2**(5): p. 1106-1113.

82. Abdelaziz, O.Y., et al., *Biological valorization of low molecular weight lignin.* Biotechnology Advances, 2016. **34**(8): p. 1318-1346.

83. Jiménez, J.I., et al., *Genomic analysis of the aromatic catabolic pathways from Pseudomonas putida KT2440.* Environmental Microbiology, 2002. **4**(12): p. 824-841.

84. Masai, E., Y. Katayama, and M. Fukuda, *Genetic and Biochemical Investigations on Bacterial Catabolic Pathways for Lignin-Derived Aromatic Compounds.* Bioscience, Biotechnology, and Biochemistry, 2007. **71**(1): p. 1-15.

85. Xu, Z., et al., *Recent advances in lignin valorization with bacterial cultures: microorganisms, metabolic pathways, and bio-products.* Biotechnology for Biofuels, 2019. **12**(1): p. 32.

86. Fairley, D.J., et al., *Aerobic Metabolism of 4-Hydroxybenzoic Acid in Archaea via an Unusual Pathway Involving an Intramolecular Migration (NIH Shift).* Applied and Environmental Microbiology, 2002. **68**(12): p. 6246-6255.

87. Zhu, D., et al., *Biodegradation of alkaline lignin by Bacillus ligniniphilus L1.* Biotechnology for Biofuels, 2017. **10**(1): p. 44.

88. Holesova, Z., et al., *Gentisate and 3-oxoadipate pathways in the yeast Candida parapsilosis: identification and functional analysis of the genes coding for 3-hydroxybenzoate 6-hydroxylase and 4-hydroxybenzoate 1-hydroxylase.* Microbiology, 2011. **157**(7): p. 2152-2163.

89. Fuchs, G., M. Boll, and J. Heider, *Microbial degradation of aromatic compounds — from one strategy to four.* Nature Reviews Microbiology, 2011. **9**: p. 803.

90. Kaufmann, F., G. Wohlfarth, and G. Diekert, *O-Demethylase from Acetobacterium dehalogenans.* European Journal of Biochemistry, 1998. **253**(3): p. 706-711.

91. Berman, M.H. and A.C. Frazer, *Importance of tetrahydrofolate and ATP in the anaerobic O-demethylation reaction for phenylmethylethers.* Applied and Environmental Microbiology, 1992. **58**(3): p. 925-931.

92. MacLean, A.M., et al., *Characterization of the β-Ketoadipate Pathway in Sinorhizobium meliloti.* Applied and Environmental Microbiology, 2006. **72**(8): p. 5403-5413.

93. Kamimura, N. and E. Masai, *The Protocatechuate 4,5-Cleavage Pathway: Overview and New Findings*, in *Biodegradative Bacteria: How Bacteria Degrade, Survive, Adapt, and Evolve*, H. Nojiri, et al., Editors. 2014, Springer Japan: Tokyo. p. 207-226.

94. Johnson, C.W. and G.T. Beckham, *Aromatic catabolic pathway selection for optimal production of pyruvate and lactate from lignin.* Metabolic Engineering, 2015. **28**: p. 240-247.

95. Ratledge, C., *Fatty acid biosynthesis in microorganisms being used for Single Cell Oil production.* Biochimie, 2004. **86**(11): p. 807-815.

96. Ratledge, C. and J.P. Wynn, *The biochemistry and molecular biology of lipid accumulation in oleaginous microorganisms.* Advances in applied microbiology, 2002. **51**: p. 1-52.

97. Lu, J., R.C. Tappel, and C.T. Nomura, *Mini-Review: Biosynthesis of Poly(hydroxyalkanoates).* Polymer Reviews, 2009. **49**(3): p. 226-248.

98. Kosa, M. and A.J. Ragauskas, *Bioconversion of lignin model compounds with oleaginous Rhodococci.* Applied Microbiology and Biotechnology, 2012. **93**(2): p. 891-900.

99. Xie, S., et al., *Advanced Chemical Design for Efficient Lignin Bioconversion.* ACS Sustainable Chemistry & Engineering, 2017. **5**(3): p. 2215-2223.

100. He, Y., et al., *Lipid Production from Dilute Alkali Corn Stover Lignin by Rhodococcus Strains.* ACS Sustainable Chemistry & Engineering, 2017. **5**(3): p. 2302-2311.

101. Kosa, M. and A.J. Ragauskas, *Lignin to lipid bioconversion by oleaginous Rhodococci.* Green Chemistry, 2013. **15**(8): p. 2070-2074.

102. Le, R.K., et al., *Conversion of corn stover alkaline pre-treatment waste streams into biodiesel via Rhodococci.* RSC Advances, 2017. **7**(7): p. 4108-4115.

103. Liu, Z.-H., et al., *Combinatorial pretreatment and fermentation optimization enabled a record yield on lignin bioconversion.* Biotechnology for Biofuels, 2018. **11**(1): p. 21.

104. Hu, M., et al., *Converting lignin derived phenolic aldehydes into microbial lipid by Trichosporon cutaneum.* Journal of Biotechnology, 2018. **281**: p. 81-86.

105. Linger, J.G., et al., *Lignin valorization through integrated biological funneling and chemical catalysis.* Proceedings of the National Academy of Sciences, 2014. **111**(33): p. 12013-12018.

106. Liu, Z.-H., et al., *Synergistic maximization of the carbohydrate output and lignin processability by combinatorial pretreatment.* Green Chemistry, 2017. **19**(20): p. 4939-4955.

107. Si, M., et al., *In Situ Lignin Bioconversion Promotes Complete Carbohydrate Conversion of Rice Straw by Cupriavidus basilensis B-8.* ACS Sustainable Chemistry & Engineering, 2018. **6**(6): p. 7969-7978.

108. Fleige, C., et al., *Investigation of the Amycolatopsis sp. Strain ATCC 39116 Vanillin Dehydrogenase and Its Impact on the Biotechnical Production of Vanillin.* Applied and Environmental Microbiology, 2013. **79**(1): p. 81-90.

109. Zulkarnain, A., et al., *Alkaline Hydrolysate of Oil Palm Empty Fruit Bunch as Potential Substrate for Biovanillin Production via Two-Step Bioconversion.* Waste and Biomass Valorization, 2018. **9**(1): p. 13-23.

110. Salleh, N., et al. *Aromatic benzaldehyde from Oryzae sativa*. in *International Conference on Food Engineering and Biotechnology. IPCBEE*. 2011.

111. Barbosa, E.d.S., et al., *VANILLIN PRODUCTION BY PHANEROCHAETE CHRYSOSPORIUM GROWN ON GREEN COCONUT AGRO-INDUSTRIAL HUSK IN SOLID STATE FERMENTATION*. Vol. 3. 2008.

112. Lesage-Meessen, L., et al., *A biotechnological process involving filamentous fungi to produce natural crystalline vanillin from maize bran.* Applied Biochemistry and Biotechnology, 2002. **102**(1): p. 141-153.

113. Lesage-Meessen, L., et al., *Fungal transformation of ferulic acid from sugar beet pulp to natural vanillin.* Journal of the Science of Food and Agriculture, 1999. **79**(3): p. 487-490.

114. van Duuren, J.B.J.H., et al., *pH-stat fed-batch process to enhance the production of cis, cis-muconate from benzoate by Pseudomonas putida KT2440-JD1.* Biotechnology Progress, 2012. **28**(1): p. 85-92.

115. van Duuren, J.B.J.H., et al., *Generation of a catR deficient mutant of P. putida KT2440 that produces cis, cis-muconate from benzoate at high rate and yield.* Journal of Biotechnology, 2011. **156**(3): p. 163-172.

116. Sonoki, T., et al., *Enhancement of protocatechuate decarboxylase activity for the effective production of muconate from lignin-related aromatic compounds.* Journal of

Biotechnology, 2014. **192**: p. 71-77.

117. Wu, W., et al., *Lignin Valorization: Two Hybrid Biochemical Routes for the Conversion of Polymeric Lignin into Value-added Chemicals.* Scientific Reports, 2017. **7**(1): p. 8420.

118. Qian, Y., et al., *Engineered Microbial Production of 2-Pyrone-4,6-Dicarboxylic Acid from Lignin Residues for Use as an Industrial Platform Chemical*. 2016. Vol. 11. 2016.

119. Perez, J.M., et al., *Funneling aromatic products of chemically depolymerized lignin into 2-pyrone-4-6-dicarboxylic acid with Novosphingobium aromaticivorans.* Green Chemistry, 2019.

120. Mycroft, Z., et al., *Biocatalytic conversion of lignin to aromatic dicarboxylic acids in Rhodococcus jostii RHA1 by re-routing aromatic degradation pathways.* Green Chemistry, 2015. **17**(11): p. 4974-4979.

121. Mahan, K.M., et al., *A Review on The Bioconversion of Lignin to Microbial Lipid with Oleaginous Rhodococcus opacus.* Journal of Biotechnology & Biomaterials, 2017: p. Medium: ED; Size: Article No. 1000262.

122. Hocking, M.B., *Vanillin: Synthetic Flavoring from Spent Sulfite Liquor.* Journal of Chemical Education, 1997. **74**(9): p. 1055.

123. Bjørsvik, H.-R. and F. Minisci, *Fine Chemicals from Lignosulfonates. 1. Synthesis of Vanillin by Oxidation of Lignosulfonates.* Organic Process Research & Development, 1999. **3**(5): p. 330-340.

124. Curran, K.A., et al., *Metabolic engineering of muconic acid production in Saccharomyces cerevisiae.* Metabolic Engineering, 2013. **15**: p. 55-66.

125. Eudes, A., et al., *Production of muconic acid in plants.* Metabolic Engineering, 2018. **46**: p. 13-19.

126. Wu, C.-M., et al., *Microbial synthesis of cis,cis-muconic acid by Sphingobacterium sp. GCG generated from effluent of a styrene monomer (SM) production plant.* Enzyme and Microbial Technology, 2004. **35**(6): p. 598-604.

127. Weber, C., et al., *Biosynthesis of cis,cis-Muconic Acid and Its Aromatic Precursors, Catechol and Protocatechuic Acid, from Renewable Feedstocks by Saccharomyces cerevisiae*. Applied and Environmental Microbiology, 2012. **78**(23): p. 8421-8430.

128. Clarkson, S.M., et al., *Construction and Optimization of a Heterologous Pathway for Protocatechuate Catabolism in Escherichia coli Enables Bioconversion of Model Aromatic*

Compounds. Applied and Environmental Microbiology, 2017. **83**(18): p. e01313-17.

129. Pang, K., R. Kotek, and A. Tonelli, *Review of conventional and novel polymerization processes for polyesters.* Progress in Polymer Science, 2006. **31**(11): p. 1009-1037.

130. Kumar, M., et al., *Genome Sequence of Pandoraea sp. ISTKB, a Lignin-Degrading Betaproteobacterium, Isolated from Rhizospheric Soil.* Genome Announcements, 2016. **4**(6): p. e01240-16.

131. DeAngelis, K., et al., *Evidence supporting dissimilatory and assimilatory lignin degradation in Enterobacter lignolyticus SCF1.* Frontiers in Microbiology, 2013. **4**(280).

132. Kumar, M., et al., *Genomic and proteomic analysis of lignin degrading and polyhydroxyalkanoate accumulating β-proteobacterium Pandoraea sp. ISTKB.* Biotechnology for Biofuels, 2018. **11**(1): p. 154.

133. Taylor, C.R., et al., *Isolation of bacterial strains able to metabolize lignin from screening of environmental samples.* Journal of Applied Microbiology, 2012. **113**(3): p. 521-530.

134. ten Have, R. and P.J.M. Teunissen, *Oxidative Mechanisms Involved in Lignin Degradation by White-Rot Fungi.* Chemical Reviews, 2001. **101**(11): p. 3397-3414.

135. Dias, A.A., et al., *Enzymatic saccharification of biologically pre-treated wheat straw with white-rot fungi.* Bioresource Technology, 2010. **101**(15): p. 6045-6050.

136. Yang, S., et al., *Understanding the factors controlling the removal of trace organic contaminants by white-rot fungi and their lignin modifying enzymes: A critical review.* Bioresource Technology, 2013. **141**: p. 97-108.

137. Chen, Y.H., et al., *Biodegradation of kraft lignin by a bacterial strain Comamonas sp. B-9 isolated from eroded bamboo slips.* Journal of Applied Microbiology, 2012. **112**(5): p. 900-906.

138. Shi, Y., et al., *Biochemical investigation of kraft lignin degradation by Pandoraea sp. B-6 isolated from bamboo slips.* Bioprocess and Biosystems Engineering, 2013. **36**(12): p. 1957-1965.

139. Numata, K. and K. Morisaki, *Screening of Marine Bacteria To Synthesize Polyhydroxyalkanoate from Lignin: Contribution of Lignin Derivatives to Biosynthesis by Oceanimonas doudoroffii.* ACS Sustainable Chemistry & Engineering, 2015. **3**(4): p. 569-573.

140. Shene, C., et al., *Production of lipids and docosahexasaenoic acid (DHA) by a native Thraustochytrium strain.* European Journal of Lipid Science and Technology, 2013. **115**(8): p. 890-900.

141. Burja, A.M., et al., *Isolation and characterization of polyunsaturated fatty acid producing Thraustochytrium species: screening of strains and optimization of omega-3 production.* Applied Microbiology and Biotechnology, 2006. **72**(6): p. 1161.

142. Anbu, P., et al., *Investigation of the physiological properties and synthesis of PUFAs from Thraustochytrids and its electrophoretic karyotypes.* Biotechnology and Bioprocess Engineering, 2007. **12**(6): p. 720-729.

143. Fawzy, M.A., *Fatty Acid Characterization and Biodiesel Production by the Marine Microalga Asteromonas gracilis: Statistical Optimization of Medium for Biomass and Lipid Enhancement.* Marine Biotechnology, 2017. **19**(3): p. 219-231.

144. Yuan, J.-P., et al., *Potential health-promoting effects of astaxanthin: A high-value carotenoid mostly from microalgae.* Molecular Nutrition & Food Research, 2011. **55**(1): p. 150-165.

145. Bianchi, T.S., *The role of terrestrially derived organic carbon in the coastal ocean: A changing paradigm and the priming effect.* Proceedings of the National Academy of Sciences, 2011. **108**(49): p. 19473-19481.

146. Hernes, P.J. and R. Benner, *Transport and diagenesis of dissolved and particulate terrigenous organic matter in the North Pacific Ocean.* Deep Sea Research Part I: Oceanographic Research Papers, 2002. **49**(12): p. 2119-2132.

147. Jain, R., et al., *Extracellular Polysaccharide Production by Thraustochytrid Protists.* Marine Biotechnology, 2005. **7**(3): p. 184-192.

148. Nagano, N., et al., *Optimization of Culture Conditions for Growth and Docosahexaenoic Acid Production by a Marine Thraustochytrid, <I>Aurantiochytrium limacinum</I> mh0186.* Journal of Oleo Science, 2009. **58**(12): p. 623-628.

149. Li, X., et al., *Inhibitory Effects of Lignin on Enzymatic Hydrolysis: The Role of Lignin Chemistry and Molecular Weight.* Renewable Energy, 2018.

150. Zhao, Y., et al., *A simplified diphenylamine colorimetric method for growth quantification.* Applied Microbiology and Biotechnology, 2013. **97**(11): p. 5069-5077.

151. Paliwal, R., S. Uniyal, and J.P.N. Rai, *Evaluating the potential of immobilized bacterial consortium for black liquor biodegradation.* Environmental Science and Pollution Research, 2015. **22**(9): p. 6842-6853.

152. Arora, D.S., M. Chander, and P.K. Gill, *Involvement of lignin peroxidase, manganese peroxidase and laccase in degradation and selective ligninolysis of wheat straw.* International Biodeterioration & Biodegradation, 2002. **50**(2): p. 115-120.

153. Sedmak, J.J., D.K. Weerasinghe, and S.O. Jolly, *Extraction and quantitation of astaxanthin*

from Phaffia rhodozyma. Biotechnology techniques, 1990. **4**(2): p. 107-112.

154. Li, W., et al., *Photocatalytic Degradation of Lignin Model Compounds and Kraft Pine Lignin by CdS/TiO2 under Visible Light Irradiation*. 2015. Vol. 10. 2015.

155. Wen, J.-L., et al., *Recent Advances in Characterization of Lignin Polymer by Solution-State Nuclear Magnetic Resonance (NMR) Methodology.* Materials, 2013. **6**(1): p. 359.

156. Xie, S., A.J. Ragauskas, and J.S. Yuan, *Lignin conversion: opportunities and challenges for the integrated biorefinery.* Industrial Biotechnology, 2016. **12**(3): p. 161-167.

157. Cheirsilp, B. and S. Torpee, *Enhanced growth and lipid production of microalgae under mixotrophic culture condition: Effect of light intensity, glucose concentration and fed-batch cultivation.* Bioresource Technology, 2012. **110**: p. 510-516.

158. Hsieh, C.-H. and W.-T. Wu, *Cultivation of microalgae for oil production with a cultivation strategy of urea limitation.* Bioresource Technology, 2009. **100**(17): p. 3921-3926.

159. Xiong, W., et al., *High-density fermentation of microalga Chlorella protothecoides in bioreactor for microbio-diesel production.* Applied Microbiology and Biotechnology, 2008. **78**(1): p. 29-36.

160. Feller, R., et al., *Polyunsaturated ω-3 and ω-6 fatty acids, total carotenoids and antioxidant activity of three marine microalgae extracts obtained by supercritical CO2 and subcritical n-butane.* The Journal of Supercritical Fluids, 2018. **133**: p. 437-443.

161. Rico, A., et al., *Pretreatment with laccase and a phenolic mediator degrades lignin and enhances saccharification of Eucalyptus feedstock.* Biotechnology for Biofuels, 2014. **7**(1): p. 6.

162. Majumdar, S., et al., *Roles of Small Laccases from Streptomyces in Lignin Degradation.* Biochemistry, 2014. **53**(24): p. 4047-4058.

163. Kamwilaisak, K. and P.C. Wright, *Investigating Laccase and Titanium Dioxide for Lignin Degradation.* Energy & Fuels, 2012. **26**(4): p. 2400-2406.

164. Chen, Q., et al., *Effects of laccase on lignin depolymerization and enzymatic hydrolysis of ensiled corn stover.* Bioresource Technology, 2012. **117**: p. 186-192.

165. Milczarek, G. and O. Inganäs, *Renewable Cathode Materials from Biopolymer/Conjugated Polymer Interpenetrating Networks.* Science, 2012. **335**(6075): p. 1468-1471.

166. Zhao, C. and J.A. Lercher, *Selective Hydrodeoxygenation of Lignin-Derived Phenolic Monomers and Dimers to Cycloalkanes on Pd/C and HZSM-5 Catalysts.* ChemCatChem, 2012. **4**(1): p. 64-68.

167. Krall, E.M., et al., *Catalyst-free lignin valorization by acetoacetylation. Structural elucidation by comparison with model compounds.* Green Chemistry, 2018. **20**(13): p. 2959-2966.

168. Singh, S.K., K. Nandeshwar, and J.D. Ekhe, *Thermochemical lignin depolymerization and conversion to aromatics in subcritical methanol: effects of catalytic conditions.* New Journal of Chemistry, 2016. **40**(4): p. 3677-3685.

169. Mahmood, N., et al., *Depolymerization of lignins and their applications for the preparation of polyols and rigid polyurethane foams: A review.* Renewable and Sustainable Energy Reviews, 2016. **60**: p. 317-329.

170. Min, K.H., et al., *The effects of culture condition on the growth property and docosahexaenoic acid production from Thraustochytrium aureum ATCC 34304.* Korean Journal of Chemical Engineering, 2012. **29**(9): p. 1211-1215.

171. Resch, M., J. Baker, and S. Decker, *Low solids enzymatic saccharification of lignocellulosic biomass.* 2015.

172. Tien, M. and T.K. Kirk, *Lignin peroxidase of Phanerochaete chrysosporium*, in *Methods in Enzymology*. 1988, Academic Press. p. 238-249.

173. Tarhan, L. and B. Tongul, *The induction of ligninolytic enzymes depending on menadione based oxidative stress and cell damages in Phanerochaete chrysosporium.* International Biodeterioration & Biodegradation, 2017. **117**: p. 1-7.

174. Pobeheim, H., et al., *Influence of trace elements on methane formation from a synthetic model substrate for maize silage.* Bioresource Technology, 2010. **101**(2): p. 836-839.

175. Keskin, T., et al., *Determining the effect of trace elements on biohydrogen production from fruit and vegetable wastes.* International Journal of Hydrogen Energy, 2018. **43**(23): p. 10666-10677.

176. Kanwal, H.K. and M.S. Reddy, *Effect of carbon, nitrogen sources and inducers on ligninolytic enzyme production by Morchella crassipes.* World Journal of Microbiology and Biotechnology, 2011. **27**(3): p. 687-691.

177. Li, Y., et al., *Cometabolic degradation of lincomycin in a Sequencing Batch Biofilm Reactor (SBBR) and its microbial community.* Bioresource Technology, 2016. **214**: p. 589-595.

178. Kuang, F., et al., *Cometabolism degradation of lignin in sequencing batch biofilm reactors.* Environmental Engineering Research, 2018. **23**(3): p. 294-300.

179. Brenelli, L., et al., *Laccase-derived lignin compounds boost cellulose oxidative enzymes AA9.* Biotechnology for Biofuels, 2018. **11**(1): p. 10.

180. Frommhagen, M., et al., *Boosting LPMO-driven lignocellulose degradation by polyphenol oxidase-activated lignin building blocks.* Biotechnology for Biofuels, 2017. **10**(1): p. 121.

181. Muraleedharan, M.N., et al., *Effect of lignin fractions isolated from different biomass sources on cellulose oxidation by fungal lytic polysaccharide monooxygenases.* Biotechnology for Biofuels, 2018. **11**(1): p. 296.

182. Westereng, B., et al., *Enzymatic cellulose oxidation is linked to lignin by long-range electron transfer.* Scientific Reports, 2015. **5**: p. 18561.

183. Li, X., et al., *A Novel Platform for Bioupgrading of Lignin to Valuable Nutraceuticals and Pharmaceuticals*, in *2018 ASABE Annual International Meeting*. 2018, ASABE: St. Joseph, MI. p. 1.

184. Longe, L.F., et al., *Importance of Mediators for Lignin Degradation by Fungal Laccase.* ACS Sustainable Chemistry & Engineering, 2018. **6**(8): p. 10097-10107.

185. Hong, C.-Y., et al., *Phanerochaete chrysosporium Multienzyme Catabolic System for in Vivo Modification of Synthetic Lignin to Succinic Acid.* ACS Chemical Biology, 2017. **12**(7): p. 1749-1759.

186. Xiao, R., et al., *Investigation on the effects of cultivation conditions, fed-batch operation, and enzymatic hydrolysate of corn stover on the astaxanthin production by Thraustochytrium striatum.* Algal Research, 2019. **39**: p. 101475.

187. Reyes, L.H. and K.C. Kao, *Growth-Coupled Carotenoids Production Using Adaptive Laboratory Evolution*, in *Synthetic Metabolic Pathways: Methods and Protocols*, M.K. Jensen and J.D. Keasling, Editors. 2018, Springer New York: New York, NY. p. 319-330.

188. Breierová, E., et al., *The Effect of Zn(II) Ions and Reactive Oxygen on the Uptake of Zinc and Production of Carotenoids by Selected Red Yeasts.* Chemistry & Biodiversity, 2018. **15**(6): p. e1800069.

189. Ma, R.Y.-N. and F. Chen, *Enhanced production of free trans-astaxanthin by oxidative stress in the cultures of the green microalga Chlorococcum sp.* Process Biochemistry, 2001. **36**(12): p. 1175-1179.

190. Pham, L.T.M., et al., *In silico-designed lignin peroxidase from Phanerochaete chrysosporium shows enhanced acid stability for depolymerization of lignin.* Biotechnology for Biofuels, 2018. **11**(1): p. 325.

191. Li, X., et al., *Inhibitory effects of lignin on enzymatic hydrolysis: The role of lignin chemistry and molecular weight.* Renewable Energy, 2018. **123**: p. 664-674.

192. Ragauskas, A.J., et al., *Lignin Valorization: Improving Lignin Processing in the*

Biorefinery. Science, 2014. **344**(6185): p. 1246843.

193. Yang, C., et al., *A Constructed Alkaline Consortium and Its Dynamics in Treating Alkaline Black Liquor with Very High Pollution Load.* PLOS ONE, 2008. **3**(11): p. e3777.

194. Carvalho, L., et al., *Methanol production via black liquor co-gasification with expanded raw material base – Techno-economic assessment.* Applied Energy, 2018. **225**: p. 570-584.

195. Darmawan, A., et al., *Enhanced process integration of black liquor evaporation, gasification, and combined cycle.* Applied Energy, 2017. **204**: p. 1035-1042.

196. Huet, M., et al., *Hydrothermal treatment of black liquor for energy and phenolic platform molecules recovery in a pulp mill.* Biomass and Bioenergy, 2016. **89**: p. 105-112.

197. Ong, B.H.Y., et al., *Hydrothermal liquefaction of Radiata Pine with Kraft black liquor for integrated biofuel production.* Journal of Cleaner Production, 2018. **199**: p. 737-750.

198. Lara, M.A., et al., *Black liquor lignin biodegradation by Trametes elegans.* International Biodeterioration & Biodegradation, 2003. **52**(3): p. 167-173.

199. Da Re, V. and L. Papinutti, *Black Liquor Decolorization by Selected White-Rot Fungi.* Applied Biochemistry and Biotechnology, 2011. **165**(2): p. 406-415.

200. Kudahettige-Nilsson, R.L., et al., *Biobutanol production by Clostridium acetobutylicum using xylose recovered from birch Kraft black liquor.* Bioresource Technology, 2015. **176**: p. 71-79.

201. Faisal, A., et al., *Zeolite MFI adsorbent for recovery of butanol from ABE fermentation broths produced from an inexpensive black liquor-derived hydrolyzate.* Biomass Conversion and Biorefinery, 2018. **8**(3): p. 679-687.

202. Xiao, R., X. Li, and Y. Zheng, *Comprehensive Study of Cultivation Conditions and Methods on Lipid Accumulation of a Marine Protist, Thraustochytrium striatum.* Protist, 2018. **169**(4): p. 451-465.

203. Zaied, M. and N. Bellakhal, *Electrocoagulation treatment of black liquor from paper industry.* Journal of Hazardous Materials, 2009. **163**(2): p. 995-1000.

204. Knill, C.J. and J.F. Kennedy, *Degradation of cellulose under alkaline conditions.* Carbohydrate Polymers, 2003. **51**(3): p. 281-300.

205. Xiao, R., et al., *Investigation of composition, structure and bioactivity of extracellular polymeric substances from original and stress-induced strains of Thraustochytrium striatum.* Carbohydrate Polymers, 2018. **195**: p. 515-524.

206. Gao, L., et al., *Extracellular polymeric substances buffer against the biocidal effect of*

H2O2 on the bloom-forming cyanobacterium Microcystis aeruginosa. Water Research, 2015. **69**: p. 51-58.

207. Yue, Z.-B., et al., *Component analysis and heavy metal adsorption ability of extracellular polymeric substances (EPS) from sulfate reducing bacteria.* Bioresource Technology, 2015. **194**: p. 399-402.

208. Zhang, C.-C., et al., *Thermodynamics of the interaction between antibiotics and extracellular polymeric substances within activated sludge.* Environmental Technology, 2019. **40**(12): p. 1525-1533.

209. Grabherr, M.G., et al., *Full-length transcriptome assembly from RNA-Seq data without a reference genome.* Nature biotechnology, 2011. **29**(7): p. 644-652.

210. Davidson, N.M. and A. Oshlack, *Corset: enabling differential gene expression analysis for de novoassembled transcriptomes.* Genome Biology, 2014. **15**(7): p. 410.

211. Gandía-Herrero, F. and F. García-Carmona, *Characterization of recombinant Beta vulgaris 4,5-DOPA-extradiol-dioxygenase active in the biosynthesis of betalains.* Planta, 2012. **236**(1): p. 91-100.

212. Zhao, X., et al., *Genomic Analysis of Genes Involved in the Biosynthesis of Very Long Chain Polyunsaturated Fatty Acids in Thraustochytrium sp. 26185.* Lipids, 2016. **51**(9): p. 1065-1075.

213. Kurosawa, K., J. Laser, and A.J. Sinskey, *Tolerance and adaptive evolution of triacylglycerol-producing Rhodococcus opacus to lignocellulose-derived inhibitors.* Biotechnology for Biofuels, 2015. **8**(1): p. 76.

Appendix A - Statistical analysis

Appendix A.1 Fermentation with aromatic compounds

(A) TFA accumulation in batch mode; (B) total carotenoids accumulation in batch mode; (C) TFA accumulation in fed-batch mode; (D) total carotenoids accumulation in fed-batch mode.

(A)

Analysis of Variance

Source	DF	Sum of Squares	Mean Square	F Ratio	Prob > F
Substrate	1	33.872400	33.8724	1330.939	0.0008*
Error	2	0.050900	0.0254		
C. Total	3	33.923300			

Means for Oneway Anova

Level	Number	Mean	Std Error	Lower 95%	Upper 95%
3,4-DHBA	2	12.5250	0.11281	12.040	13.010
4-HBA	2	6.7050	0.11281	6.220	7.190

Std Error uses a pooled estimate of error variance

Means Comparisons

Comparisons for all pairs using Tukey-Kramer HSD

Confidence Quantile

q*	Alpha
4.30265	0.05

HSD Threshold Matrix

Abs(Dif)-HSD

	3,4-DHBA	4-HBA
3,4-DHBA	-0.6864	5.1336
4-HBA	5.1336	-0.6864

Positive values show pairs of means that are significantly different.

Connecting Letters Report

Level		Mean
3,4-DHBA	A	12.525000
4-HBA	B	6.705000

Levels not connected by same letter are significantly different.

(B)

Analysis of Variance

Source	DF	Sum of Squares	Mean Square	F Ratio	Prob > F
Substrate	1	0.00024398	0.000244	4.0959	0.1803
Error	2	0.00011914	0.000060		
C. Total	3	0.00036312			

Means for Oneway Anova

Level	Number	Mean	Std Error	Lower 95%	Upper 95%
3,4-DHBA	2	0.110310	0.00546	0.08683	0.13379
4-HBA	2	0.125930	0.00546	0.10245	0.14941

Std Error uses a pooled estimate of error variance

Means Comparisons

Comparisons for all pairs using Tukey-Kramer HSD

Confidence Quantile

q*	Alpha
4.30265	0.05

HSD Threshold Matrix

Abs(Dif)-HSD

	4-HBA	3,4-DHBA
4-HBA	-0.03321	-0.01759
3,4-DHBA	-0.01759	-0.03321

Positive values show pairs of means that are significantly different.

Connecting Letters Report

Level		Mean
4-HBA	A	0.12592950
3,4-DHBA	A	0.11030950

Levels not connected by same letter are significantly different.

(C)

Analysis of Variance

Source	DF	Sum of Squares	Mean Square	F Ratio	Prob > F
Substrate	1	53.290000	53.2900	32.7969	0.0292*
Error	2	3.249700	1.6248		
C. Total	3	56.539700			

Means for Oneway Anova

Level	Number	Mean	Std Error	Lower 95%	Upper 95%
3,4-DHBA	2	22.2150	0.90135	18.337	26.093
4-HBA	2	14.9150	0.90135	11.037	18.793

Std Error uses a pooled estimate of error variance

Means Comparisons

Comparisons for all pairs using Tukey-Kramer HSD

Confidence Quantile

q*	Alpha
4.30265	0.05

HSD Threshold Matrix

Abs(Dif)-HSD

	3,4-DHBA	4-HBA
3,4-DHBA	-5.4846	1.8154
4-HBA	1.8154	-5.4846

Positive values show pairs of means that are significantly different.

Connecting Letters Report

Level		Mean
3,4-DHBA	A	22.215000
4-HBA	B	14.915000

Levels not connected by same letter are significantly different.

(D)

Analysis of Variance

Source	DF	Sum of Squares	Mean Square	F Ratio	Prob > F
Substrate	1	0.01913754	0.019138	71.7363	0.0137*
Error	2	0.00053355	0.000267		
C. Total	3	0.01967109			

Means for Oneway Anova

Level	Number	Mean	Std Error	Lower 95%	Upper 95%
3,4-DHBA	2	0.268667	0.01155	0.21897	0.31836
4-HBA	2	0.130328	0.01155	0.08064	0.18002

Std Error uses a pooled estimate of error variance

Means Comparisons

Comparisons for all pairs using Tukey-Kramer HSD

Confidence Quantile

q*	Alpha
4.30265	0.05

HSD Threshold Matrix

Abs(Dif)-HSD

	3,4-DHBA	4-HBA
3,4-DHBA	-0.07028	0.06806
4-HBA	0.06806	-0.07028

Positive values show pairs of means that are significantly different.

Connecting Letters Report

Level		Mean
3,4-DHBA	A	0.26866650
4-HBA	B	0.13032800

Levels not connected by same letter are significantly different.

Appendix A.2 Aromatic compounds fermentation with/without pH control

(A) cell mass concentration; (B) TFA accumulation; (C) total carotenoids accumulation.

(A)

Analysis of Variance

Source	DF	Sum of Squares	Mean Square	F Ratio	Prob > F
Treatment	3	1.5006158	0.500205	103.8976	0.0003*
Error	4	0.0192576	0.004814		
C. Total	7	1.5198735			

Means for Oneway Anova

Level	Number	Mean	Std Error	Lower 95%	Upper 95%
3,4-DHBA with pH control	2	1.79531	0.04906	1.6591	1.9315
3,4-DHBA without pH control	2	1.87504	0.04906	1.7388	2.0113
4-HBA with pH control	2	0.92558	0.04906	0.7894	1.0618
4-HBA without pH control	2	1.02134	0.04906	0.8851	1.1576

Std Error uses a pooled estimate of error variance

Means Comparisons

Comparisons for all pairs using Tukey-Kramer HSD

Confidence Quantile

q*	Alpha
4.07085	0.05

HSD Threshold Matrix

Abs(Dif)-HSD

	3,4-DHBA without pH control	3,4-DHBA with pH control	4-HBA without pH control	4-HBA with pH control
3,4-DHBA without pH control	-0.28246	-0.20274	0.57123	0.66699
3,4-DHBA with pH control	-0.20274	-0.28246	0.49151	0.58727
4-HBA without pH control	0.57123	0.49151	-0.28246	-0.18670
4-HBA with pH control	0.66699	0.58727	-0.18670	-0.28246

Positive values show pairs of means that are significantly different.

Connecting Letters Report

Level		Mean
3,4-DHBA without pH control	A	1.8750350
3,4-DHBA with pH control	A	1.7953105
4-HBA without pH control	B	1.0213420
4-HBA with pH control	B	0.9255825

Levels not connected by same letter are significantly different.

(B)

Analysis of Variance

Source	DF	Sum of Squares	Mean Square	F Ratio	Prob > F
Treatment	3	61.571038	20.5237	1058.604	<.0001*
Error	4	0.077550	0.0194		
C. Total	7	61.648588			

Means for Oneway Anova

Level	Number	Mean	Std Error	Lower 95%	Upper 95%
3,4-DHBA with pH control	2	11.5250	0.09846	11.252	11.798
3,4-DHBA without pH control	2	12.5250	0.09846	12.252	12.798
4-HBA with pH control	2	6.3500	0.09846	6.077	6.623
4-HBA without pH control	2	6.7050	0.09846	6.432	6.978

Std Error uses a pooled estimate of error variance

Means Comparisons

Comparisons for all pairs using Tukey-Kramer HSD

Confidence Quantile

q*	Alpha
4.07085	0.05

HSD Threshold Matrix

Abs(Dif)-HSD

	3,4-DHBA without pH control	3,4-DHBA with pH control	4-HBA without pH control	4-HBA with pH control
3,4-DHBA without pH control	-0.5668	0.4332	5.2532	5.6082
3,4-DHBA with pH control	0.4332	-0.5668	4.2532	4.6082
4-HBA without pH control	5.2532	4.2532	-0.5668	-0.2118
4-HBA with pH control	5.6082	4.6082	-0.2118	-0.5668

Positive values show pairs of means that are significantly different.

Connecting Letters Report

Level		Mean
3,4-DHBA without pH control	A	12.525000
3,4-DHBA with pH control	B	11.525000
4-HBA without pH control	C	6.705000
4-HBA with pH control	C	6.350000

Levels not connected by same letter are significantly different.

(C)

Analysis of Variance

Source	DF	Sum of Squares	Mean Square	F Ratio	Prob > F
Treatment	3	0.00232445	0.000775	19.6287	0.0074*
Error	4	0.00015789	0.000039		
C. Total	7	0.00248235			

Means for Oneway Anova

Level	Number	Mean	Std Error	Lower 95%	Upper 95%
3,4-DHBA with pH control	2	0.115481	0.00444	0.10315	0.12782
3,4-DHBA without pH control	2	0.110310	0.00444	0.09797	0.12264
4-HBA with pH control	2	0.080081	0.00444	0.06775	0.09242
4-HBA without pH control	2	0.125930	0.00444	0.11359	0.13826

Std Error uses a pooled estimate of error variance

Means Comparisons

Comparisons for all pairs using Tukey-Kramer HSD

Confidence Quantile

q*	Alpha
4.07085	0.05

HSD Threshold Matrix

Abs(Dif)-HSD

	4-HBA without pH control	3,4-DHBA with pH control	3,4-DHBA without pH control	4-HBA with pH control
4-HBA without pH control	-0.02558	-0.01513	-0.00996	0.02027
3,4-DHBA with pH control	-0.01513	-0.02558	-0.02040	0.00982
3,4-DHBA without pH control	-0.00996	-0.02040	-0.02558	0.00465
4-HBA with pH control	0.02027	0.00982	0.00465	-0.02558

Positive values show pairs of means that are significantly different.

Connecting Letters Report

Level		Mean
4-HBA without pH control	A	0.12592950
3,4-DHBA with pH control	A	0.11548100
3,4-DHBA without pH control	A	0.11030950
4-HBA with pH control	B	0.08008100

Levels not connected by same letter are significantly different.

Appendix A.3 Direct fermentation of three technical lignins

(A) Cell mass concentration; (B) lignin conversion percentage; (C) TFA accumulation; (D) total carotenoids accumulation.

(A)

Analysis of Variance

Source	DF	Sum of Squares	Mean Square	F Ratio	Prob > F
Types of lignin	2	0.02595468	0.012977	31.3741	0.0097*
Error	3	0.00124090	0.000414		
C. Total	5	0.02719558			

Means for Oneway Anova

Level	Number	Mean	Std Error	Lower 95%	Upper 95%
AL CS	2	1.29115	0.01438	1.2454	1.3369
EOL LP	2	1.21165	0.01438	1.1659	1.2574
KPL	2	1.37275	0.01438	1.3270	1.4185

Std Error uses a pooled estimate of error variance

Means Comparisons

Comparisons for all pairs using Tukey-Kramer HSD

Confidence Quantile

q*	Alpha
4.17871	0.05

HSD Threshold Matrix

Abs(Dif)-HSD

	KPL	AL CS	EOL LP
KPL	-0.08499	-0.00339	0.07611
AL CS	-0.00339	-0.08499	-0.00549
EOL LP	0.07611	-0.00549	-0.08499

Positive values show pairs of means that are significantly different.

Connecting Letters Report

Level		Mean
KPL	A	1.3727500
AL CS	A B	1.2911500
EOL LP	B	1.2116500

Levels not connected by same letter are significantly different.

(B)

Analysis of Variance

Source	DF	Sum of Squares	Mean Square	F Ratio	Prob > F
Types of lignin	2	4.6668813	2.33344	2.0801	0.2712
Error	3	3.3653603	1.12179		
C. Total	5	8.0322417			

Means for Oneway Anova

Level	Number	Mean	Std Error	Lower 95%	Upper 95%
AL CS	2	24.8406	0.74893	22.457	27.224
EOL LP	2	22.6806	0.74893	20.297	25.064
KPL	2	23.7296	0.74893	21.346	26.113

Std Error uses a pooled estimate of error variance

Means Comparisons

Comparisons for all pairs using Tukey-Kramer HSD

Confidence Quantile

q*	Alpha
4.17871	0.05

HSD Threshold Matrix

Abs(Dif)-HSD

	AL CS	KPL	EOL LP
AL CS	-4.4259	-3.3149	-2.2659
KPL	-3.3149	-4.4259	-3.3769
EOL LP	-2.2659	-3.3769	-4.4259

Positive values show pairs of means that are significantly different.

Connecting Letters Report

Level		Mean
AL CS	A	24.840550
KPL	A	23.729550
EOL LP	A	22.680550

Levels not connected by same letter are significantly different.

(C)

Analysis of Variance

Source	DF	Sum of Squares	Mean Square	F Ratio	Prob > F
Types of lignin	2	38.002397	19.0012	10.8656	0.0422*
Error	3	5.246255	1.7488		
C. Total	5	43.248652			

Means for Oneway Anova

Level	Number	Mean	Std Error	Lower 95%	Upper 95%
AL CS	2	24.0806	0.93508	21.105	27.056
EOL LP	2	17.9315	0.93508	14.956	20.907
KPL	2	20.6276	0.93508	17.652	23.603

Std Error uses a pooled estimate of error variance

Means Comparisons

Comparisons for all pairs using Tukey-Kramer HSD

Confidence Quantile

q*	Alpha
4.17871	0.05

HSD Threshold Matrix

Abs(Dif)-HSD

	AL CS	KPL	EOL LP
AL CS	-5.5259	-2.0729	0.6232
KPL	-2.0729	-5.5259	-2.8298
EOL LP	0.6232	-2.8298	-5.5259

Positive values show pairs of means that are significantly different.

Connecting Letters Report

Level		Mean
AL CS	A	24.080550
KPL	A B	20.627550
EOL LP	B	17.931450

Levels not connected by same letter are significantly different.

(D)

Analysis of Variance

Source	DF	Sum of Squares	Mean Square	F Ratio	Prob > F
Types of lignin	2	0.00212529	0.001063	121.0304	0.0014*
Error	3	0.00002634	8.78e-6		
C. Total	5	0.00215163			

Means for Oneway Anova

Level	Number	Mean	Std Error	Lower 95%	Upper 95%
AL CS	2	0.057800	0.00210	0.05113	0.06447
EOL LP	2	0.102100	0.00210	0.09543	0.10877
KPL	2	0.068900	0.00210	0.06223	0.07557

Std Error uses a pooled estimate of error variance

Means Comparisons

Comparisons for all pairs using Tukey-Kramer HSD

Confidence Quantile

q*	Alpha
4.17871	0.05

HSD Threshold Matrix

Abs(Dif)-HSD

	EOL LP	KPL	AL CS
EOL LP	-0.01238	0.02082	0.03192
KPL	0.02082	-0.01238	-0.00128
AL CS	0.03192	-0.00128	-0.01238

Positive values show pairs of means that are significantly different.

Connecting Letters Report

Level		Mean
EOL LP	A	0.10210000
KPL	B	0.06890000
AL CS	B	0.05780000

Levels not connected by same letter are significantly different.

Appendix A.4 Technical lignins fermentation with different loadings of laccase

(A) cell mass concentration; (B) TFA accumulation; (C) total carotenoids accumulation.

(A)

Analysis of Variance

Source	DF	Sum of Squares	Mean Square	F Ratio	Prob > F
Laccase loading	4	0.02796347	0.006991	0.2716	0.8846
Error	5	0.12869866	0.025740		
C. Total	9	0.15666213			

Means for Oneway Anova

Level	Number	Mean	Std Error	Lower 95%	Upper 95%
0	2	1.47065	0.11345	1.1790	1.7623
1	2	1.44205	0.11345	1.1504	1.7337
2	2	1.57460	0.11345	1.2830	1.8662
0.1	2	1.42980	0.11345	1.1382	1.7214
0.5	2	1.44415	0.11345	1.1525	1.7358

Std Error uses a pooled estimate of error variance

Means Comparisons

Comparisons for all pairs using Tukey-Kramer HSD

Confidence Quantile

q*	Alpha
4.01150	0.05

HSD Threshold Matrix

Abs(Dif)-HSD

	2	0	0.5	1	0.1
2	-0.64359	-0.53964	-0.51314	-0.51104	-0.49879
0	-0.53964	-0.64359	-0.61709	-0.61499	-0.60274
0.5	-0.51314	-0.61709	-0.64359	-0.64149	-0.62924
1	-0.51104	-0.61499	-0.64149	-0.64359	-0.63134
0.1	-0.49879	-0.60274	-0.62924	-0.63134	-0.64359

Positive values show pairs of means that are significantly different.

Connecting Letters Report

Level		Mean
2	A	1.5746000
0	A	1.4706500
0.5	A	1.4441500
1	A	1.4420500
0.1	A	1.4298000

Levels not connected by same letter are significantly different.

(B)

Analysis of Variance

Source	DF	Sum of Squares	Mean Square	F Ratio	Prob > F
Laccase loading	4	14.604740	3.65118	6.7862	0.0297*
Error	5	2.690150	0.53803		
C. Total	9	17.294890			

Means for Oneway Anova

Level	Number	Mean	Std Error	Lower 95%	Upper 95%
0	2	18.4100	0.51867	17.077	19.743
1	2	20.0950	0.51867	18.762	21.428
2	2	19.0350	0.51867	17.702	20.368
0.1	2	21.2600	0.51867	19.927	22.593
0.5	2	17.8950	0.51867	16.562	19.228

Std Error uses a pooled estimate of error variance

Means Comparisons

Comparisons for all pairs using Tukey-Kramer HSD

Confidence Quantile

q*	Alpha
4.01150	0.05

HSD Threshold Matrix

Abs(Dif)-HSD

	0.1	1	2	0	0.5
0.1	-2.9425	-1.7775	-0.7175	-0.0925	0.4225
1	-1.7775	-2.9425	-1.8825	-1.2575	-0.7425
2	-0.7175	-1.8825	-2.9425	-2.3175	-1.8025
0	-0.0925	-1.2575	-2.3175	-2.9425	-2.4275
0.5	0.4225	-0.7425	-1.8025	-2.4275	-2.9425

Positive values show pairs of means that are significantly different.

Connecting Letters Report

Level		Mean
0.1	A	21.260000
1	A B	20.095000
2	A B	19.035000
0	A B	18.410000
0.5	B	17.895000

Levels not connected by same letter are significantly different.

(C)

Analysis of Variance

Source	DF	Sum of Squares	Mean Square	F Ratio	Prob > F
Laccase loading	4	0.00004072	0.000010	2.4538	0.1758
Error	5	0.00002075	4.149e-6		
C. Total	9	0.00006147			

Means for Oneway Anova

Level	Number	Mean	Std Error	Lower 95%	Upper 95%
0	2	0.054500	0.00144	0.05080	0.05820
1	2	0.056700	0.00144	0.05300	0.06040
2	2	0.060400	0.00144	0.05670	0.06410
0.1	2	0.055350	0.00144	0.05165	0.05905
0.5	2	0.056600	0.00144	0.05290	0.06030

Std Error uses a pooled estimate of error variance

Means Comparisons

Comparisons for all pairs using Tukey-Kramer HSD

Confidence Quantile

q*	Alpha
4.01150	0.05

HSD Threshold Matrix

Abs(Dif)-HSD

	2	1	0.5	0.1	0
2	-0.00817	-0.00447	-0.00437	-0.00312	-0.00227
1	-0.00447	-0.00817	-0.00807	-0.00682	-0.00597
0.5	-0.00437	-0.00807	-0.00817	-0.00692	-0.00607
0.1	-0.00312	-0.00682	-0.00692	-0.00817	-0.00732
0	-0.00227	-0.00597	-0.00607	-0.00732	-0.00817

Positive values show pairs of means that are significantly different.

Connecting Letters Report

Level		Mean
2	A	0.06040000
1	A	0.05670000
0.5	A	0.05660000
0.1	A	0.05535000
0	A	0.05450000

Levels not connected by same letter are significantly different.

Appendix A.5 Effects of nitrogen source type on KPL fermentation

(A) cell concentration; (B) lignin utilization; (C) cell concentrations from fermentation with organic nitrogen source only and with organic nitrogen source/KPL.

(A)

Analysis of Variance

Source	DF	Sum of Squares	Mean Square	F Ratio	Prob > F
Nitrogen source	4	1.0605400	0.265135	8.6589	0.0180*
Error	5	0.1531000	0.030620		
C. Total	9	1.2136400			

Means for Oneway Anova

Level	Number	Mean	Std Error	Lower 95%	Upper 95%
NaNO3	2	5.56500	0.12373	5.2469	5.8831
NH4Cl	2	5.88000	0.12373	5.5619	6.1981
Peptone	2	6.28000	0.12373	5.9619	6.5981
Urea	2	5.70000	0.12373	5.3819	6.0181
YE	2	6.40500	0.12373	6.0869	6.7231

Std Error uses a pooled estimate of error variance

Means Comparisons

Comparisons for all pairs using Tukey-Kramer HSD

Confidence Quantile

q*	Alpha
4.01150	0.05

HSD Threshold Matrix

Abs(Dif)-HSD

	YE	Peptone	NH4Cl	Urea	NaNO3
YE	-0.70196	-0.57696	-0.17696	0.00304	0.13804
Peptone	-0.57696	-0.70196	-0.30196	-0.12196	0.01304
NH4Cl	-0.17696	-0.30196	-0.70196	-0.52196	-0.38696
Urea	0.00304	-0.12196	-0.52196	-0.70196	-0.56696
NaNO3	0.13804	0.01304	-0.38696	-0.56696	-0.70196

Positive values show pairs of means that are significantly different.

Connecting Letters Report

Level			Mean
YE	A		6.4050000
Peptone	A	B	6.2800000
NH4Cl	A	B C	5.8800000
Urea		B C	5.7000000
NaNO3		C	5.5650000

Levels not connected by same letter are significantly different.

(B)

Analysis of Variance

Source	DF	Sum of Squares	Mean Square	F Ratio	Prob > F
Nitrogen source	4	214.65053	53.6626	56.7156	0.0002*
Error	5	4.73085	0.9462		
C. Total	9	219.38138			

Means for Oneway Anova

Level	Number	Mean	Std Error	Lower 95%	Upper 95%
NaNO3	2	7.7656	0.68781	5.998	9.534
NH4Cl	2	16.4862	0.68781	14.718	18.254
Peptone	2	6.6030	0.68781	4.835	8.371
Urea	2	4.2778	0.68781	2.510	6.046
YE	2	3.5508	0.68781	1.783	5.319

Std Error uses a pooled estimate of error variance

Means Comparisons

Comparisons for all pairs using Tukey-Kramer HSD

Confidence Quantile

q*	Alpha
4.01150	0.05

HSD Threshold Matrix

Abs(Dif)-HSD

	NH4Cl	NaNO3	Peptone	Urea	YE
NH4Cl	-3.9020	4.8185	5.9812	8.3063	9.0334
NaNO3	4.8185	-3.9020	-2.7394	-0.4142	0.3128
Peptone	5.9812	-2.7394	-3.9020	-1.5769	-0.8498
Urea	8.3063	-0.4142	-1.5769	-3.9020	-3.1750
YE	9.0334	0.3128	-0.8498	-3.1750	-3.9020

Positive values show pairs of means that are significantly different.

Connecting Letters Report

Level			Mean
NH4Cl	A		16.486150
NaNO3		B	7.765600
Peptone		B C	6.602950
Urea		B C	4.277800
YE		C	3.550750

Levels not connected by same letter are significantly different.

(C)

Analysis of Variance

Source	DF	Sum of Squares	Mean Square	F Ratio	Prob > F
Treatment	5	0.9189417	0.183788	4.9594	0.0383*
Error	6	0.2223500	0.037058		
C. Total	11	1.1412917			

Means for Oneway Anova

Level	Number	Mean	Std Error	Lower 95%	Upper 95%
Peptone	2	5.82500	0.13612	5.4919	6.1581
Peptone+KPL	2	6.28000	0.13612	5.9469	6.6131
Urea	2	5.69500	0.13612	5.3619	6.0281
Urea+KPL	2	5.70000	0.13612	5.3669	6.0331
YE	2	6.06000	0.13612	5.7269	6.3931
YE+KPL	2	6.40500	0.13612	6.0719	6.7381

Std Error uses a pooled estimate of error variance

Means Comparisons

Comparisons for all pairs using Tukey-Kramer HSD

Confidence Quantile

q*	Alpha
3.97998	0.05

HSD Threshold Matrix

Abs(Dif)-HSD

	YE+KPL	Peptone+KPL	YE	Peptone	Urea+KPL	Urea
YE+KPL	-0.76617	-0.64117	-0.42117	-0.18617	-0.06117	-0.05617
Peptone+KPL	-0.64117	-0.76617	-0.54617	-0.31117	-0.18617	-0.18117
YE	-0.42117	-0.54617	-0.76617	-0.53117	-0.40617	-0.40117
Peptone	-0.18617	-0.31117	-0.53117	-0.76617	-0.64117	-0.63617
Urea+KPL	-0.06117	-0.18617	-0.40617	-0.64117	-0.76617	-0.76117
Urea	-0.05617	-0.18117	-0.40117	-0.63617	-0.76117	-0.76617

Positive values show pairs of means that are significantly different.

Connecting Letters Report

Level		Mean
YE+KPL	A	6.4050000
Peptone+KPL	A	6.2800000
YE	A	6.0600000
Peptone	A	5.8250000
Urea+KPL	A	5.7000000
Urea	A	5.6950000

Levels not connected by same letter are significantly different.

Appendix A.6 Effects of growth factors on KPL fermentation.

(A) cell concentration; (B) lignin utilization.

(A)

Analysis of Variance

Source	DF	Sum of Squares	Mean Square	F Ratio	Prob > F
Treatment	2	0.03663333	0.018317	5.6649	0.0958
Error	3	0.00970000	0.003233		
C. Total	5	0.04633333			

Means for Oneway Anova

Level	Number	Mean	Std Error	Lower 95%	Upper 95%
Mineral	2	5.79500	0.04021	5.6670	5.9230
Mineral+vitamin	2	5.74500	0.04021	5.6170	5.8730
Vitamin	2	5.61000	0.04021	5.4820	5.7380

Std Error uses a pooled estimate of error variance

Means Comparisons

Comparisons for all pairs using Tukey-Kramer HSD

Confidence Quantile

q*	Alpha
4.17871	0.05

HSD Threshold Matrix

Abs(Dif)-HSD

	Mineral	Mineral+vitamin	Vitamin
Mineral	-0.23761	-0.18761	-0.05261
Mineral+vitamin	-0.18761	-0.23761	-0.10261
Vitamin	-0.05261	-0.10261	-0.23761

Positive values show pairs of means that are significantly different.

Connecting Letters Report

Level		Mean
Mineral	A	5.7950000
Mineral+vitamin	A	5.7450000
Vitamin	A	5.6100000

Levels not connected by same letter are significantly different.

(B)

Analysis of Variance

Source	DF	Sum of Squares	Mean Square	F Ratio	Prob > F
Treatment	3	149.11746	49.7058	59.9092	0.0009*
Error	4	3.31875	0.8297		
C. Total	7	152.43621			

Means for Oneway Anova

Level	Number	Mean	Std Error	Lower 95%	Upper 95%
Mineral	2	21.8544	0.64408	20.066	23.643
Mineral+vitamin	2	26.5330	0.64408	24.745	28.321
No treatment	2	16.4862	0.64408	14.698	18.274
Vitamin	2	15.9665	0.64408	14.178	17.755

Std Error uses a pooled estimate of error variance

Means Comparisons

Comparisons for all pairs using Tukey-Kramer HSD

Confidence Quantile

q*	Alpha
4.07085	0.05

HSD Threshold Matrix

Abs(Dif)-HSD

	Mineral+vitamin	Mineral	No treatment	Vitamin
Mineral+vitamin	-3.7080	0.9706	6.3388	6.8585
Mineral	0.9706	-3.7080	1.6602	2.1799
No treatment	6.3388	1.6602	-3.7080	-3.1884
Vitamin	6.8585	2.1799	-3.1884	-3.7080

Positive values show pairs of means that are significantly different.

Connecting Letters Report

Level		Mean
Mineral+vitamin	A	26.533000
Mineral	B	21.854400
No treatment	C	16.486150
Vitamin	C	15.966500

Levels not connected by same letter are significantly different.

Appendix A.7 Effects of cometabolism on lignin utilization percentage

Analysis of Variance

Source	DF	Sum of Squares	Mean Square	F Ratio	Prob > F
Glucose concentration	3	477.62517	159.208	99.2647	0.0003*
Error	4	6.41551	1.604		
C. Total	7	484.04068			

Means for Oneway Anova

Level	Number	Mean	Std Error	Lower 95%	Upper 95%
0	2	23.7296	0.89551	21.243	26.216
2	2	32.3620	0.89551	29.876	34.848
5	2	37.3993	0.89551	34.913	39.886
10	2	44.9828	0.89551	42.496	47.469

Std Error uses a pooled estimate of error variance

Means Comparisons

Comparisons for all pairs using Tukey-Kramer HSD

Confidence Quantile

q*	Alpha
4.07085	0.05

HSD Threshold Matrix

Abs(Dif)-HSD

	10	5	2	0
10	-5.156	2.428	7.465	16.098
5	2.428	-5.156	-0.118	8.514
2	7.465	-0.118	-5.156	3.477
0	16.098	8.514	3.477	-5.156

Positive values show pairs of means that are significantly different.

Connecting Letters Report

Level		Mean
10	A	44.982800
5	B	37.399300
2	B	32.362000
0	C	23.729550

Levels not connected by same letter are significantly different.

Appendix A.8 Enzyme production from fungal fermentation under different conditions

(A) LiP; (B) MnP; (C) Laccase.

(A)

Analysis of Variance

Source	DF	Sum of Squares	Mean Square	F Ratio	Prob > F
Treatment	3	1859.0216	619.674	142.0686	0.0002*
Error	4	17.4472	4.362		
C. Total	7	1876.4688			

Means for Oneway Anova

Level	Number	Mean	Std Error	Lower 95%	Upper 95%
GA	2	8.3871	1.4768	4.287	12.487
GS	2	7.6882	1.4768	3.588	11.788
RA	2	38.4946	1.4768	34.394	42.595
RS	2	38.5484	1.4768	34.448	42.649

Std Error uses a pooled estimate of error variance

Means Comparisons

Comparisons for all pairs using Tukey-Kramer HSD

Confidence Quantile

q*	Alpha
4.07085	0.05

HSD Threshold Matrix

Abs(Dif)-HSD

	RS	RA	GA	GS
RS	-8.502	-8.448	21.659	22.358
RA	-8.448	-8.502	21.606	22.304
GA	21.659	21.606	-8.502	-7.803
GS	22.358	22.304	-7.803	-8.502

Positive values show pairs of means that are significantly different.

Connecting Letters Report

Level		Mean
RS	A	38.548400
RA	A	38.494600
GA	B	8.387100
GS	B	7.688200

Levels not connected by same letter are significantly different.

(B)

Analysis of Variance

Source	DF	Sum of Squares	Mean Square	F Ratio	Prob > F
Treatment	3	93.191999	31.0640	27.2292	0.0040*
Error	4	4.563345	1.1408		
C. Total	7	97.755344			

Means for Oneway Anova

Level	Number	Mean	Std Error	Lower 95%	Upper 95%
GA	2	11.9658	0.75526	9.869	14.063
GS	2	12.1573	0.75526	10.060	14.254
RA	2	5.2722	0.75526	3.175	7.369
RS	2	5.2017	0.75526	3.105	7.299

Std Error uses a pooled estimate of error variance

Means Comparisons

Comparisons for all pairs using Tukey-Kramer HSD

Confidence Quantile

q*	Alpha
4.07085	0.05

HSD Threshold Matrix

Abs(Dif)-HSD

	GS	GA	RA	RS
GS	-4.3481	-4.1565	2.5370	2.6076
GA	-4.1565	-4.3481	2.3455	2.4160
RA	2.5370	2.3455	-4.3481	-4.2775
RS	2.6076	2.4160	-4.2775	-4.3481

Positive values show pairs of means that are significantly different.

Connecting Letters Report

Level		Mean
GS	A	12.157300
GA	A	11.965750
RA	B	5.272200
RS	B	5.201650

Levels not connected by same letter are significantly different.

(C)

Analysis of Variance

Source	DF	Sum of Squares	Mean Square	F Ratio	Prob > F
Treatment	3	18.131036	6.04368	17.9384	0.0088*
Error	4	1.347650	0.33691		
C. Total	7	19.478686			

Means for Oneway Anova

Level	Number	Mean	Std Error	Lower 95%	Upper 95%
GA	2	2.80555	0.41043	1.666	3.9451
GS	2	4.98615	0.41043	3.847	6.1257
RA	2	2.50000	0.41043	1.360	3.6395
RS	2	0.75000	0.41043	-0.390	1.8895

Std Error uses a pooled estimate of error variance

Means Comparisons

Comparisons for all pairs using Tukey-Kramer HSD

Confidence Quantile

q*	Alpha
4.07085	0.05

HSD Threshold Matrix

Abs(Dif)-HSD

	GS	GA	RA	RS
GS	-2.3629	-0.1823	0.1233	1.8733
GA	-0.1823	-2.3629	-2.0573	-0.3073
RA	0.1233	-2.0573	-2.3629	-0.6129
RS	1.8733	-0.3073	-0.6129	-2.3629

Positive values show pairs of means that are significantly different.

Connecting Letters Report

Level			Mean
GS	A		4.9861500
GA	A	B	2.8055500
RA		B	2.5000000
RS		B	0.7500000

Levels not connected by same letter are significantly different.

Appendix A.9 Simultaneous lignin depolymerization and fermentation

(A) cell concentration; (B) lignin utilization percentage; (C) TFA accumulation; (D) total carotenoids accumulation.

(A)

Analysis of Variance

Source	DF	Sum of Squares	Mean Square	F Ratio	Prob > F
Treatment	4	283864.73	70966.2	563.2192	<.0001*
Error	5	630.01	126.0		
C. Total	9	284494.73			

Means for Oneway Anova

Level	Number	Mean	Std Error	Lower 95%	Upper 95%
KPL	2	5.880	7.9373	-14.5	26.28
KPL_F	2	50.000	7.9373	29.6	70.40
KPL_R	2	179.000	7.9373	158.6	199.40
KPL_S	2	33.000	7.9373	12.6	53.40
KPL_T	2	461.000	7.9373	440.6	481.40

Std Error uses a pooled estimate of error variance

Means Comparisons

Comparisons for all pairs using Tukey-Kramer HSD

Confidence Quantile

q*	Alpha
4.01150	0.05

HSD Threshold Matrix

Abs(Dif)-HSD

	KPL_T	KPL_R	KPL_F	KPL_S	KPL
KPL_T	-45.03	236.97	365.97	382.97	410.09
KPL_R	236.97	-45.03	83.97	100.97	128.09
KPL_F	365.97	83.97	-45.03	-28.03	-0.91
KPL_S	382.97	100.97	-28.03	-45.03	-17.91
KPL	410.09	128.09	-0.91	-17.91	-45.03

Positive values show pairs of means that are significantly different.

Connecting Letters Report

Level		Mean
KPL_T	A	461.00000
KPL_R	B	179.00000
KPL_F	C	50.00000
KPL_S	C	33.00000
KPL	C	5.88000

Levels not connected by same letter are significantly different.

(B)

Analysis of Variance

Source	DF	Sum of Squares	Mean Square	F Ratio	Prob > F
Treatment	4	246.5366	61.6090	66.3421	<.0001*
Error	5	46.44641	9.2893		
C. Total	9	292.80543			

Means for Oneway Anova

Level	Number	Mean	Std Error	Lower 95%	Upper 95%
KPL	2	16.4862	2.1551	10.946	22.026
KPL_F	2	22.8285	2.1551	17.289	28.368
KPL_R	2	28.0093	2.1551	22.469	33.549
KPL_S	2	28.8597	2.1551	23.320	34.400
KPL_T	2	29.7101	2.1551	24.170	35.250

Std Error uses a pooled estimate of error variance

Means Comparisons

Comparisons for all pairs using Tukey-Kramer HSD

Confidence Quantile

q*	Alpha
4.01150	0.05

HSD Threshold Matrix

Abs(Dif)-HSD

	KPL_T	KPL_S	KPL_R	KPL_F	KPL
KPL_T	-12.226	-11.376	-10.526	-5.345	0.998
KPL_S	-11.376	-12.226	-11.376	-6.195	0.147
KPL_R	-10.526	-11.376	-12.226	-7.046	-0.703
KPL_F	-5.345	-6.195	-7.046	-12.226	-5.884
KPL	0.998	0.147	-0.703	-5.884	-12.226

Positive values show pairs of means that are significantly different.

Connecting Letters Report

Level		Mean
KPL_T	A	29.710100
KPL_S	A	28.859700
KPL_R	A B	28.009300
KPL_F	A B	22.828500
KPL	B	16.486150

Levels not connected by same letter are significantly different.

(C)

Analysis of Variance

Source	DF	Sum of Squares	Mean Square	F Ratio	Prob > F
Treatment	4	579.81100	144.953	134.2889	<.0001*
Error	5	5.39705	1.079		
C. Total	9	585.20805			

Means for Oneway Anova

Level	Number	Mean	Std Error	Lower 95%	Upper 95%
KPL	2	20.6250	0.73465	18.737	22.513
KPL_F	2	37.6500	0.73465	35.762	39.538
KPL_R	2	41.7000	0.73465	39.812	43.588
KPL_S	2	38.4000	0.73465	36.512	40.288
KPL_T	2	39.6500	0.73465	37.762	41.538

Std Error uses a pooled estimate of error variance

Means Comparisons

Comparisons for all pairs using Tukey-Kramer HSD

Confidence Quantile

q*	Alpha
4.01150	0.05

HSD Threshold Matrix

Abs(Dif)-HSD

	KPL_R	KPL_T	KPL_S	KPL_F	KPL
KPL_R	-4.168	-2.118	-0.868	-0.118	16.907
KPL_T	-2.118	-4.168	-2.918	-2.168	14.857
KPL_S	-0.868	-2.918	-4.168	-3.418	13.607
KPL_F	-0.118	-2.168	-3.418	-4.168	12.857
KPL	16.907	14.857	13.607	12.857	-4.168

Positive values show pairs of means that are significantly different.

Connecting Letters Report

Level		Mean
KPL_R	A	41.700000
KPL_T	A	39.650000
KPL_S	A	38.400000
KPL_F	A	37.650000
KPL	B	20.625000

Levels not connected by same letter are significantly different.

(D)

Analysis of Variance

Source	DF	Sum of Squares	Mean Square	F Ratio	Prob > F
Treatment	4	0.06187405	0.015469	308.6665	<.0001*
Error	5	0.00025057	0.000050		
C. Total	9	0.06212462			

Means for Oneway Anova

Level	Number	Mean	Std Error	Lower 95%	Upper 95%
KPL	2	0.068900	0.00501	0.05603	0.08177
KPL_F	2	0.277800	0.00501	0.26493	0.29067
KPL_R	2	0.237850	0.00501	0.22498	0.25072
KPL_S	2	0.281300	0.00501	0.26843	0.29417
KPL_T	2	0.246850	0.00501	0.23398	0.25972

Std Error uses a pooled estimate of error variance

Means Comparisons

Comparisons for all pairs using Tukey-Kramer HSD

Confidence Quantile

q*	Alpha
4.01150	0.05

HSD Threshold Matrix

Abs(Dif)-HSD

	KPL_S	KPL_F	KPL_T	KPL_R	KPL
KPL_S	-0.02840	-0.02490	0.00605	0.01505	0.18400
KPL_F	-0.02490	-0.02840	0.00255	0.01155	0.18050
KPL_T	0.00605	0.00255	-0.02840	-0.01940	0.14955
KPL_R	0.01505	0.01155	-0.01940	-0.02840	0.14055
KPL	0.18400	0.18050	0.14955	0.14055	-0.02840

Positive values show pairs of means that are significantly different.

Connecting Letters Report

Level		Mean
KPL_S	A	0.28130000
KPL_F	A	0.27780000
KPL_T	B	0.24685000
KPL_R	B	0.23785000
KPL	C	0.06890000

Levels not connected by same letter are significantly different.

Appendix A.10 Effects of NH_4Cl concentration on black liquor fermentation

(A) cell mass concentration; (B) conversion of total aromatics; (C) TFA accumulation; (D) carotenoids accumulation.

(A)

Analysis of Variance

Source	DF	Sum of Squares	Mean Square	F Ratio	Prob > F
N concentration	6	13.279501	2.21325	100.9755	<.0001*
Error	7	0.153431	0.02192		
C. Total	13	13.432932			

Means for Oneway Anova

Level	Number	Mean	Std Error	Lower 95%	Upper 95%
0.5	2	3.23895	0.10469	2.9914	3.4865
1	2	4.34355	0.10469	4.0960	4.5911
2	2	4.55775	0.10469	4.3102	4.8053
4	2	4.13295	0.10469	3.8854	4.3805
8	2	2.67620	0.10469	2.4287	2.9237
12	2	2.57440	0.10469	2.3269	2.8219
16	2	1.76355	0.10469	1.5160	2.0111

Std Error uses a pooled estimate of error variance

Means Comparisons

Comparisons for all pairs using Tukey-Kramer HSD

Confidence Quantile

q*	Alpha
3.96388	0.05

HSD Threshold Matrix

Abs(Dif)-HSD

	2	1	4	0.5	8	12	16
2	-0.5869	-0.3727	-0.1621	0.7319	1.2947	1.3965	2.2073
1	-0.3727	-0.5869	-0.3763	0.5177	1.0805	1.1823	1.9931
4	-0.1621	-0.3763	-0.5869	0.3071	0.8699	0.9717	1.7825
0.5	0.7319	0.5177	0.3071	-0.5869	-0.0241	0.0777	0.8885
8	1.2947	1.0805	0.8699	-0.0241	-0.5869	-0.4851	0.3258
12	1.3965	1.1823	0.9717	0.0777	-0.4851	-0.5869	0.2240
16	2.2073	1.9931	1.7825	0.8885	0.3258	0.2240	-0.5869

Positive values show pairs of means that are significantly different.

Connecting Letters Report

Level		Mean
2	A	4.5577500
1	A	4.3435500
4	A	4.1329500
0.5	B	3.2389500
8	B C	2.6762000
12	C	2.5744000
16	D	1.7635500

Levels not connected by same letter are significantly different.

(B)

Analysis of Variance

Source	DF	Sum of Squares	Mean Square	F Ratio	Prob > F
N concentration	6	2528.1927	421.365	697.5048	<.0001*
Error	7	4.2287	0.604		
C. Total	13	2532.4214			

Means for Oneway Anova

Level	Number	Mean	Std Error	Lower 95%	Upper 95%
0.5	2	45.4766	0.54959	44.177	46.776
1	2	60.1947	0.54959	58.895	61.494
2	2	62.7153	0.54959	61.416	64.015
4	2	55.0667	0.54959	53.767	56.366
8	2	47.9670	0.54959	46.667	49.267
12	2	31.4077	0.54959	30.108	32.707
16	2	23.9284	0.54959	22.629	25.228

Std Error uses a pooled estimate of error variance

Means Comparisons

Comparisons for all pairs using Tukey-Kramer HSD

Confidence Quantile

q*	Alpha
3.96388	0.05

HSD Threshold Matrix

Abs(Dif)-HSD

	2	1	4	8	0.5	12	16
2	-3.081	-0.560	4.568	11.667	14.158	28.227	35.706
1	-0.560	-3.081	2.047	9.147	11.637	25.706	33.185
4	4.568	2.047	-3.081	4.019	6.509	20.578	28.057
8	11.667	9.147	4.019	-3.081	-0.590	13.478	20.958
0.5	14.158	11.637	6.509	-0.590	-3.081	10.988	18.467
12	28.227	25.706	20.578	13.478	10.988	-3.081	4.398
16	35.706	33.185	28.057	20.958	18.467	4.398	-3.081

Positive values show pairs of means that are significantly different.

Connecting Letters Report

Level		Mean
2	A	62.715300
1	A	60.194650
4	B	55.066700
8	C	47.967000
0.5	C	45.476600
12	D	31.407700
16	E	23.928400

Levels not connected by same letter are significantly different.

(C)

Analysis of Variance

Source	DF	Sum of Squares	Mean Square	F Ratio	Prob > F
N concentration	6	21.004487	3.50075	28.6276	0.0001*
Error	7	0.856000	0.12229		
C. Total	13	21.860487			

Means for Oneway Anova

Level	Number	Mean	Std Error	Lower 95%	Upper 95%
0.5	2	6.87800	0.24727	6.2933	7.4627
1	2	7.18500	0.24727	6.6003	7.7697
2	2	7.44000	0.24727	6.8553	8.0247
4	2	5.19500	0.24727	4.6103	5.7797
8	2	4.27500	0.24727	3.6903	4.8597
12	2	4.81000	0.24727	4.2253	5.3947
16	2	4.77000	0.24727	4.1853	5.3547

Std Error uses a pooled estimate of error variance

Means Comparisons

Comparisons for all pairs using Tukey-Kramer HSD

Confidence Quantile

q*	Alpha
3.96388	0.05

HSD Threshold Matrix

Abs(Dif)-HSD

	2	1	0.5	4	12	16	8
2	-1.3861	-1.1311	-0.8241	0.8589	1.2439	1.2839	1.7789
1	-1.1311	-1.3861	-1.0791	0.6039	0.9889	1.0289	1.5239
0.5	-0.8241	-1.0791	-1.3861	0.2969	0.6819	0.7219	1.2169
4	0.8589	0.6039	0.2969	-1.3861	-1.0011	-0.9611	-0.4661
12	1.2439	0.9889	0.6819	-1.0011	-1.3861	-1.3461	-0.8511
16	1.2839	1.0289	0.7219	-0.9611	-1.3461	-1.3861	-0.8911
8	1.7789	1.5239	1.2169	-0.4661	-0.8511	-0.8911	-1.3861

Positive values show pairs of means that are significantly different.

Connecting Letters Report

Level		Mean
2	A	7.4400000
1	A	7.1850000
0.5	A	6.8780000
4	B	5.1950000
12	B	4.8100000
16	B	4.7700000
8	B	4.2750000

Levels not connected by same letter are significantly different.

(D)

Analysis of Variance

Source	DF	Sum of Squares	Mean Square	F Ratio	Prob > F
N concentration	6	0.00460855	0.000768	0.7335	0.6392
Error	7	0.00732975	0.001047		
C. Total	13	0.01193830			

Means for Oneway Anova

Level	Number	Mean	Std Error	Lower 95%	Upper 95%
0.5	2	0.221500	0.02288	0.16739	0.27561
1	2	0.242400	0.02288	0.18829	0.29651
2	2	0.244700	0.02288	0.19059	0.29881
4	2	0.199250	0.02288	0.14514	0.25336
8	2	0.227950	0.02288	0.17384	0.28206
12	2	0.217500	0.02288	0.16339	0.27161
16	2	0.193600	0.02288	0.13949	0.24771

Std Error uses a pooled estimate of error variance

Means Comparisons

Comparisons for all pairs using Tukey-Kramer HSD

Confidence Quantile

q*	Alpha
3.96388	0.05

HSD Threshold Matrix

Abs(Dif)-HSD

	2	1	8	0.5	12	4	16
2	-0.12827	-0.12597	-0.11152	-0.10507	-0.10107	-0.08282	-0.07717
1	-0.12597	-0.12827	-0.11382	-0.10737	-0.10337	-0.08512	-0.07947
8	-0.11152	-0.11382	-0.12827	-0.12182	-0.11782	-0.09957	-0.09392
0.5	-0.10507	-0.10737	-0.12182	-0.12827	-0.12427	-0.10602	-0.10037
12	-0.10107	-0.10337	-0.11782	-0.12427	-0.12827	-0.11002	-0.10437
4	-0.08282	-0.08512	-0.09957	-0.10602	-0.11002	-0.12827	-0.12262
16	-0.07717	-0.07947	-0.09392	-0.10037	-0.10437	-0.12262	-0.12827

Positive values show pairs of means that are significantly different.

Connecting Letters Report

Level		Mean
2	A	0.24470000
1	A	0.24240000
8	A	0.22795000
0.5	A	0.22150000
12	A	0.21750000
4	A	0.19925000
16	A	0.19360000

Levels not connected by same letter are significantly different.

Appendix A.11 Effects of fed-batch mode on black liquor fermentation

(A) cell mass concentration; (B) TFA accumulation; (C) total carotenoids accumulation.

(A)

Analysis of Variance

Source	DF	Sum of Squares	Mean Square	F Ratio	Prob > F
Sample #	5	13.145087	2.62902	612.3098	<.0001*
Error	6	0.025762	0.00429		
C. Total	11	13.170849			

Means for Oneway Anova

Level	Number	Mean	Std Error	Lower 95%	Upper 95%
BA_D8	2	3.22850	0.04633	3.1151	3.3419
BA_D12	2	2.83564	0.04633	2.7223	2.9490
BA_D16	2	2.82862	0.04633	2.7152	2.9420
FB_D8	2	4.82578	0.04633	4.7124	4.9392
FB_D12	2	5.12424	0.04633	5.0109	5.2376
FB_D16	2	5.14179	0.04633	5.0284	5.2552

Std Error uses a pooled estimate of error variance

Means Comparisons

Comparisons for all pairs using Tukey-Kramer HSD

Confidence Quantile

q*	Alpha
3.97998	0.05

HSD Threshold Matrix

Abs(Dif)-HSD

	FB_D16	FB_D12	FB_D8	BA_D8	BA_D12	BA_D16
FB_D16	-0.2608	-0.2432	0.0552	1.6525	2.0454	2.0524
FB_D12	-0.2432	-0.2608	0.0377	1.6349	2.0278	2.0348
FB_D8	0.0552	0.0377	-0.2608	1.3365	1.7294	1.7364
BA_D8	1.6525	1.6349	1.3365	-0.2608	0.1321	0.1391
BA_D12	2.0454	2.0278	1.7294	0.1321	-0.2608	-0.2538
BA_D16	2.0524	2.0348	1.7364	0.1391	-0.2538	-0.2608

Positive values show pairs of means that are significantly different.

Connecting Letters Report

Level			Mean
FB_D16	A		5.1417865
FB_D12	A		5.1242350
FB_D8		B	4.8257795
BA_D8		C	3.2285035
BA_D12		D	2.8356360
BA_D16		D	2.8286160

Levels not connected by same letter are significantly different.

(B)

Analysis of Variance

Source	DF	Sum of Squares	Mean Square	F Ratio	Prob > F
Sample #	5	96.001667	19.2003	353.0555	<.0001*
Error	6	0.326300	0.0544		
C. Total	11	96.327967			

Means for Oneway Anova

Level	Number	Mean	Std Error	Lower 95%	Upper 95%
BA_D8	2	6.9200	0.16490	6.517	7.323
BA_D12	2	5.3150	0.16490	4.912	5.718
BA_D16	2	4.4500	0.16490	4.047	4.853
FB_D8	2	7.2550	0.16490	6.852	7.658
FB_D12	2	10.3100	0.16490	9.907	10.713
FB_D16	2	12.6200	0.16490	12.217	13.023

Std Error uses a pooled estimate of error variance

Means Comparisons

Comparisons for all pairs using Tukey-Kramer HSD

Confidence Quantile

q*	Alpha
3.97998	0.05

HSD Threshold Matrix

Abs(Dif)-HSD

	FB_D16	FB_D12	FB_D8	BA_D8	BA_D12	BA_D16
FB_D16	-0.9281	1.3819	4.4369	4.7719	6.3769	7.2419
FB_D12	1.3819	-0.9281	2.1269	2.4619	4.0669	4.9319
FB_D8	4.4369	2.1269	-0.9281	-0.5931	1.0119	1.8769
BA_D8	4.7719	2.4619	-0.5931	-0.9281	0.6769	1.5419
BA_D12	6.3769	4.0669	1.0119	0.6769	-0.9281	-0.0631
BA_D16	7.2419	4.9319	1.8769	1.5419	-0.0631	-0.9281

Positive values show pairs of means that are significantly different.

Connecting Letters Report

Level			Mean
FB_D16	A		12.620000
FB_D12		B	10.310000
FB_D8		C	7.255000
BA_D8		C	6.920000
BA_D12		D	5.315000
BA_D16		D	4.450000

Levels not connected by same letter are significantly different.

Analysis of Variance

Source	DF	Sum of Squares	Mean Square	F Ratio	Prob > F
Sample #	5	0.01434738	0.002869	7.1387	0.0165*
Error	6	0.00241178	0.000402		
C. Total	11	0.01675916			

Means for Oneway Anova

Level	Number	Mean	Std Error	Lower 95%	Upper 95%
BA_D8	2	0.162580	0.01418	0.12789	0.19727
BA_D12	2	0.146500	0.01418	0.11181	0.18119
BA_D16	2	0.129350	0.01418	0.09466	0.16404
FB_D8	2	0.163900	0.01418	0.12921	0.19859
FB_D12	2	0.178975	0.01418	0.14429	0.21366
FB_D16	2	0.239255	0.01418	0.20457	0.27394

Std Error uses a pooled estimate of error variance

Means Comparisons

Comparisons for all pairs using Tukey-Kramer HSD

Confidence Quantile

q*	Alpha
3.97998	0.05

HSD Threshold Matrix

Abs(Dif)-HSD

	FB_D16	FB_D12	FB_D8	BA_D8	BA_D12	BA_D16
FB_D16	-0.07979	-0.01951	-0.00444	-0.00312	0.01296	0.03011
FB_D12	-0.01951	-0.07979	-0.06472	-0.06340	-0.04732	-0.03017
FB_D8	-0.00444	-0.06472	-0.07979	-0.07847	-0.06239	-0.04524
BA_D8	-0.00312	-0.06340	-0.07847	-0.07979	-0.06371	-0.04656
BA_D12	0.01296	-0.04732	-0.06239	-0.06371	-0.07979	-0.06264
BA_D16	0.03011	-0.03017	-0.04524	-0.04656	-0.06264	-0.07979

Positive values show pairs of means that are significantly different.

Connecting Letters Report

Level			Mean
FB_D16	A		0.23925500
FB_D12	A	B	0.17897500
FB_D8	A	B	0.16390000
BA_D8	A	B	0.16258000
BA_D12		B	0.14650000
BA_D16		B	0.12935000

Levels not connected by same letter are significantly different.

Appendix A.12 Effects of initial pH on black liquor fermentation

(A) cell mass concentration; (B) conversion of total aromatics; (C) TFA accumulation; (D) total carotenoids accumulation.

(A)

Analysis of Variance

Source	DF	Sum of Squares	Mean Square	F Ratio	Prob > F
Initial pH	6	43.894139	7.31569	327.5081	<.0001*
Error	7	0.156362	0.02234		
C. Total	13	44.050501			

Means for Oneway Anova

Level	Number	Mean	Std Error	Lower 95%	Upper 95%
7	2	5.02108	0.10568	4.771	5.2710
8	2	4.71215	0.10568	4.462	4.9620
9	2	3.90130	0.10568	3.651	4.1512
10	2	2.92195	0.10568	2.672	3.1718
11	2	2.12510	0.10568	1.875	2.3750
12	2	0.23055	0.10568	-0.019	0.4804
13	2	0.54720	0.10568	0.297	0.7971

Std Error uses a pooled estimate of error variance

Means Comparisons

Comparisons for all pairs using Tukey-Kramer HSD

Confidence Quantile

q*	Alpha
3.96388	0.05

HSD Threshold Matrix

Abs(Dif)-HSD

	7	8	9	10	11	13	12
7	-0.5924	-0.2835	0.5273	1.5067	2.3035	3.8814	4.1981
8	-0.2835	-0.5924	0.2184	1.1978	1.9946	3.5725	3.8892
9	0.5273	0.2184	-0.5924	0.3869	1.1838	2.7617	3.0783
10	1.5067	1.1978	0.3869	-0.5924	0.2044	1.7823	2.0990
11	2.3035	1.9946	1.1838	0.2044	-0.5924	0.9855	1.3021
13	3.8814	3.5725	2.7617	1.7823	0.9855	-0.5924	-0.2758
12	4.1981	3.8892	3.0783	2.0990	1.3021	-0.2758	-0.5924

Positive values show pairs of means that are significantly different.

Connecting Letters Report

Level		Mean
7	A	5.0210750
8	A	4.7121500
9	B	3.9013000
10	C	2.9219500
11	D	2.1251000
13	E	0.5472000
12	E	0.2305500

Levels not connected by same letter are significantly different.

(B)

Analysis of Variance

Source	DF	Sum of Squares	Mean Square	F Ratio	Prob > F
Initial pH	6	5191.6582	865.276	92.0301	<.0001*
Error	7	65.8147	9.402		
C. Total	13	5257.4729			

Means for Oneway Anova

Level	Number	Mean	Std Error	Lower 95%	Upper 95%
7	2	53.6262	2.1682	48.50	58.753
8	2	45.1234	2.1682	40.00	50.250
9	2	44.3430	2.1682	39.22	49.470
10	2	41.4858	2.1682	36.36	46.613
11	2	23.0076	2.1682	17.88	28.135
12	2	3.1533	2.1682	-1.97	8.280
13	2	3.4641	2.1682	-1.66	8.591

Std Error uses a pooled estimate of error variance

Means Comparisons

Comparisons for all pairs using Tukey-Kramer HSD

Confidence Quantile

q*	Alpha
3.96388	0.05

HSD Threshold Matrix

Abs(Dif)-HSD

	7	8	9	10	11	13	12
7	-12.154	-3.652	-2.871	-0.014	18.464	38.008	38.318
8	-3.652	-12.154	-11.374	-8.517	9.961	29.505	29.816
9	-2.871	-11.374	-12.154	-9.297	9.181	28.725	29.035
10	-0.014	-8.517	-9.297	-12.154	6.324	25.867	26.178
11	18.464	9.961	9.181	6.324	-12.154	7.389	7.700
13	38.008	29.505	28.725	25.867	7.389	-12.154	-11.844
12	38.318	29.816	29.035	26.178	7.700	-11.844	-12.154

Positive values show pairs of means that are significantly different.

Connecting Letters Report

Level		Mean
7	A	53.626150
8	A	45.123400
9	A	44.343000
10	A	41.485800
11	B	23.007600
13	C	3.464050
12	C	3.153300

Levels not connected by same letter are significantly different.

(C)

Analysis of Variance

Source	DF	Sum of Squares	Mean Square	F Ratio	Prob > F
Initial pH	3	178.94470	59.6482	26.6896	0.0042*
Error	4	8.93954	2.2349		
C. Total	7	187.88424			

Means for Oneway Anova

Level	Number	Mean	Std Error	Lower 95%	Upper 95%
7	2	12.7989	1.0571	9.864	15.734
8	2	15.3910	1.0571	12.456	18.326
9	2	17.3258	1.0571	14.391	20.261
10	2	4.8987	1.0571	1.964	7.834

Std Error uses a pooled estimate of error variance

Means Comparisons

Comparisons for all pairs using Tukey-Kramer HSD

Confidence Quantile

q*	Alpha
4.07085	0.05

HSD Threshold Matrix

Abs(Dif)-HSD

	9	8	7	10
9	-6.0857	-4.1509	-1.5588	6.3414
8	-4.1509	-6.0857	-3.4937	4.4065
7	-1.5588	-3.4937	-6.0857	1.8145
10	6.3414	4.4065	1.8145	-6.0857

Positive values show pairs of means that are significantly different.

Connecting Letters Report

Level		Mean
9	A	17.325800
8	A	15.390950
7	A	12.798900
10	B	4.898685

Levels not connected by same letter are significantly different.

(D)

Analysis of Variance

Source	DF	Sum of Squares	Mean Square	F Ratio	Prob > F
Initial pH	3	0.00105876	0.000353	3.3532	0.1365
Error	4	0.00042099	0.000105		
C. Total	7	0.00147976			

Means for Oneway Anova

Level	Number	Mean	Std Error	Lower 95%	Upper 95%
7	2	0.221350	0.00725	0.20121	0.24149
8	2	0.202740	0.00725	0.18260	0.22288
9	2	0.189100	0.00725	0.16896	0.20924
10	2	0.201755	0.00725	0.18161	0.22190

Std Error uses a pooled estimate of error variance

Means Comparisons

Comparisons for all pairs using Tukey-Kramer HSD

Confidence Quantile

q*	Alpha
4.07085	0.05

HSD Threshold Matrix

Abs(Dif)-HSD

	7	8	10	9
7	-0.04176	-0.02315	-0.02217	-0.00951
8	-0.02315	-0.04176	-0.04078	-0.02812
10	-0.02217	-0.04078	-0.04176	-0.02911
9	-0.00951	-0.02812	-0.02911	-0.04176

Positive values show pairs of means that are significantly different.

Connecting Letters Report

Level		Mean
7	A	0.22135000
8	A	0.20274000
10	A	0.20175500
9	A	0.18910000

Levels not connected by same letter are significantly different.

Appendix A.13 Effects of initial pH on glucose fermentation

(A) cell mass concentration; (B) glucose consumption; (C) TFA accumulation; (D) total carotenoids accumulation.

(A)

Analysis of Variance

Source	DF	Sum of Squares	Mean Square	F Ratio	Prob > F
Initial pH	4	0.09997380	0.024993	24.2132	0.0018*
Error	5	0.00516112	0.001032		
C. Total	9	0.10513492			

Means for Oneway Anova

Level	Number	Mean	Std Error	Lower 95%	Upper 95%
3	2	2.18534	0.02272	2.1269	2.2437
4	2	2.04493	0.02272	1.9865	2.1033
5	2	1.94384	0.02272	1.8854	2.0022
6	2	1.94665	0.02272	1.8882	2.0050
7	2	1.91154	0.02272	1.8531	1.9699

Std Error uses a pooled estimate of error variance

Means Comparisons

Comparisons for all pairs using Tukey-Kramer HSD

Confidence Quantile

q*	Alpha
4.01150	0.05

HSD Threshold Matrix

Abs(Dif)-HSD

	3	4	6	5	7
3	-0.12888	0.01153	0.10981	0.11262	0.14492
4	0.01153	-0.12888	-0.03060	-0.02779	0.00451
6	0.10981	-0.03060	-0.12888	-0.12608	-0.09378
5	0.11262	-0.02779	-0.12608	-0.12888	-0.09658
7	0.14492	0.00451	-0.09378	-0.09658	-0.12888

Positive values show pairs of means that are significantly different.

Connecting Letters Report

Level		Mean
3	A	2.1853400
4	B	2.0449300
6	B C	1.9466450
5	B C	1.9438400
7	C	1.9115400

Levels not connected by same letter are significantly different.

(B)

Analysis of Variance

Source	DF	Sum of Squares	Mean Square	F Ratio	Prob > F
Initial pH	4	284.70452	71.1761	16.7963	0.0042*
Error	5	21.18803	4.2376		
C. Total	9	305.89255			

Means for Oneway Anova

Level	Number	Mean	Std Error	Lower 95%	Upper 95%
3	2	57.1083	1.4556	53.366	60.850
4	2	56.0547	1.4556	52.313	59.796
5	2	48.1930	1.4556	44.451	51.935
6	2	46.1350	1.4556	42.393	49.877
7	2	43.8892	1.4556	40.147	47.631

Std Error uses a pooled estimate of error variance

Means Comparisons

Comparisons for all pairs using Tukey-Kramer HSD

Confidence Quantile

q*	Alpha
4.01150	0.05

HSD Threshold Matrix

Abs(Dif)-HSD

	3	4	5	6	7
3	-8.2579	-7.2043	0.6574	2.7154	4.9612
4	-7.2043	-8.2579	-0.3961	1.6619	3.9077
5	0.6574	-0.3961	-8.2579	-6.1999	-3.9541
6	2.7154	1.6619	-6.1999	-8.2579	-6.0121
7	4.9612	3.9077	-3.9541	-6.0121	-8.2579

Positive values show pairs of means that are significantly different.

Connecting Letters Report

Level		Mean
3	A	57.108250
4	A B	56.054700
5	B C	48.192950
6	C	46.134950
7	C	43.889150

Levels not connected by same letter are significantly different.

(C)

Analysis of Variance

Source	DF	Sum of Squares	Mean Square	F Ratio	Prob > F
Initial pH	4	49.241839	12.3105	7.1027	0.0271*
Error	5	8.666090	1.7332		
C. Total	9	57.907929			

Means for Oneway Anova

Level	Number	Mean	Std Error	Lower 95%	Upper 95%
3	2	18.7744	0.93092	16.381	21.167
4	2	16.3387	0.93092	13.946	18.732
5	2	16.1039	0.93092	13.711	18.497
6	2	17.9076	0.93092	15.515	20.301
7	2	12.3157	0.93092	9.923	14.709

Std Error uses a pooled estimate of error variance

Means Comparisons

Comparisons for all pairs using Tukey-Kramer HSD

Confidence Quantile

q*	Alpha
4.01150	0.05

HSD Threshold Matrix

Abs(Dif)-HSD

	3	6	4	5	7
3	-5.2812	-4.4144	-2.8455	-2.6107	1.1775
6	-4.4144	-5.2812	-3.7123	-3.4775	0.3107
4	-2.8455	-3.7123	-5.2812	-5.0464	-1.2582
5	-2.6107	-3.4775	-5.0464	-5.2812	-1.4930
7	1.1775	0.3107	-1.2582	-1.4930	-5.2812

Positive values show pairs of means that are significantly different.

Connecting Letters Report

Level		Mean
3	A	18.774400
6	A	17.907600
4	A B	16.338700
5	A B	16.103900
7	B	12.315700

Levels not connected by same letter are significantly different.

(D)

Analysis of Variance

Source	DF	Sum of Squares	Mean Square	F Ratio	Prob > F
Initial pH	4	0.00166301	0.000416	1.5392	0.3200
Error	5	0.00135058	0.000270		
C. Total	9	0.00301359			

Means for Oneway Anova

Level	Number	Mean	Std Error	Lower 95%	Upper 95%
3	2	0.202625	0.01162	0.17275	0.23250
4	2	0.204725	0.01162	0.17485	0.23460
5	2	0.232180	0.01162	0.20231	0.26205
6	2	0.201460	0.01162	0.17159	0.23133
7	2	0.195055	0.01162	0.16518	0.22493

Std Error uses a pooled estimate of error variance

Means Comparisons

Comparisons for all pairs using Tukey-Kramer HSD

Confidence Quantile

q*	Alpha
4.01150	0.05

HSD Threshold Matrix

Abs(Dif)-HSD

	5	4	3	6	7
5	-0.06593	-0.03847	-0.03637	-0.03521	-0.02880
4	-0.03847	-0.06593	-0.06383	-0.06266	-0.05626
3	-0.03637	-0.06383	-0.06593	-0.06476	-0.05836
6	-0.03521	-0.06266	-0.06476	-0.06593	-0.05952
7	-0.02880	-0.05626	-0.05836	-0.05952	-0.06593

Positive values show pairs of means that are significantly different.

Connecting Letters Report

Level		Mean
5	A	0.23218000
4	A	0.20472500
3	A	0.20262500
6	A	0.20146000
7	A	0.19505500

Levels not connected by same letter are significantly different.

Appendix B - Copyright permissions

Appendix B.1 Copyright permission for Figure 1.4

SPRINGER NATURE LICENSE TERMS AND CONDITIONS

Jul 21, 2019

This Agreement between Xiang Li ("You") and Springer Nature ("Springer Nature") consists of your license details and the terms and conditions provided by Springer Nature and Copyright Clearance Center.

License Number	4631960020949
License date	Jul 18, 2019
Licensed Content Publisher	Springer Nature
Licensed Content Publication	Nature Reviews Microbiology
Licensed Content Title	Microbial degradation of aromatic compounds — from one strategy to four
Licensed Content Author	Georg Fuchs, Matthias Boll, Johann Heider
Licensed Content Date	Oct 3, 2011
Licensed Content Volume	9
Licensed Content Issue	11
Type of Use	Thesis/Dissertation
Requestor type	academic/university or research institute
Format	electronic
Portion	figures/tables/illustrations
Number of figures/tables/illustrations	2
High-res required	no
Will you be translating?	no
Circulation/distribution	1,001 to 2,000
Author of this Springer Nature content	no
Title	Lignin bioconversion to value-added products by marine protist, Thraustochytrium striatum
Institution name	Kansas State University
Expected presentation date	Dec 2019
Portions	Figures 3 &5
Requestor Location	Xiang Li 2215 College Ave Apt 275 Manhattan, KS 66502 United States Attn:

Appendix B.2 Copyright permission for Figure 1.5A

ELSEVIER LICENSE
TERMS AND CONDITIONS

Jul 21, 2019

This Agreement between Xiang Li ("You") and Elsevier ("Elsevier") consists of your license details and the terms and conditions provided by Elsevier and Copyright Clearance Center.

License Number	4631960895121
License date	Jul 18, 2019
Licensed Content Publisher	Elsevier
Licensed Content Publication	Biochimie
Licensed Content Title	Fatty acid biosynthesis in microorganisms being used for Single Cell Oil production
Licensed Content Author	Colin Ratledge
Licensed Content Date	Nov 1, 2004
Licensed Content Volume	86
Licensed Content Issue	11
Licensed Content Pages	9
Start Page	807
End Page	815
Type of Use	reuse in a thesis/dissertation
Intended publisher of new work	other
Portion	figures/tables/illustrations
Number of figures/tables/illustrations	1
Format	electronic
Are you the author of this Elsevier article?	No
Will you be translating?	No
Original figure numbers	Figure 3
Title of your thesis/dissertation	Lignin bioconversion to value-added products by marine protist, Thraustochytrium striatum

Publisher of new work	Kansas State University
Expected completion date	Dec 2019
Estimated size (number of pages)	1
Requestor Location	Xiang Li 2215 College Ave Apt 275 Manhattan, KS 66502 United States Attn:
Publisher Tax ID	98-0397604

Appendix B.3 Copyright permission for Figure 1.6A

7/18/2019 Rightslink® by Copyright Clearance Center

Copyright Clearance Center RightsLink® Home Account Info Help LIVE CHAT

ACS Publications Most Trusted. Most Cited. Most Read.

Title: Breaking Down Lignin to High-Value Chemicals: The Conversion of Lignocellulose to Vanillin in a Gene Deletion Mutant of Rhodococcus jostii RHA1

Author: Paul D. Sainsbury, Elizabeth M. Hardiman, Mark Ahmad, et al

Publication: ACS Chemical Biology

Publisher: American Chemical Society

Date: Oct 1, 2013

Copyright © 2013, American Chemical Society

Logged in as: Xiang Li

Account #: 3001484188

LOGOUT

PERMISSION/LICENSE IS GRANTED FOR YOUR ORDER AT NO CHARGE

This type of permission/license, instead of the standard Terms & Conditions, is sent to you because no fee is being charged for your order. Please note the following:

- Permission is granted for your request in both print and electronic formats, and translations.
- If figures and/or tables were requested, they may be adapted or used in part.
- Please print this page for your records and send a copy of it to your publisher/graduate school.
- Appropriate credit for the requested material should be given as follows: "Reprinted (adapted) with permission from (COMPLETE REFERENCE CITATION). Copyright (YEAR) American Chemical Society." Insert appropriate information in place of the capitalized words.
- One-time permission is granted only for the use specified in your request. No additional uses are granted (such as derivative works or other editions). For any other uses, please submit a new request.

If credit is given to another source for the material you requested, permission must be obtained from that source.

Appendix B.4 Copyright permission for Figure 1.6B

Order Details

Green chemistry

Billing Status: **N/A**

Order detail ID:	71949053
ISSN:	1463-9270
Publication Type:	e-Journal
Volume:	
Issue:	
Start page:	
Publisher:	ROYAL SOCIETY OF CHEMISTRY
Author/Editor:	Royal Society of Chemistry (Great Britain)

Permission Status: Granted

Permission type: Republish or display content
Type of use: Thesis/Dissertation
Order License Id: 4631970485752

Requestor type	Academic institution
Format	Electronic
Portion	chart/graph/table/figure
Number of charts/graphs/tables/figures	1
The requesting person/organization	Xiang Li
Title or numeric reference of the portion(s)	Figure 1
Title of the article or chapter the portion is from	Biocatalytic conversion of lignin to aromatic dicarboxylic acids in Rhodococcus jostii RHA1 by re-routing aromatic degradation pathways
Editor of portion(s)	N/A
Author of portion(s)	Zoe Mycroft, Maria Gomis, Paul Mines, Paul Law and Timothy D. H. Bugg
Volume of serial or monograph	N/A
Issue, if republishing an article from a serial	11
Page range of portion	4975
Publication date of portion	July 9th, 2015
Rights for	Main product and any product related to main product
Duration of use	Life of current edition
Creation of copies for the disabled	no
With minor editing privileges	yes
For distribution to	Worldwide
In the following language(s)	Original language of publication
With incidental promotional use	no
Lifetime unit quantity of new product	Up to 4,999
Title	Lignin bioconversion to value-added products by marine protist, Thraustochytrium striatum
Institution name	Kansas State University
Expected presentation date	Dec 2019